Face Milling Tool Geometry And Cutting Performance Of Silicon-nitride Tool Materials.

INFORMATION TO USERS

This reproduction was made from a copy of a document sent to us for microfilming. While the most advanced technology has been used to photograph and reproduce this document, the quality of the reproduction is heavily dependent upon the quality of the material submitted.

The following explanation of techniques is provided to help clarify markings or notations which may appear on this reproduction.

1. The sign or "target" for pages apparently lacking from the document photographed is "Missing Page(s)". If it was possible to obtain the missing page(s) or section, they are spliced into the film along with adjacent pages. This may have necessitated cutting through an image and duplicating adjacent pages to assure complete continuity.

2. When an image on the film is obliterated with a round black mark, it is an indication of either blurred copy because of movement during exposure, duplicate copy, or copyrighted materials that should not have been filmed. For blurred pages, a good image of the page can be found in the adjacent frame. If copyrighted materials were deleted, a target note will appear listing the pages in the adjacent frame.

3. When a map, drawing or chart, etc., is part of the material being photographed, a definite method of "sectioning" the material has been followed. It is customary to begin filming at the upper left hand corner of a large sheet and to continue from left to right in equal sections with small overlaps. If necessary, sectioning is continued again—beginning below the first row and continuing on until complete.

4. For illustrations that cannot be satisfactorily reproduced by xerographic means, photographic prints can be purchased at additional cost and inserted into your xerographic copy. These prints are available upon request from the Dissertations Customer Services Department.

5. Some pages in any document may have indistinct print. In all cases the best available copy has been filmed.

University Microfilms International
300 N. Zeeb Road
Ann Arbor, MI 48106

Lehtihet, El-Amine

FACE MILLING TOOL GEOMETRY AND CUTTING PERFORMANCE OF SILICON-NITRIDE TOOL MATERIALS

Lehigh University PH.D. 1985

PLEASE NOTE:

In all cases this material has been filmed in the best possible way from the available copy. Problems encountered with this document have been identified here with a check mark __✓__.

1. Glossy photographs or pages _____
2. Colored illustrations, paper or print _____
3. Photographs with dark background _____
4. Illustrations are poor copy _____
5. Pages with black marks, not original copy _____
6. Print shows through as there is text on both sides of page _____
7. Indistinct, broken or small print on several pages ✓
8. Print exceeds margin requirements _____
9. Tightly bound copy with print lost in spine _____
10. Computer printout pages with indistinct print _____
11. Page(s) _____ lacking when material received, and not available from school or author.
12. Page(s) _____ seem to be missing in numbering only as text follows.
13. Two pages numbered _____. Text follows.
14. Curling and wrinkled pages _____
15. Other _____

University
Microfilms
International

FACE MILLING TOOL GEOMETRY AND CUTTING PERFORMANCE OF SILICON NITRIDE TOOL MATERIALS

by

El-Amine Lehtihet

A Dissertation

Presented to the Graduate Committee

of Lehigh University

in Candidacy for the Degree of

Doctor of Philosophy

in

Industrial Engineering

Lehigh University

1985

Approved and recommended for acceptance as a dissertation in partial fulfillment of the requirements for the degree of Doctor of Philosophy in Industrial Engineering.

5/9/85
(date)

Professor in Charge

Accepted 5/9/85
(date)

Special committee directing the doctoral work of El-Amine Lehtihet

Chairman

Acknowledgements

I would like to express my gratitude to all members of my committee for their involvement with this dissertation. I am particularly indebted to Prof. G.E. Kane for the inspiration, guidance and relentless encouragements throughout these years. The lessons in cutting tools will undoubtedly be remembered but those in kindness and humility will be cherished and the hardest to emulate. My thanks go also to Mr. W. Scheithauer, Jr. and his colleagues at G.T.E. Sylvania for support, cooperation and the opportunity to look at these new tools. I was fortunate enough to meet and learn from Prof. S. Monro and sincerely thank him for many delicate attentions over these years. Last but not least, I would like to thank Prof. A.F. Gould for his help, kindness and the opportunity to attend Lehigh.

TABLE OF CONTENTS

(Table of Contents - cont.)

List of Tables

List of Figures

(List of Figures - cont.)

ABSTRACT

An evaluation of two different grades of silicon nitride based cutting tools was conducted to assess their suitability for face milling. Two edge geometries were used and the emphasis of the study was on the identification and control of the geometric variables responsible for premature tool failure. When machining with tools having a honed edge only, it was shown that both the angle of engagement ε_i and the angle of exit ε_o were potential sources of premature tool failure. It was also shown that by confining the location of the initial tool/workpiece contact point to the face of the tool and operating in an area below a feed/ε_o dependent exit breakage boundary, the face milling of steel workpieces was possible. The notion of controlling the location of initial tool/workpiece contact and its progress was extended to a tool having a K-land edge preparation by simulating tool engagement on a computer-aided design station with solid modelling capability. As the angle of engagement was varied, the computer model revealed that this preparation was capable of both potentially favorable and unfavorable entry conditions. The experimental tests showed that brittle failure was absent when initial contact location was confined to the K-land. However, as the angle of engagement took on large positive values, the initial contact point shifted to the minor cutting edge and the tool failed by fracture. Under these conditions, the presence of a K-land was clearly redundant. The use of ε_i as an independent variable allowed

meaningful comparisons among tool grades and edge preparations to be made. This approach is suggested as a rational way of evaluating ceramic tool geometries in face milling. When milling different steels, the SNT grade was found to be more crater resistant than the AY6 grade but the latter proved to be substantially tougher. An attempt to provide crater resistance through Al_2O_3 coating was unsuccessful as the coating showed poor adherence. Neither silicon nitride grade was capable of face milling titanium or nickel alloys. When face milling a hypereutectic silicon aluminum, the AY6 grade was found to be superior to a C-2 grade of tungsten carbide but neither grade matched the performance of pollycrystalline diamond tools.

1. INTRODUCTION AND OBJECTIVES

1.1 Introduction

Ceramic cutting tools, made essentially out of aluminum oxide were experimented with in metal machining operations as far back as 1905. However, early recognition of this material's potential as a cutting tool and subsequent refinements did not necessarily ensure its acceptance in the manufacturing field. Commenting on the difficulties encountered by ceramic cutting tools in the machining industry, E. Dow Whitney of the University of Florida [*] states that: "Misuse, misunderstanding and prejudgement of failure have suppressed general acceptance and application for years". While indiscriminate attempts to use ceramic tools must have contributed to the general lack of acceptance, their inherent brittleness is undoubtedly the physical property most responsible for their confinement to today's narrow window of application. In their drive to overcome the brittleness problem, metal cutting practitioners devised tool edge configurations better suited to accommodate the fragility of these tools. This development allowed ceramics to perform adequately in the high speed turning of cast iron and steel. Still, interrupted type operations are scrupulously avoided and

---

E. Dow Whitney, "Ceramic and ceramic cutting tool technology" Carbide and tool journal, May-June 1980.

and most users are apprehensive about the catastrophic failures associated with thest tools. In spite of these difficulties, interest in ceramic tools did not subside. Compared to the abundance of ceramic tool raw materials, the major constituents of cemented carbide tools are experiencing rising costs and decreasing availability. Difficult to machine materials are still in need for tool performances beyond the reach of cemented carbides. It is therefore not surprising that these considerations have renewed interest in ceramic type tooling and today, predictions of acceptance and increased utilization are optimistic. A consequence of this renewed interest in ceramics is the recent appearance of a new family of tools based on silicon nitride rather than aluminum oxide. The present study will try to address the use of some silicon nitride compositions.

1.2 Objectives and Approach

The recent development of silicon nitride based tools for machining purposes has brought the promise of a substantially tougher tool which retains the desirable characteristics of conventional ceramics. To the extent that toughness, as measured by the fracture toughness coefficient K_{iC}, is any indication of the impact resistance of a tool under actual cutting conditions, these new compositions raise the possibility of expanding the application

range of ceramics to cover interrupted cuts. G.T.E. SYLVANIA has recently joined a handful of tool manufacturers in the development of silicon nitride based tools. The proposed study deals with the feasibility of using some of their compositions in face milling, with particular emphasis placed on the selection of the geometric parameters of the process. The ability to withstand impacts under interrupted cutting conditions will be evaluated with the intent to adapt these tools to the milling of some difficult to machine materials. Specifically, steel, titanium and nickel alloys were retained. The ability of these tools to withstand abrasive wear will be evaluated against a hypereutectic silicon aluminum alloy. This alloy is finding increasing utilization in the automobile industry but its high silicon content presents some machining difficulties.

As metal cutting practitioners familiar with the development of cemented carbide tools will recall, these tools met with some considerable difficulties when first used in interrupted cutting. Their toughness was not comparable to that of high speed steel tools and they could not be used in the same way. The adoption of negative rake geometry allowed the user to compensate for the decrease in toughness and still benefit from the superior wear qualities of cemented carbides. This is but one example of the judicious selection of geometric variables controlled by the user,

so that the tool is presented to the work in a manner which enhances its advantages while masking its shortcomings. As an approach to evaluating the performance of silicon nitride tools in face milling, it is proposed to review the face milling operation, assess the tool requirements for interrupted cutting and expose some geometric considerations characteristic of tool engagement and disengagement during the cut. Particular attention will be paid to the notion that a great deal of control can be exerted on how the tool impacts the work during intermittent cuts. The role played by geometric edge preparations will be evaluated in this context. Identification of the characteristics of the process as well as the problems inherent to face milling will help define the geometric variables over which control can be exercised for optimum performance. It is felt that only then can meaningful experiments be designed to assess the suitability and performance of the compositions under study.

2. OVERVIEW OF CERAMIC TOOLS

2.1 Historical Development

Although ceramic cutting tools are often looked upon as a new development in cutting tool technology, they are reported [1] to have been considered in metal removal in Germany as far back as 1905. Their introduction for machining purposes therefore preceded that of the more familiar tungsten carbides by some twenty years. Patents for aluminum oxide tools were subsequently granted in England (1912) and Germany (1913). The next phase in the evolution of these tools is attributed to Ryschkewitsh whose development work in Germany resulted in the first commercially produced tool ("DEGUSSIT") as well as the first reported use in production during World War II [1,2]. After the war, extensive work was reported to be taking place in the Soviet Union [3]. Two standard ceramics under the names of "Thermokorund" and "Microlit" were developed, tested and reported to be in use for the production machining of a steel equivalent to SAE 3330 [3]. Although in the United States, work on these tools started as early as 1935, further development lagged behind the previously mentioned countries. Interest was generated only after the first success stories arrived from Europe. The Rodman Laboratory of Watertown Arsenal demonstrated that ceramics could machine steel in turning [4] and experimental work was initiated to assess milling performance. The mid-fifties saw renewed interest

in ceramics for the high speed machining of grey cast iron and steel rolls in the automobile and steel industries. Subsequently, several commercial grades appeared, including General Electric's "0-30" and Carborundum's "STUPALOX". Later years saw the introduction of cermets which combined titanium carbide with aluminum oxide and resulted in a material of higher strength. New compositions and advances in ceramic tool formulation are continuing today.

2.2 Fabrication Methods

Over the years, several processing methods have been developed to produce ceramic tools. While there may be some nuances in the methods among different tool manufacturers, some of the most common processes are similar in principle to those used to prepare cemented carbides. A brief review of cold pressing with sintering, hot pressing and hot isostatic pressing follows.

2.2.1 Cold pressing and sintering:

In this process, alumina powder, usually obtained through thermal or chemical decomposition technique is mixed with additives and ball-milled to achieve some uniformity and size control in the mixture. A mechanical or hydraulic press is then used to compact the material into its near net shape, and at this stage, geometric features such as holes etc. can be added. The inserts are then sintered at high temperature in a controlled atmosphere without the

application of pressure. Sintering basically takes advantage of the tendency of two particles to bond together when brought into contact at high temperature. Grain growth and diffusion take place across the contact surfaces and lead to an adequate cementing of the particles. The characteristics of the resulting product are strongly dependent on the duration and temperature of the sintering process. Taken at high level, these two variables will promote the high density and fine grain size desirable in the product; at a lower level, they will produce a fine microstructure which is also desirable. This contradictory requirement is resolved by a careful control of the conditions and the necessary addition of MgO and T_iO for grain growth inhibition and ease of sintering. Other variables that are controlled are the raw material's particle size, shape and composition. Upon completion of the sintering process, the inserts are ready for finishing. In this operation, they are usually cam-ground, finish-ground and finally "blanchard" ground on the top, bottom and periphery. Typical strength for cold pressed alumina is around 90,000 psi with a density averaging 3.95 g/cm^3 and a 91-93 R_A hardness.

2.2.2 Hot pressing:

Hot pressing is credited with playing a major role in the improvement of ceramic tool inserts. The process is essentially the same as the previously described sintering except for the application of pressure in addition to heat. The result is said [1] to

give better densification with lower temperature and time requirements. Grain boundary sliding, particle fragmentation, plastic deformation and accelerated diffusion are some of the phenomena which are said [1] to aid in the ease of densification. Typically, alumina powder is placed in a graphite die designed to mold either a large disc or an individual insert. The disc is inserted in a specially designed hot press furnace whose atmosphere differs from that normally encountered in sintering because of the presence of carbon containing gases. As the temperature in the furnace is raised, pressure is gradually applied through a graphite plunger. Typical runs are made at around 3000 psi 700°C for an hour, with only a few minutes at maximum temperature. Upon removal from the furnace, top and bottom are "Blanchard" and rough ground. If the material was molded into a large disc shape, the disc is usually glued onto a flat grinding plate and diamond slitting wheels are used to cut the approximate shape. The rough-sized inserts are then cam-ground to specifications and special edge preparations put on by finish grinding. Hot pressed materials, usually of the cermet type (70% aluminum oxide and 30% titanium carbide approximately) are reported to possess higher rupture strength, to be denser and have a smaller average grain size than their cold pressed and sintered counterparts. Typical values for a hot pressed cermet are 100,000 to 120,000 psi, 4.1-4.25 g/cm^3, 92-94 R_A and 1-2 μm grain size.

2.2.3 Hot isostatic pressing (HIP)

HIP or "hot isostatic pressing" is basically a modification of the hot pressing process. In this procedure, gaseous pressure is used as the pressure medium. Typical steps in the processing of the raw material involve milling and grinding, pressing, presintering, HIP sintering and grinding. The resulting products are claimed to be very dense materials with an unusually small grain size [5].

2.3 Properties

The environment in which a cutting tool has to operate is a particularly hostile one. The tool has to endure mechanical and thermal stresses, abrasion, chemical reactions and a variety of other conditions which will ultimately drive it to fail through one or a combination of mechanisms. The strong chemical bond present in the structure of ceramics and the absence of a variety of slip systems make it possible for these materials to have high hardness and to retain this hardness at elevated temperature. These two qualities made the ceramic material an attractive candidate for consideration as a potential cutting tool. In contrast, the physical property most responsible for the stagnation in the evolution and usage of ceramic tools is their inherent brittleness. Typically, the transverse rupture strength of ceramic tools is roughly equal to one-third that of cemented carbides. On the other hand, compresssive strength is appreciably high and comparable

to that of cemented carbides. Although there is evidence [6] that chemical reactions occur during machining with ceramics, these tools are shown [7] to be the least reactive in contact with different metals. Their low thermal conductivity results in most of the machining heat being carried away by the chip, leaving the workpiece relatively cool. This property, however, makes the tool very susceptible to thermal shock, and it is reported [1] to be inferior to tungsten carbide in this respect.

2.4 Application in Metal Cutting

2.4.1 Evolution of edge preparation

As pointed out in section 2.1, ceramic cutting tools of the alumina type preceded the introduction of tungsten carbide for metal machining. The early enthusiasm that greeted their reappearance in the 50's and saw these tools as a replacement for tungsten carbide was dampened very quickly by the realization that there were very serious limitations to their use. If wear resistance and the tool's chemical stability were judged a major improvement, the edge of the tool, in contrast, had a tendency to chip very readily or fail in a catastrophic manner. This precluded ceramic tools from being considered for many operations. To metal cutting practitioners, it became apparent very quickly that ceramic tools could not be used in the same way as their carbide or high speed steel counterparts. Commenting on turning tests they carried out at Ohio State, H.D. Moore and D.R. Kibbey [8] state that "the best tool from any

of the early tests developed a small chip on the second pass, which seemed to correct the geometry in such a way that the tool had an almost indefinite life. If the small chip was in fact a correction of geometry, then, it should be possible to duplicate the correction by grinding the tool before use." A similar observation must have been made in Russia, since some of their translated work [3] also showed the above-mentioned correction of conventional geometry. The result was the grinding of a land of specific width and inclination all around the periphery of the tool. Although this special preparation of the tool edge carries with it some disadvantages with respect to the metal shearing process, it reduced the severe chipping that was characteristic of tools without it [8]. It is thought to be beneficial to the cutting edge by redirecting the load so as to eliminate the cantelever type of loading that invaraibly shattered the tool. Redirecting the load then, if it happens, would allow the user to "mask" the brittleness of ceramics while taking full advantage of their adequate compressive strength. The tool edge is thought to be further enhanced because the presence of the land increases the included angle of the wedge to a value greater than 90°. Generating a slight hone on the cutting edge by tumbling the tool in an abrasive medium is another way used to alleviate the brittleness problem. The honed edge is thought to eliminate possible edge cracks resulting from the finish grinding operation and, therefore, enhance resistance to chipping. Today,

a variety of edge preparations are used and offered by ceramic tool manufacturers. Fig. 1 shows a cross-section of an SNG insert with a land ground around the periphery, and different combinations of edge preparations commonly found in ceramic tools. It should be noted that the adoption of the K-land on ceramic tools has resulted in a proliferation of standards among cutting tool manufacturers who, at best, offer a vague rule-of-thumb to help the user decide on what edge preparation is best for a particular application. While these preparations eliminated the overwhelming chipping and fracture predominant in sharp ceramic edges, they are shown to result [9] in a significant decrease in tool life during continuous cutting. Substantial increases in cutting forces with increasing hone radius and land width were said to be the probable cause of the decrease in tool life. Nevertheless, for ceramic tools, this development allowed them to perform in continuous cutting and their tool life was determined by mechanisms other than brittle premature chipping.

2.4.2 Ceramic wear mechanisms

Under severe machining conditions, photographic and microscopic evidence are reported [1] to show that plastic deformation is one of the wear mechanisms in alumina. Plastic deformation is thought to cause a reorientation of material which is subsequently removed. This deformation process is thought by King and Wheldon [1] to lead to the nucleation of surface cracks often observed in ceramics.

a. hone only

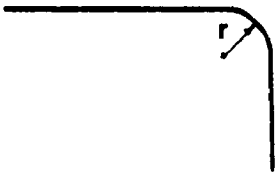

b. K-land only

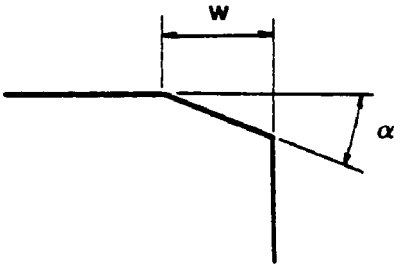

c. K-land + hone

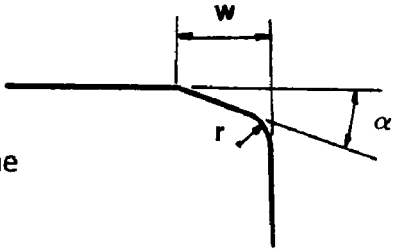

d. double K-land + hone

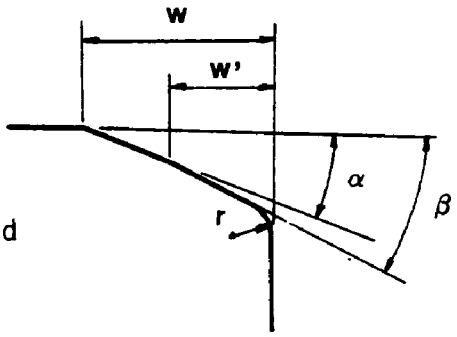

Figure 1: Ceramic edge preparations

This particular pattern of cracks, often referred to as "comb-cracks" because of their orientation and spacing with respect to the cutting edge, has been described by Pekelharing [9]. He found that on cutting a given material, usually steel, with the depth of cut kept constant, a "comb-crack threshold" could be specified as a function of the cutting speed and feed. He also reported about experiments carried out to seek the cause of the "comb-cracks". When molten iron was poured over part of the protruding tip of a ceramic insert embedded in moulding sand, the same type of cracks were found after the tip had cooled. This and other considerations led him to believe that "comb-cracking" results mainly from high thermal stresses localized in the crater area behind the cutting edge. Although the appearance of "comb-cracks" does not necessarily imply that tool failure is imminent, their presence is nevertheless undesirable as it slowly enhances wear development and disintegration of the crater area. It represents, therefore, an important shortcoming of refractory materials such as ceramics. Another source of tool deterioration when machining with ceramic tools is wear promoted by chemical reaction. Although aluminum oxide turned out to be the least reactive material in tests designed to assess the degree of chemical reaction between potential tool materials and selected metals [10], the severe temperature and pressure conditions present at the tool-chip interface will promote chemical reactions. King and Wheldon [1] report that when alumina and iron are heated

in an oxidizing atmosphere, a reaction that results in the formation of a layer of the spinal $FeOAL_2O_3$ occurs and this may represent a potential source of crater wear through the shearing of this layer by the moving chip. Finally, it is also reported that some ceramic tools exhibited wear through microspalling, a process in which whole alumina grains are suddenly removed.

2.4.3 Current use

Within the spectrum of today's cutting tools, ceramics occupy a very modest place and are used almost exclusively in the high speed finishing type of operations. They address a number of materials including super alloys, hard chill cast irons and high strength steels. Although the adoption of special edge preparations, better toughness of the cermets and more rigid machine tools have lessened to some extent the earlier restrictions imposed on ceramics, they are still excluded from interrupted operations. Research in ceramics has continued to seek new and tougher ceramic tools and a clear manifestation of the continuing interest in ceramic tools is the recent development of a family of cutting tools based on silicon nitride. These tools raise the prospect of an expanded role for ceramics. While most of the information concerning these tools is still proprietary, some basic facts relating to their development and properties are beginning to emerge. The following is an overview of these tools.

2.5 Silicon Nitride-Based Ceramics

Silicon nitride possesses a number of properties which are very desirable for a potential cutting tool material. High strength, good wear resistance, high decomposition temperature, good oxidation, resistance and thermal shock properties are all responsible for the recent appearance of this material as the basis for a new cutting tool family. However, the low self-diffusivity of this material prevents maximum densification under normal sintering conditions. It is, therefore, prepared by hot pressing at 1700-1800°C with the addition of suitable compounds such as M_gO. It appears [12] that even the hot pressed product is inadequate due to the formation of a glassy phase associated with magnesium oxide. This glassy phase compromises the high-temperature properties of this material. Gazza [13] reportedly showed that the properties can be enhanced by substituting yttria to magnesia. The result was a more refractory grain-boundary phase. Silicon nitride also gave birth to a group of ceramics known as "sialons." They are silicon nitride-based materials with additions of aluminum and oxygen. They are said [12] to have been discovered independently in Japan and England. Their existence seems to have been brought about by the realization that α-silicon nitride was a defect structure in which some nitrogen atoms are replaced by oxygen [12]. This in turn, according to Jack [12], raised the possibility of substituting more oxygen to nitrogen through the application of the principles

governing the replacement of a higher valency atom by a lower valency one in the mineral silicates. In other words, simultaneously replacing Si^{4+} by AL^{3+} and introducing other atoms like Mg^{2+} and Li^{+} for charge compensation would lead to a variety of new materials. The resulting materials possessed strength, hardness, wear and thermal resistance that made them attractive for use in turbine engine components. These same properties also qualified them as potential cutting tools and generated a number of investigations and reports [14,15,16]. Today, a number of companies are marketing silicon nitride-based tools or have such tools under development. Very little is known about the composition or preparation of these tools due to the proprietary nature of this information. It appears that they are either based on the complex compound of Si-AL-O-N (Sialon) or on silicon nitride with additions of yttria, alumina and titanium carbide. Their properties appear to represent a considerable improvement over the best ceramic or cermet tools with respect to strength. Trent [17] reports transverse rupture strengths for sintered syalon and hot pressed silicon nitride well in excess of twice those commonly associated with alumina. Fracture toughness is also shown to average over three times that of alumina. Field tests are reported to show excellent performance against cast iron in turning as well as in milling. Machining of high temperature alloys in turning as well as in interrupted cutting has been claimed [18] although such claims are not always substantiated by data.

3. THE FACE MILLING OPERATION

3.1 Description of the Process

Milling is a basic machining process whereby a workpiece is fed to a rotating cutter in a direction perpendicular to the axis of the cutter. The surface is generated by the progressive formation and removal of chips from the workpiece. In face milling, the generated surface is flat and at right angle to the cutter axis of rotation. This surface is the result of the cutting actions of the portions of the teeth located on both the periphery and face of the cutter. The basic concept and motions involved in face milling are illustrated in Fig. 2. The operation usually involves the use of a multitooth cutter consisting of a large diameter cutter body with a number of inserted tools mechanically secured to the body. Most face milling operations are performed with throwaway inserts. As the working cutting edge on the insert wears out, a new edge can be presented to the work by indexing the insert. As all edges of the insert are worn, the insert is then replaced by a new one. The important geometric variables of an insert held in a face milling cutter are the axial rake (γa), the radial rake (γr) and the corner angle (C). These angles are defined relative to a reference plane which contains the axis of rotation of the face mill and passes through the point of the tool. Axial and radial rakes are measured in planes perpendicular to the reference plane but lie in different directions. The radial rake lies in a plane parallel to the machined

surface and the axial rake lies in a plane perpendicular to it. The corner angle (c) lies in the reference plane and is the angle between the axis of rotation and the projection of the cutting edge. Fig. 3 illustrates these angles. These angles determine the true rake angle, which directly affects the shear angle in the chip removal process. Face milling cuts can be performed in a variety of ways depending on the cutter position relative to the workpiece. Three characteristic positions are illustrated in Fig. 4. The trajectory of the milling tooth in face milling has been shown by Martelloti [19] to be trochoidal. For the sake of simplicity, illustrations of milling cuts will approximate it by circular arcs. The complicated nature of this path results in a variable undeformed chip thickness along the cutting path. In neutral milling, the cutter centerline is equally spaced from both entry and exit. This causes the chip thickness to be minimum at the points where the tooth enters and leaves the work, and maximum at the level of the neutral line. Moving the centerline of the cutter above or below the neutral line alters the entry and exit chip thicknesses and results in what is commonly referred to as down or up milling respectively. This periodic variation of the chip thickness causes a pulsation of the cutting force resulting in dynamic loading. As the tool engages the work, it will be subjected to an impact, and as it emerges from the cut, the loading on the tool will suddenly be relaxed to zero. The relative position of the centerline of the

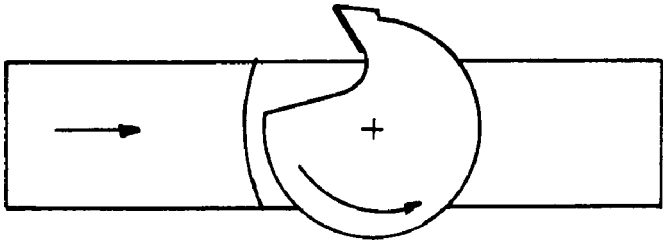

Figure 2: Tool/work motions in face milling

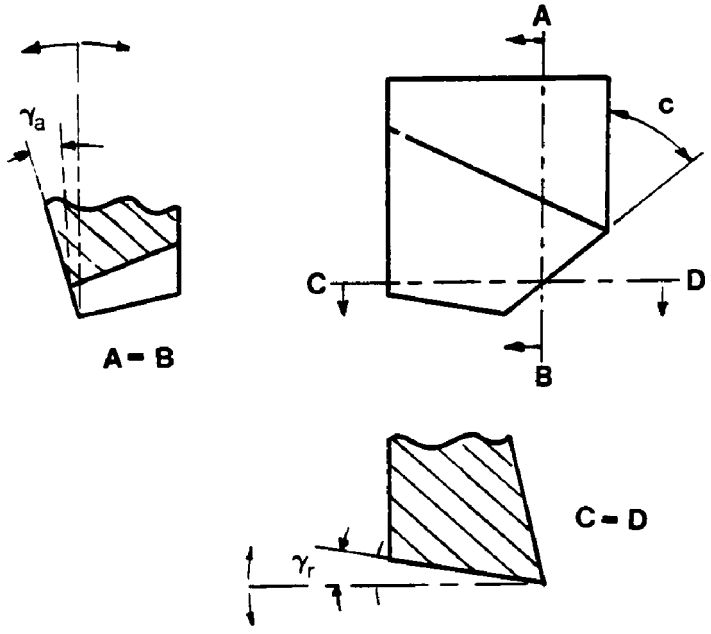

Figure 3: Milling tooth angles

Figure 4: Face milling modes

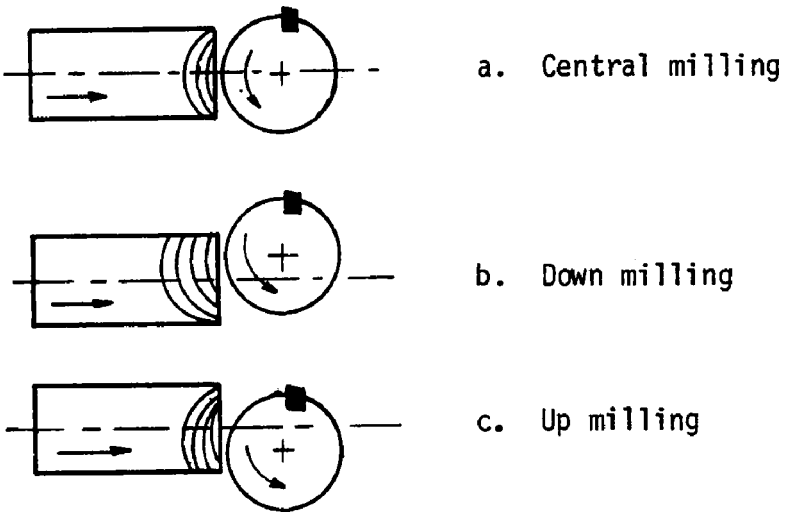

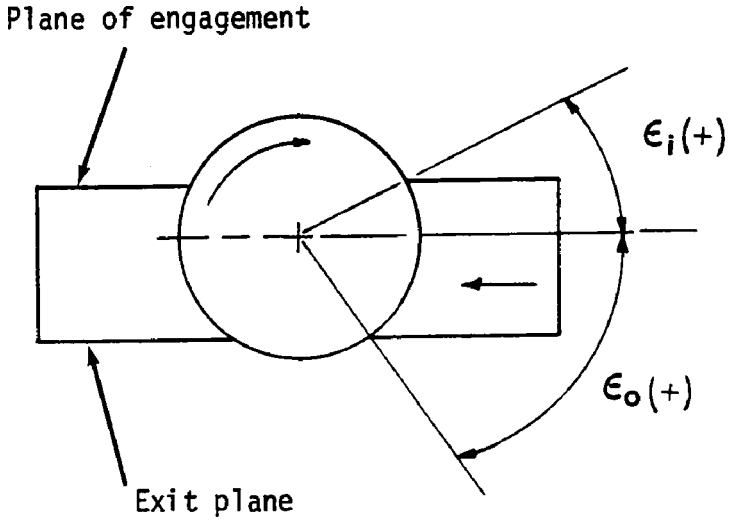

Figure 5: Angle of engagement ϵ_i and angle of exit ϵ_o.

cutter with respect to the workpiece defines the angles at which the tooth engages the work and disengages from it. These angles will be referred to as angle of engagement ε_i(in) and angle of disengagement ε_o (out). Fig. 5 illustrates how these angles are defined. By convention, positive and negative signs correspond to the centerline of the cutter below or above the plane of engagement for ε_i. The reverse holds for the disengagement angle ε_o.

3.2 Demands on the Tool

Compared to a continuous turning operation, metal removal by face milling adds some important dimensions to the properties required of a cutting tool. The intermittent nature of the cutting process in milling subjects the tool to at least one impact per revolution. Furthermore, after each impact, the tool is required to exit from the workpiece by tearing off the chip from the parent material and experiencing a sudden change in loading. Comparative machining experiments in milling and turning reported by Loladze [20] highlight the more severe tool requirements imposed by interrupted cutting. For the same tools and work material, equivalent cutting conditions and common wear criterion, the ratio of linear distance cut by turning to that cut by milling was well over 100. The disparity between the two operations was attributed to the intermittent nature of milling. In any cutting operation, brittle failure is thought to occur when conditions are such that for a

given tool, tool material and geometry, the normal stress reaches the ultimate strength of the material. Loladze [20] shows that there exists a value of uncut chip thickness at which the stresses on the tool reach a critical level. Failure is reported to occur at this so called "breaking feed". Tests carried out using a planing operation with a photoelastic tool material so as to freeze the stresses on the tool were reported [20] to show a considerable change in the stress conditions of the tool as it went from entry to full cut and finally to exit. The same phenomenon was reported to occur in milling and it was estimated that all other conditions being constant, the critical uncut chip thickness for milling should be about half that of turning.

Another factor which distinguishes interrupted cuts from continuous ones in terms of the stresses imposed on the tool is the cyclic heating and cooling of the cutting tip resulting from intermittent contact with the workpiece material. Various opinions have been emitted on the effect of the resulting cyclic thermal stresses [20,21,22] but it appears that a combination of cyclic and mechanical shock is the probable cause of the commonly observed "comb cracks" pattern seen on cemented carbides in the intermittent cutting of certain materials. The same phenomenon was observed in ceramic tools [1,9].

The considerations mentioned above seem to suggest that there are three critical properties controlling the brittle failure of a

cutting tool in intermittent cutting. These are:

a - The ultimate tensile strength

b - The ultimate compressive strength

c - The thermal shock resistance.

It is worth noting that these are properties inherent to the tool material and for a ceramic type of tooling, they include the physical property that constitutes its major weakness. It is therefore not difficult to see why ceramic tools are excluded from interrupted cuts. In the earlier discussion concerning the development and use of ceramic tools, it was seen how the detrimental effect of the brittle nature of ceramics was minimized for turning operations through the adoption of a correction in the geometry of the edge. The land that was ground around the edge eliminated most of the gross chipping that was causing premature tool failure in ceramics, by presumably shifting the loading from tension to compression. While considerable endeavor has gone into treating the edge of the tool for increased strength, the approach to interrupted cutting with ceramics seems to have stopped short of the realization that a great deal of control can be exercised on where the initial impact occurs on the tool and how it progresses until full engagement is reached. Indeed, cemented carbides, despite their higher toughness, faced a similar problem under intermittent cutting, and the importance of initial contact location between the tool and the workpiece in face milling was recognized as early as 1946.

3.3 Geometric Considerations in Face Milling

When cemented carbides were applied in the face milling of steel, their brittle nature resulted in a short tool life usually controlled by chipping or fracture. This led to the adoption of negative rake angles which would presumably shift the load so that it is applied in compression rather than in tension. Other remedies included the use of the double negative rake angles discussed by A.O. Schmidt [23] as well as the thinning out of the chips through the use of corner angles [24]. A more important development was the realization that the position of the face mill relative to the work had a strong influence on the life of carbide tips. F. Lucht [25] reported on extensive testing done on steel which showed a dramatic dependence of tool life on cutter position. Lucht constructed a wooden model of the tooth shape and workpiece and used this device to visualize the location of the initial impact between the tool and the work. The results of these experiments will be discussed in a later section of this report. In the same year, a paper by M. Kronenberg [26] appeared in the transactions of the A.S.M.E. and gave a detailed mathematical model for the determination of the tool/workpiece point of initial contact. Because this concept will be used later on in the testing of ceramic tools, Kronenberg's derivation is reproduced here.

3.3.1 Kronenberg's analysis of initial contact

Fig. 6.a is a reproduction of the transparent model Kronenberg used to analyze the initial contact relationships. The figure represents a milling tooth with a straight cutting edge at an instant prior to contact. At this point, the tooth's position and orientation in space relative to the plane of engagement is determined by three parameters: the axial rake (γa), the radial rake (γr) and the angle of engagement (ε_i). Given the straight cutting edge of the tooth, the area of contact can be approximated by a parallelogram S-T-U-V. Points U and V represent points inside the face of the tool while S and T are the contact points on the periphery of the tool. In the model, the plane of engagement of the workpiece intersects the planar tool face according to a straight line L-M. Since the model represents an instant prior to contact, it is assumed that the incremental rotation needed to make contact will cause the tool to travel parallel to itself in a straight line rather than a circular path. In the case represented in Fig. 6a, it is evident that as the tool moves parallel to itself, point U on the tool will be the first point to reach its counterpart on the workpiece. The movement of the tool parallel to itself will also cause the intersection line L-M to move parallel to itself towards the contact zone. It is clear that when point U on the tool contacts its counterpart on the work, point L on the intersection line will have reached this point, too. Further movement

of the tool parallel to itself will cause the intersection line to move parallel to itself, sweeping the area of contact S-T-U-V until the last point on the tool contacts the work and full engagement is reached. Therefore, in order to determine the point of the tool that will contact the work first, it is only necessary to determine the inclination of the intersection line between the tool face and the plane of engagement of the workpiece. The next step is to relate the direction of intersection line L-M to the angles describing the geometry of the tool and its positional relationship with respect to the workpiece. In Fig. 6.b, it can be seen that the direction of line L-M can be easily described by angle i' included between lines L-M and L-N (LN being a perpendicular line dropped from L to the base of the plane of engagement and contained in this plane). Point P on the base of the tool face is constructed such that plane LNP is perpendicular to the radial line. According to its definition, the axial rake of the tool is measured in the direction of cutter rotation (i.e. perpendicular to the radial line) and therefore angle $\hat{PLN}$ represents the negative axial rake γ_a used in the figure. The radial rake (which is also negative in the figure) γ_r is defined by the intersection angle between the base of the tool face and the radial line. The angle of engagement ϵ_i is defined by the intersection of the radial line and the plane of engagement. Triangles LNP, NPM, the radial line and base of the plane of engagement are reproduced in Fig. 6c for clarity.

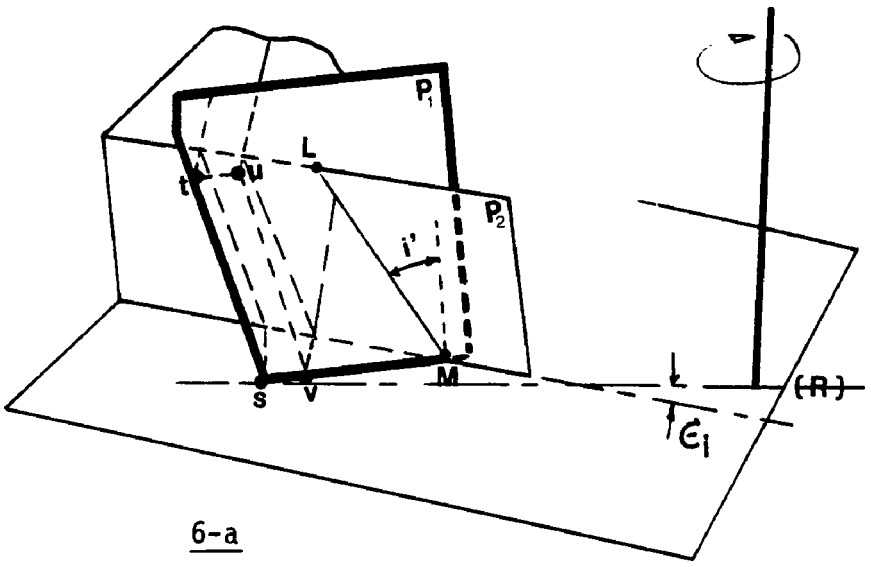

6-a

Figure 6 a,b,c: Kronenberg's tool/work model
(Trans. ASME. April 1946, pp. 217-228)

P_1: Plane of the tool face

P_2: Plane of engagement

R: Radial line

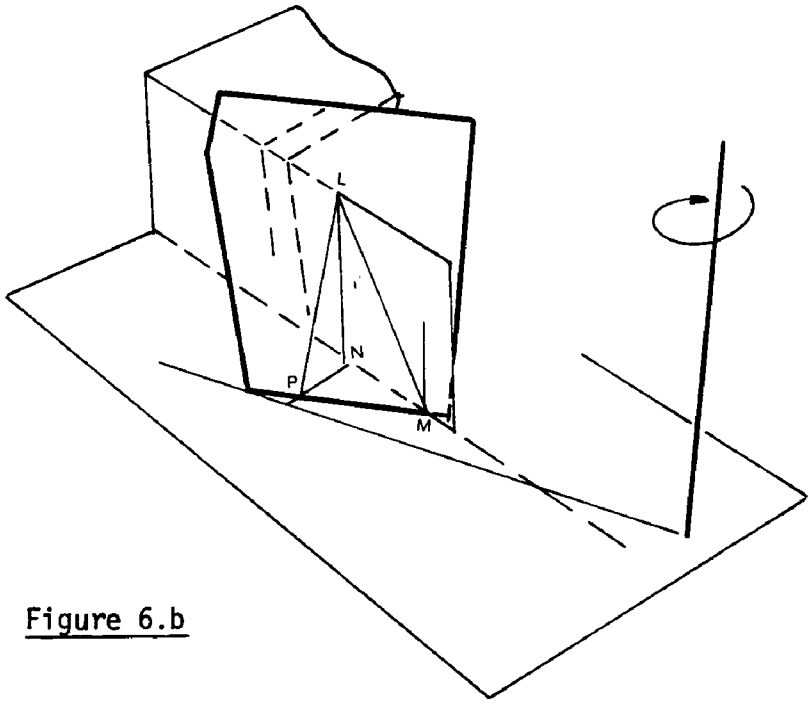

Figure 6.b

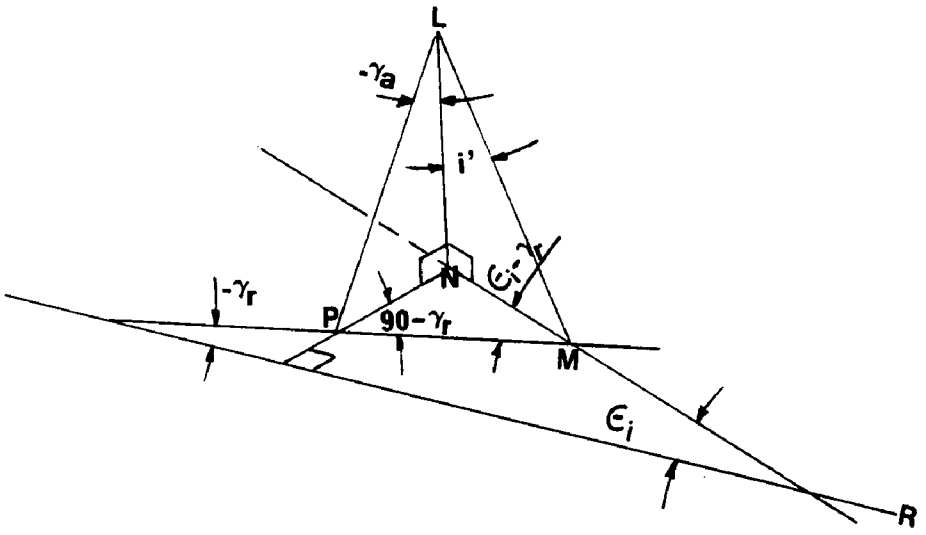

Figure 6.c

From Fig. 6.c

$$\tan(i') = NM/LN \text{ and } LN = NP/\tan(-\gamma a)$$

$$\tan(i') = \tan(-\gamma a)\cdot NM/NP$$

From triangle NPM, the following relation can be written:

$$NM/\sin(90+\gamma r) = NP/\sin(\varepsilon_i-\gamma r)$$

$$NM/NP = \sin(90+\gamma r)/\sin(\varepsilon_i-\gamma r)$$

$$NM/NP = \{\sin(90)\cos(\gamma r)+\cos(90)\sin(\gamma r)\}/\sin(\varepsilon_i-\gamma r)$$

$$NM/NP = \cos(\gamma r)/\sin(\varepsilon_i-\gamma r)$$

$$\text{Therefore } \tan(i') = \tan(-\gamma a)\cos(\gamma r)/\sin(\varepsilon_i-\gamma r)$$

$$= \tan(\gamma a)\cos(\gamma r)/\sin(\gamma r-\varepsilon_i)$$

A simpler equation can be obtained by projecting angle i' on a reference plane. The reference plane is a vertical plane erected on the radial line. Thus it is a plane making an angle ε_i (the angle of engagement) with the workpiece plane of engagement. Let i equal the projection of angle i' on the reference plane. The projection of line LN on the reference plane is a line of the same length since both planes are vertical. The projection of line NM on the reference plane is a line of length $NM\cdot\cos(\varepsilon_i)$ since the two planes are set at an angle ε_i.

Therefore $\tan(i) = NM\cdot\cos(\varepsilon_i)/LN = \tan(i')\cdot\cos(\varepsilon_i)$

The relationship between i, the rake angles and ε_i becomes

$$\tan(i) = \tan(i')\cdot\cos(\varepsilon_i) = \tan(\gamma a)\cdot\cos(\gamma r)\cdot\cos(\varepsilon_i)/\sin(\gamma r-\varepsilon_i)$$

$$\tan(i) = \tan(\gamma a) \cdot \frac{\cos(\gamma r)\cos(\varepsilon_i)}{\sin(\gamma r)\cos(\varepsilon_i)-\sin(\varepsilon_i)\cos(\gamma r)}$$

$$= \tan(\gamma a)\cdot\left[\frac{\sin(\gamma r)\cos(\varepsilon_i)}{\cos(\gamma r)\cos(\varepsilon_i)} - \frac{\sin(\varepsilon_i)\cos(\gamma r)}{\cos(\gamma r)\cos(\varepsilon_i)}\right]^{-1}$$

$$= \tan(\gamma a)\cdot\left[\frac{\sin(\gamma r)}{\cos(\gamma r)} - \frac{\sin(\varepsilon_i)}{\cos(\varepsilon_i)}\right]^{-1}$$

and finally

$$\tan(i) = \frac{\tan(\gamma a)}{\tan(\gamma r)-\tan(\varepsilon_i)} \quad . \qquad (1)$$

In order to use the corner angle C of the tool, it is useful to project angle C' (see Fig. 6.a: C' is the angle made by the edge of the workpiece left by the previous tooth and a vertical line in the plane of engagement) on the reference plane. If C is the corner angle of the tool, then it is mathematically equal to the projection of C' on the reference plane, i.e. $\tan(C) = \tan(C')\cdot\cos(\varepsilon_i)$. So equation (1) allows the determination of the inclination of the tool/workpiece intersection line. In his analysis, Kronenberg [26] also specifies the geometric conditions which determine on which side of the chip cross-section the intersection line should be placed. The analysis is also augmented by a series of monograms which allow a graphical determination of the point of initial contact and progress of contact for any shape of a planar tool edge. An example of the initial contact determination method is illustrated in Fig. 7. In this figure, the periphery of the tool is

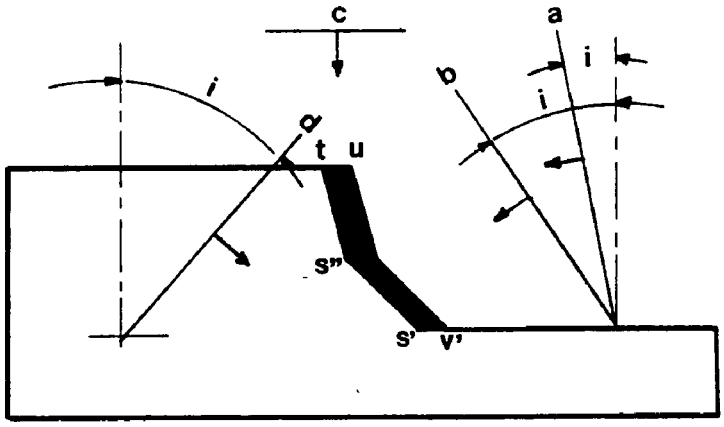

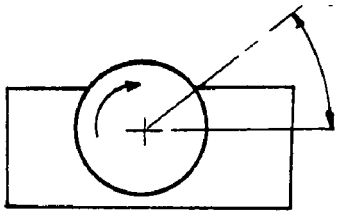

a. $\epsilon_i = +40°$

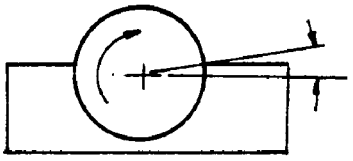

b. $\epsilon_i = +5°$

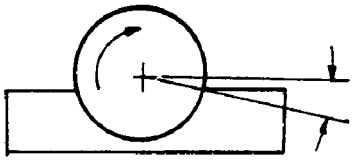

c. $\epsilon_i = -10°$

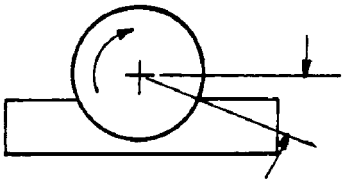

d. $\epsilon_i = -20°$

Figure 7: Example of initial contact determination.

assumed to be made up of a double corner angle (45° angle followed by a 15° angle). The shape of the chip cross-section for a certain feed/tooth is represented by the cross hatched area. The tool is assumed to have negative axial and radial rakes of -10° each. Four cases representing different positions of the face mill with respect to the engagement plane are considered. These different positions of the face mill are represented by the values assigned to the angle of engagement ε_i.

case a) $\varepsilon_i = 40°$

For $\varepsilon_i = 40°$, the inclination of the intersection line is given by $i=\tan^{-1}[\tan(-10)/(\tan(-10)-\tan(40))=9.8°$. Because $\varepsilon_i > \gamma_r$, the intersection line is positioned at point A. By moving the intersection line parallel to itself towards the chip cross section, it can be seen that point V', a point on the minor cutting edge of the tool will be the first point on the tool to contact the work-piece. As contact progresses, further movement of the intersection line shows that point V' will be followed by points S', U, S" and T in sequence.

case b) $\varepsilon_i = 5°$

For $\varepsilon_i = 5°$, the inclination of the intersection line is given by $i=\tan^{-1}[\tan(-10)/(\tan(-10)-\tan(5))]=33.8°$. Since $\varepsilon_i > \gamma_r$, the intersection line is still at A. Movement of the intersection line parallel to itself in the direction of the chip cross-section shows initial contact at point U followed by V', T, S' and S".

case c) $\varepsilon_i = -10°$

For $\varepsilon_i = -10°$, the inclination of the intersection line is given by $i=\tan^{-1}[\tan(-10)/(\tan(-10)-\tan(-10))]\rightarrow 90°$. Since $\varepsilon_i=\gamma r$ and $\gamma a<0$, initial contact is along line UT. Movement of the intersection line parallel to itself shows that the chip cross-section will be intercepted from the top down. Line S'V' on the minor cutting edge of the tool will be the last part to enter the cut.

case d) $\varepsilon_i = -20°$

For $\varepsilon_i = -20°$, the inclination of the intersection line is given by $i=\tan^{-1}[\tan(10)/(\tan(-10)-\tan(-20))] = -43.2°$. Since $\gamma r>\varepsilon_i$, the intersection line is placed at point B now. Movement of this intersection line parallel to itself shows initial contact at T, followed by U, S", S' and V.

The above example shows that for a given set of axial and radial rake angles, the variation of the cutter position with respect to the workpiece plane of engagement can result in a radical change in the location of the point of initial contact on the tool. The progress of contact until full engagement is reached is also different. If the notion that the area of contact on the tool is made up of regions (the sharp edge or tool point for example) which are more sensitive to impace or shock than others (like the face of the tool), then the ability to control the location of the initial point of contact on the tool and the progress of contact

until full engagement can be very important in the case of brittle materials. Intuitively, when using a cutting tool having a relatively sharp edge, it would be desirable to have the initial impact occur deep in the face of the tool (point U for example in Fig. 7) rather than on a sensitive point of the edge. Kronenberg and others carried out extensive testing of this concept. The results will be discussed in a later section so that they can be interpreted in terms of initial impact location at entry as well as in terms of the exit conditions of the tool.

3.3.2 Exit conditions

While Kronenberg's analysis shows that the choice of geometric variables can result in radically different contact conditions which may be damaging to the tool, the exit regime of the tool from the workpiece has also been suspected to represent a potential source of difficulty under certain conditions. In his photoelastic studies of the planing and milling operations, Loladze [20] found that the value of the principal stresses reached its maximum at the exit phase. A.J. Pekelharing [27] and others [28,29,30,31] also noticed that the exit condition could be harmful. Pekelharing [27] carried out an extensive study of the exit failure of carbide tools during orthogonal cutting. His first conclusion seems to be that sharp carbide tools (edge radius <5 μm) fracture at the exit from an orthogonal cut irrespective of feeds and speeds. In his study of the phenomenon, Pekelharing then identifies a type

of chip formation at exit which seems to be responsible for the exit failure of carbide tools. This type of chip is characterized by the formation of a "foot" at its base. Fig. 8 illustrates Pekelharing's view of foot formation at the base of the chip during the exit phase in intermittent cutting. Pekelharing ventures that the separation of the foot of the chip from the parent workpiece is the result of plastic shearing rather than brittle failure. This plastic shearing is said to result in a zone of "negative shear" which results in excessive loads being applied on the tip of the tool until separation occurs. Dangerous loading is also said to occur due to the progressive change in load distribution and concentration on the tip of the cutting edge resulting from the gradual rotation of the foot. Finite element studies reported by Pekelharing [27] tend to support this idea. In these studies, exit conditions were simulated under a plane stress condition and the resulting stress distribution in the workpiece showed a pattern of maximum shear stresses that Pekelharing treats as a possible negative shear zone. The geometry associated with the exit plane as well as the tool geometry are two factors that have been identified as having an effect on the exit failure. In his orthogonal tests, Pekelharing [27] notes that an alteration of the 90° angle that the exit phase makes which the machined surface causes the foot formation and consequently breakage to cease. By cutting chamfers of different angles on the exit plane of the workpiece, Pekelharing

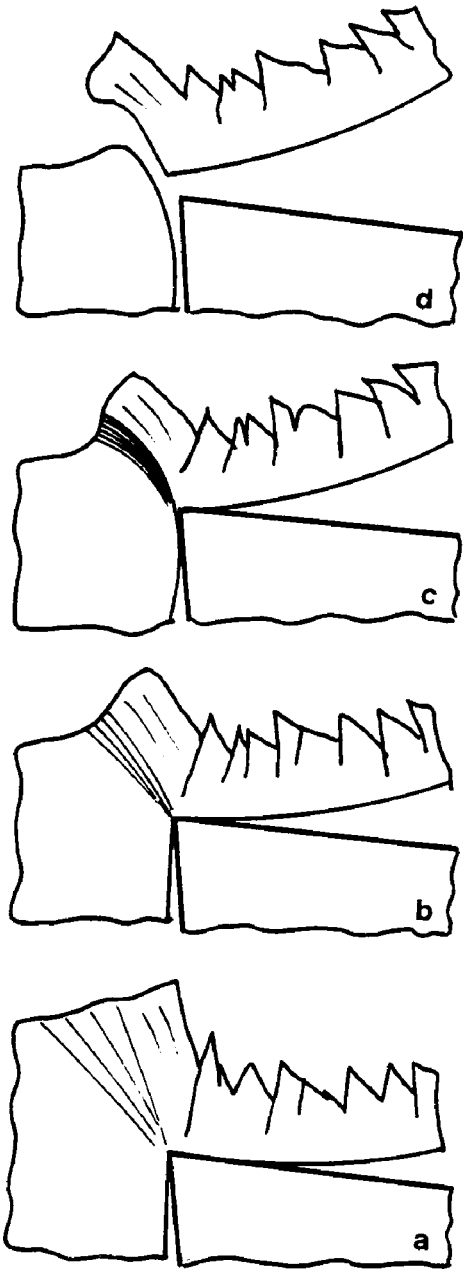

Figure 8: Progressive foot formation at exit according to Van Lutterwelt and Pekelharing. Annals of the C.I.R.P. Vol. 27/1/1978, pp. 6.

[27] is able to identify zones under which exit is safe and zones which result in foot formation and breakage. The influence of the exit plane angle with respect to the machined surface was recently confirmed by M.C. Shaw et al. [32]. Pekelharing also notes that although cutting with rounded or chamfered edges also results in foot formation as well as chip rotation, these tools do not experience the breakage associated with sharp tools. No explanation is offered for this behavior. Pekelharing et al. [33,34] recently reported on some experiments using carbide tools in face milling. These experiments were carried out to test the influence of the exit failure of cemented carbides in face milling. The tests used commercially available milling grades of cemented carbide tools on steel. A total of ten (10) different geometries (mostly variations in corner angles) were examined. The tests systematically varied the angle of disengagement (exit angle) ε_o while keeping the angle of engagement ε_i constant and equal to 90°. A 90° angle of engagement means that the tool enters the cut at minimum chip thickness of zero and therefore the shock of entry is nonexistent. A preparatory cut with a spare carbide tool was made to mill through the plane of the rectangular workpiece which is parallel to the feed motion so that the tests proper would see constant ε_i and ε_o. The tests sought to determine those values of ε_o which resulted in safe exits and those which resulted in relatively early breakage due to foot formation. The criterion for a safe exit

classification was arbitrarily set at 100 revolutions of the cutter. Cutter diameter, feed and speed were the other variables and were taken at three levels each. The main conclusions of these tests are listed below.

- Irrespective of feeds and speeds, an increase in cutter diameter increases the range of dangerous exit conditions in the direction of more negative ε_o values. This seems to imply that length of cut is a significant variable. When the length of cut taken by the largest diameter was modified so that it equaled that of the smallest cutter diameter, the range of dangerous exits was narrowed considerably. No explanation was offered for this observation.

- For some cutter diameters, an increase in the uncut chip thickness results in an increase in the dangerous exit zone.

- Higher speeds had a tendency to decrease the dangerous exit zone.

While these experiments seem to clearly establish the role of the exit angle ε_o as a potential source of breakage in face milling, they also indicate that other yet undetermined parameters may also have an effect.

3.4 Influence of Initial Contact on Tool Life

Upon the realization that the relative position of the cutter diameter with respect to the workpiece plane of engagement would

influence the life of the tool, a certain number of studies seeking to explain the phenomenon were undertaken by various researchers over the years. The results of these studies will be discussed below within the context of entry as well as exit conditions.

3.4.1 Lucht's tests

Lucht [25] carried out a systematic investigation of cutter offset with respect to the workpiece plane of engagement. He used a double negative cutter of 203 mm diameter (8 in) on a steel workpiece of constant width equal to 31 mm (1.5 in). The carbide tool used had a double corner angle resulting in a sharp point at the junction of the two corners. Figure 9 shows a reproduction of the graphical results published by Lucht. The figure clearly shows a sharp decline in tool life as the angle of engagement ε_i increases. The application of Kronenberg's analysis of initial contact to Lucht's tool shows that those regions of high tool life (ε_i=0,10°) correspond to an initial contact point deep in the face of the tool (point A, or E followed by A in figure 9) while the low tool life regions correspond to a type of contact starting on the minor cutting edge of the tool (points E followed by F). However, in this experiment, it should be noted that as the cutter is shifted to increase the value of ε_i, this same action results in a decrease of ε_o because of the constant width of the workpiece. Keeping in mind the possible effect of dangerous exit conditions discussed by Pekelharing [27,33,34], Lucht's experiment may very well result in

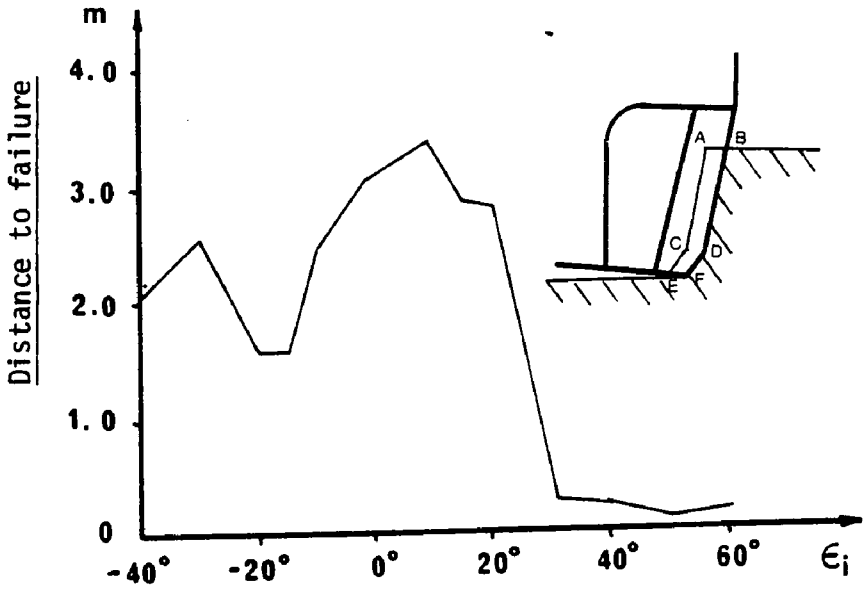

Figure 9: Lucht's Tests. Trnas. A.S.M.E., April 1946.

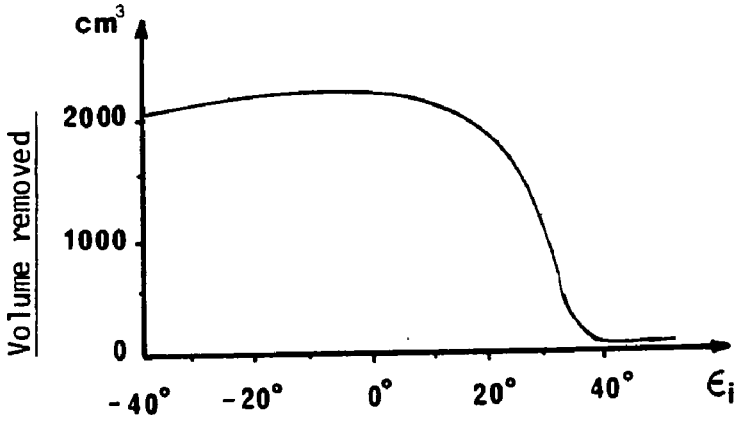

Figure 10: Kronenberg's Tests. Annals of the C.I.R.P., Vol. XVIII (1971).

the confounding of two effects: as ε_i is increased, this results in a decrease of ε_o and the low tool life shown for $\varepsilon_i \geq 30°$ may be due to either effect or a combination of both. This possibility is further reinforced by the observation that Lucht makes at ε_i = 45°. At this particular test point, Lucht notes that the tool life is negligible. He further notes that the tool life at this point can be increased many times if the width of cut is increased (i.e. more positive ε_o). The possibility of exit failure is also reinforced by Lucht's observation that failure seems to start at the sharp point constituting the junction of the two corner angles. The application of Kronenberg's analysis to Lucht's tool shows that the last point on the foot to exit from the cut is the sharp point at the junction of the two corner angles. If the type of foot formation described by Pekelharing is present, then the companion shear stress will be born by this point on the tool and breakage is not surprising. So while there is some evidence of the influence of entry conditions as expressed by values of ε_i on the tool life, caution should be used in the interpretation of the apparent reduction in tool life for large values of ε_i.

3.4.2 Kronenberg's tests

After formulating the fundamental principles of initial contact location and progress of engagement between the tool and workpiece, Kronenberg [35] reports on some experiments carried out to investigate the influence of initial contact point location on tool

life. The experiments used a 305 mm (12 in) diameter double negative cutter. The exact geometry of the carbide tool is not specified but the corner angle was reported to equal 30°. In his experiment, Kronenberg used workpieces of variable width so that at each test point, the length of the tool path was constant and equal to 80 mm (3.14 in). Figure 10 shows the results of these tests. It can be seen that initial contact at point U seems to be very desirable while tool life starts decreasing very sharply as initial contact moves progressively to point V on the minor cutting edge of the tool. Just as with Lucht's data, a word of caution is necessary in light of the potentially damaging effects of the exit conditions described by Pekelharing. Kronenberg's decision to hold the length of the tool path constant results in a variable exit condition at each test point, just as in the case of Lucht's data. It is worth noting that for $\varepsilon_i \geq 30°$, the values of the disengagement angles ε_o correspond to the dangerous exit region mentioned by Pekelharing [34]. So it may very well be that in the right hand side of the curve, again, two effects, entry and exit, are confounded.

3.4.3 Okushima and Hoshi's tests [30]

In their tests, Okushima and Hoshi use cutters of different diameters to set up experiments which allow a distinction between the effects of the angle of engagement and disengagement. Without any attempts to explain the differences of tool life obtained, they conclude that both the angle of engagement and the angle of

disengagement have an influence on the cutter life. More specifically, they find that small angles of engagement and large angles of disengagement provide a good tool life. In contrast, large angles of engagement and small angles of disengagement result in a small tool life characterized by chipping and fracture. When Kronenberg's analysis for the determination of the point of initial contact is applied to those test points showing the influence of the angle of engagement on tool life, it is found that good tool life is obtained under a T or U type of contact, while poor tool life results from initial contact on the minor cutting edge of the tool.

3.4.4 Opitz and Beckhaus's tests

Opitz and Beckhaus [36], in a paper summarizing some work done in Aachen [31], push the notion of initial contact location in face milling one step further. The idea they try to convey states basically that the larger the area deep in the face of the tool that contacts the work before the sensitive edge or tool point enters the cut, the better the survival chances of the tool. To express this idea, they consider a chip cross section approximated by a parallelogram S-T-U-V shown in Fig. 11. Opitz and Beckhaus define the partial areas of engagement F_S, F_T and F_V as the areas of the cross section crossed by the intersection line before point S, T or V are contacted respectively. For the case of a tool capable of a U type of contact (i.e. a tool with $\gamma a<0$), a plot of F_T and

F_V in function of the angle of engagement exhibits a definite maximum. Experimental tests carried out by systematically varying the angle of engagement of a high speed steel cutter on high strength austenitic steel show that the values of ε_i which maximize tool life, correspond to those ε_i values which maximize the plot of F_T and F_V. The tool life results are essentially of the same general shape as those obtained by Lucht [25] or Kronenberg [35] Opitz and Beckhaus do not give any data concerning the width of the workpieces used in their tests. Consequently, it is not possible to check what kind of exit conditions were present at the different test points. However, the problem of exit failure was raised during the discussion of the paper and Opitz acknowledges that the potentially harmful effects of the exit conditions were considered but it was clear that the dominant failure mechanism was due to unfavorable entry conditions.

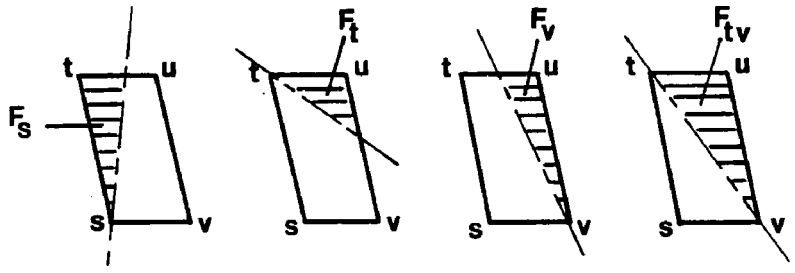

Figure 11: Partial areas of engagement. Opitz & Beckhauss Annals of the C.I.R.P., Vol. XVIII (1971).

4. FACE MILLING WITH CERAMICS

4.1 Implications for Ceramic Tools

The previous discussion concerning the influence of entry and/or exit conditions on the performance of cemented carbides and high speed steel tools in the face milling operation clearly shows that it is possible to optimize tool life, or, at least avoid premature tool failure by a careful selection of the geometric parameters of the process. It should be noted that the variables controlling the location of the initial contact point on the tool and its progress are variables chosen by the user and are independent of the tool material properties. It is also clear that within the constraints imposed by a particular workpiece size, there is always some latitude with respect to the choice of tool material, tool preparation, tool geometry, milling cutter size, milling cutter style and finally cutter/workpiece relative position. The ultimate decision will undoubtedly involve a compromise but the important aspect here is that all factors should be considered. Consideration of all these factors, and particularly the geometric factors controlling the entrance and exit of the tool becomes critical when contemplating face milling with ceramic tools. Indeed, if the experiments described in section 3.4 suggest that cemented carbide tools and high speed steel tools are sensitive to entrance and exit conditions, then at least similar sensitivity should be expected of ceramic tools due to their far greater brittleness. This proposition was adopted as

the basis for the testing of silicon nitride based tools in face milling. When viewed in the context of the efforts made throughout the years to treat the edge of ceramic tools by grinding a land for protection against brittle failure, the potential sensitivity of ceramic tools to different initial contact conditions raises a number of interesting questions.

a) The role of the K-Land

Section 2.4.1 talked about the correction of geometry introduced on ceramic tools for purposes of easing the brittleness problem. In addition to increasing the included angle of the tool, this preparation is thought [8, 51] to result in a compressive load which eliminates the cantilever type of loading. Should ceramic tools be sensitive to the location of initial impact, then it may be possible to exploit the presence of a K-land by choosing the geometric parameters so that a large portion of the initial contact area occurs on the K-land, away from the fragile cutting edge. By absorbing most of the impact on the K-land, it may very well be possible to protect the cutting edge from brittle fracture. It is therefore necessary to determine the manner in which a K-land tool contacts the workpiece and how contact changes as ε_i is changed.

b) The angle of the K-land

Commercially available ceramic tools come in a variety of shapes (round, square, triangular) as well as edge preparations. K-land angles being offered have a range from 0° (no K-land on the tool) to

as high as 35°. If the initial contact of a K-land tool with the workpiece has an influence on tool life, then the following considerations arise:

- If two tools having two different K-land angles are tested under the same conditions (same face mill, ε_i and ε_o), these tools will not see the same initial contact with the workpiece because their axial and radial angles will be different. If a significant difference in performance is detected after the test, it will not be possible to conclude whether it was due to the different included angles, or whether it was due to the different contact conditions. Under these circumstances, it would then be necessary to determine an equivalent contact condition for both tools so that the two possible effects are not confounded.
- Should the above considerations be feasible and meaningful, then this testing procedure constitutes a rational way of deciding on the optimum angle needed on a K-land. By determining equivalent impact conditions for different K-land angles, the strengthening effect of a particular K-land can be evaluated free of the effect of initial contact condition.

c) The width of the K-land

In addition to its angle, a K land is also specified by its width. The width of the K-land can also have an effect because of the following considerations:

- If the width of the K-land is equal to or greater than the chip cross-section at entry, then the location of the initial contact point and progress of this contact until full engagement is determined by the axial and radial rakes resulting from the K-land.
- If the width of the K-land is less than the chip cross section at entry, then the initial point of contact and its progress until full engagement will be a function of the two distinct sets of rake angles present on the tool face: one set of rake angles imparted by the K-land and another set imparted by the cutter geometry.

In view of these consideration it seems very important to determine the way in which the introduction of a K-land around the tool edge affects initial contact location and its progress until full engagement is reached.

4.2 Visualization of Initial Contact

4.2.1 Tool with a K-land

Face milling is done with a variety of insert shapes. The tools under consideration in this study are mostly SNG 433 inserts. The discussion on contact determination will therefore be limited to SNG inserts with a rounded tool nose.

When an SNG insert is used in face milling, its geometry, namely the axial, radial and corner angles are solely determined by the

geometry of the face mill pocket. If a K-land of a certain angle and width is ground around the cutting edge of the tool, then the resulting geometry is substantially different from that imparted by the face mill. Figure 12 illustrates a portion of a tool having a K-land ground around the periphery. On the straight portion of the cutting edge, axial and radial rakes become augmented by different amounts which are function of the angle of the K-land and the angles present on the face mill pocket. On the curved portion of the cutting edge representing the nose radius, axial and radial rakes continuously change along the curvature, their values at a particular point being also function of the K-land angle, the angles present in the face mill pocket and the value of the corner angle at that point. Furthermore, the presence of a K-land also changes the tool face. Along the straight portion of the cutting edge, the face of the tool is still planar while around the nose radius, the K-land introduces a surface of revolution. The use of Kronenberg's analysis for initial contact determination is no longer applicable in this case since the method assumes a planar tool face with constant axial and radial rake angles. With reference to the intersection line between the tool face and the plane of engagement in Kronenberg's analysis, it is clear that the intersection between a K-land tool and the plane of engagement will be a straight line over the planar portion of the cutting edge and a curve around the tool nose. So another method must be found to determine the contact condition between a K-land tool and a workpiece.

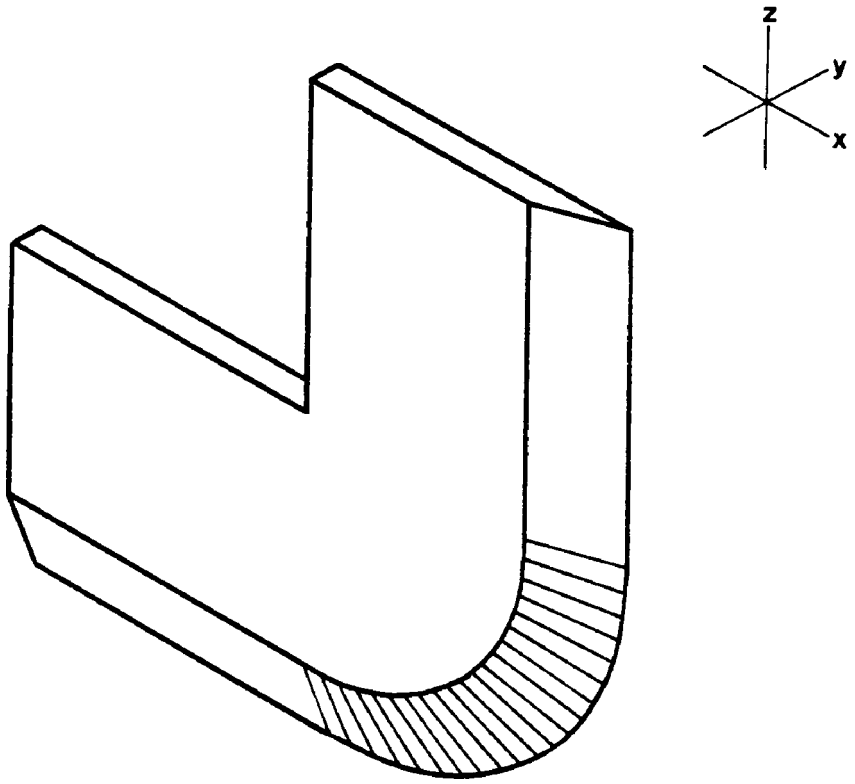

Figure 12: Tool with a K-land

4.2.2 Computer graphic model

A convenient way to visualize the way in which a K-land tool will contact the workpiece is to model the operation on a computer aided design station. Such a system must have the software capability to allow the modelling of solid three-dimensional objects. It must also allow the user to combine separate objects into one and display the intersection boundaries of the product. If these capabilities exist, they are sufficient for the visualization of initial contact between any tool shape and a workpiece through the following steps. The relevant part of the tool edge can be modelled as a three-dimension solid having the geometric features of the tool under consideration. Once created, this solid can be manipulated in space through a series of operations so that it reflects the spatial position it would take if it was held in a specific face milling cutter. A second solid can be created to model the workpiece and more specifically, the workpiece's plane of engagement. Once the two solids are built, they can then be positioned with respect to one another to simulate a relative position of the face mill with respect to the workpiece equal to a given angle ε_i. At this stage, the tool simulates an instant prior to contact and an incremental rotation of the tool will cause it to make contact with the solid representing the workpiece. The intersection line between the two solids can be viewed.

The above mentioned procedure was implemented through the use of IBM's Geometric Data Processor (GDP). GDP is an interactive

graphic system used for the modeling and design of three-dimensional objects. This system uses a number of primitive components from which any complex object or part can be modelled. This can be done through the addition and substraction of the various primitives which make up the desired part. The system combines different primitives or objects through a MERGE command. This feature is critical to the modelling of tool/workpiece contact since it will allow the display of the intersection line between tool and workpiece when contact occurs. This software is available in the Industrial Engineering Department's Computer Integrated Manufacturing laboratory. The package is run on an IBM 4341 and the work station comprises an IBM 3277 GA terminal linked to a Tektronix 618 graphic display terminal. A Tektronix Hardcopy Unit is also attached to the station. As mentioned before, the package is an interactive one and it is impractical to list here a detailed listing of all the steps used to model the contact of an SNG 433 tool having a K-land. Instead, a general outline of the procedure is given.

Step 1: Create an SNG 433 tool with a K-land

In this step, the tip of an SNG-433 ceramic tool having a K land .2 mm (.008 in) wide and an angle of 20° is created by constructing a polygon representing the cross section of a tool part similar to the tool part displayed in Figure 12. This polygon A,B,C,D, is constructed to the specifications of the K-land and its longest side is limited to the length of the tool's nose radius as shown in Figure

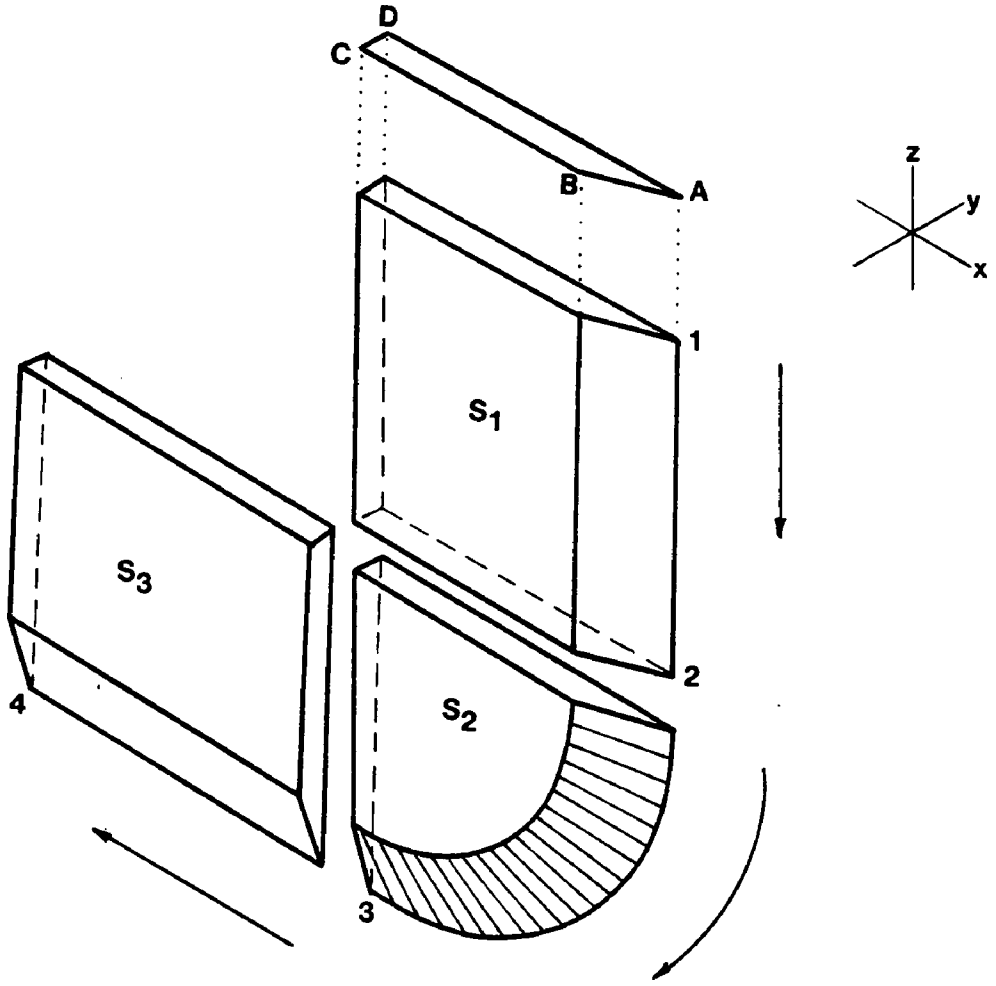

Figure 13: Creation of a SNG 433 Tool with a K-land on the graphic system.

13. This polygon is placed perpendicular to the Z-X plane and such that AD is contained in this plane. The polygon is then translated down, parallel to the Z axis by an amount equal to the nose radius. This procedure creates a solid object S_1. Polygon $A_2B_2C_2D_2$ which represents the base of S_1 is then selected to generate the next part. This polygon is rotated about an axis passing through C_2D_2, perpendicular to the Z-X plane. The rotation is in a clockwise direction and equal to 90°. This procedure generates the tool nose with a K-land around it. The surface of revolution generated by the K-land is approximated by planar facets. Refaceting can be done at this stage until the desired smoothness is achieved. The new object is called S_2. The final part of the tool is created by selecting polygon $A_3B_3C_2D_2$ and translating it parallel to the X axis, from right to left, by an amount equal to the nose radius. The new object is S_3. At this point, the tool part can be formed by merging S_1, S_2 and S_3. This command takes the three separate objects S_1, S_2 and S_3 and combines them into one object representing part of an SNG-433 tool with a K-land.

Step 2: Tool orientation

Once the tool is created, it has to be positioned in space so that it has the axial rake, radial rake and corner angles that the face mill would give it. This is done through a series of three rotations. Keeping in mind the definitions of these angles given in

section 3.1, the problem here is to find three successive rotations about particular axes so that the end result is a tool having the desired axial rake γ_a, radial rake γ_r and corner angle C. Consider Figure 14 and consider the three rotations needed to operate on plane P_1 so that it has an axial rake γ_a, radial rake γ_r, and so that OO' makes a corner angle equal to C.

a) Anti-clockwise rotation about x to give plane P_1 an axial rake γ_a.

b) Consider the new set of axes xy'z'. The next step is to find the angle α so that an anticlockwise rotation about z' results in a radial rake γ_r. From Figure 14.a we have

$$\tan(\gamma r) = AB/OA \quad \text{and} \quad \tan(\alpha) = AB'/OA$$

$$\cos(\gamma a) = AB'/AB$$

and therefore $\tan(\alpha) = \tan(\gamma r)\cdot\cos(\gamma a)$

so $\alpha = \tan^{-1}\{\tan(\gamma r)\cdot\cos(\gamma a)\}$

c) The next step is a clockwise rotation of the segment OO' in the plane P_1 about an axis perpendicular to P_1 and passing through O. The rotation should be by an angle β so that the projection of OO' on the plane ZX makes an angle C (the corner angle) with the vertical axis Z. First, project β onto the z'x plane. From Figure 14.b,

$$O'A' = OO'\cdot\cos(\beta) \; ; \; OA' = OO'\cdot\sin(\beta)$$

$$OA'' = OA'\cdot\cos(\alpha) = OA'\cdot\sin(\beta)\cdot\cos(\alpha)$$

Let θ be the projection of β in the Z'x plane

$\tan(\theta) = OA''|O'A' = OO'\cdot\sin(\beta)\cdot\cos(\alpha)|OO'\cdot\cos(\beta)$

$\tan(\theta) = \tan(\beta)\cdot\cos(\alpha)$

Now θ is projected from the Z'x plane onto the Zx plane. It should equal the desired corner angle C. From Figure 14.c, let O" be the projection of O' on the Zx plane.

$O''A_2 = O''A_1\cdot\cos(\gamma a)$

$\tan(\theta) = \theta A_1|O''A_1$ and $O''A_1 = OA_1|\tan(\theta)$

$O''A_2 = OA_1\cdot\cos(\gamma a)|\tan(\theta)$

$\tan(C) = A_3A_2/O''A_2$ and $OA_1 = A_3A_2$

$\tan(C) = \tan(\theta)/\cos(\gamma a)$

so $\tan(\beta)=\tan(\theta)/\cos(\gamma a)=\tan(C)\cdot\cos(\gamma a)/\cos(\alpha)$

The tool created in step 1 can then be positioned in the following manner. Place the tool in the xyz coordinate system so that its major and minor cutting edges coincide with the z and (-x) axis respectively. The tool can then be positioned through the following rotations:

- Rotate about z, anticlockwise by γa.
- Rotate about the major cutting edge, anticlockwise (looking down) by $\alpha = \mathrm{Tan}^{-1}\{\mathrm{Tan}(\gamma r)\cdot\cos(\gamma a)\}$.
- Rotate clockwise about an axis perpendicular to the plane of the tool and passing through its tip by an angle

  $\beta = \tan^{-1}\{\tan C\cdot\cos(\gamma a)/\cos(\alpha)\}$

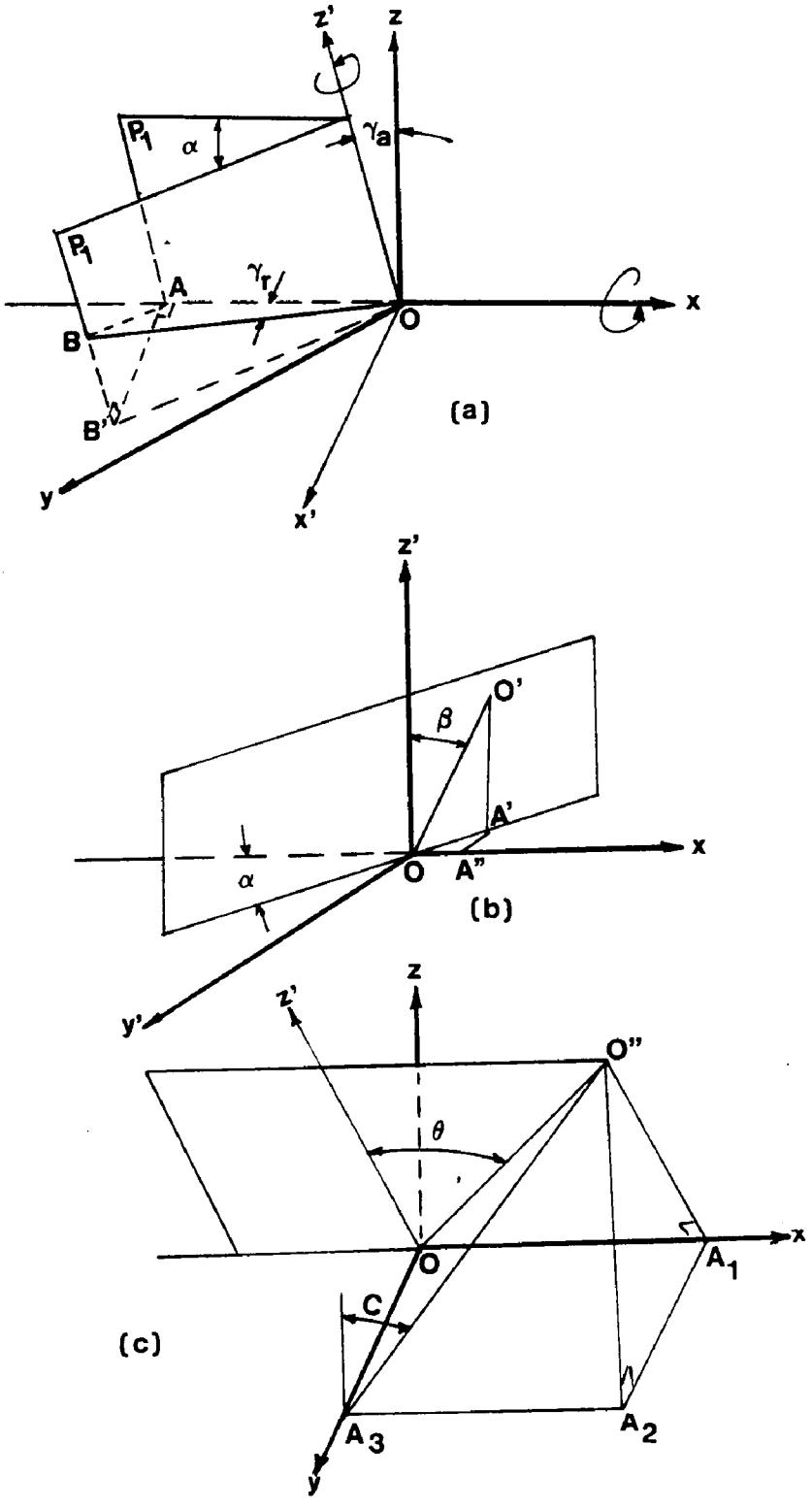

Figure 14: Tool orientation procedure

Step 3: Create a workpiece

Ideally, the workpiece should be simulated by a plane representing the plane of engagement. Unfortunately, this is not possible in the system. So a plane is approximated by a very thin cuboid. When the cuboid is thin enough, it is good enough for the purposes of this exercise.

Step 4: Tool/workpiece position

Tool and workpiece are now ready to be positioned relative to each other. To simulate an angle of engagement ε_1, the tool's point of tangency to the x-y plane is translated to the origin of the coordinate system (x,y,z)=(0,0,0). The tool is assumed to be held in a face mill of radius R, rotating about an axis of rotation, perpendicular to the xy plane and located at (-R,0,0). From this position, the tool can be rotated about the imaginary centerline of the face mill by any angle ε_1. Once the tool is rotated by an angle ε_i, the thin cuboid representing the workpiece can be taken to the tool. The cuboid is positioned perpendicular to the x-y plane, parallel to the x axis and such that an incremental rotation of the tool about its center of rotation will cause the two objects to contact each other, in an area away from the area of the chip cross section that would result from a feed f$\leq$width of the K-land.

Step 5: Visualization of contact

An incremental rotation of the tool about its center of rotation should now bring the tool/workpiece intersection close to the K-land. At this point the two objects can be combined into a single object by

using the MERGE command. After the MERGE operation is executed, the system displays the two objects combined and the intersection between tool and workpiece can be viewed from any desired position. The progress of contact can be viewed by unmerging the objects, incrementing the tool rotation and merging the two objects again. The new intersection line will then be displayed by the system. This process can be repeated until the projected area of contact on the tool has cleared the plane of engagement. Figure 15 shows different stages of a tool breaking through the plane of engagement. The figure represents a model of an SNG 433 tool with a .008x20° K land simulated in a double negative face mill of γ_a = -5°; γ_r = -5.6° and C = 15°. The angle of engagement was set at ε_i = -30°.

4.2.3 Results of the analysis

The method described in section 3.3.2 was applied to an SNG 433 tool with a .008x20° K land ground around its periphery. The tool was modelled assuming it would be held in a 101.6 mm (4 in) diameter face mill. This face milling cutter is a double negative cutter having an axial rake γ_a = -5°, radial rake γ_r = -5.6° and a corner angle C=15°.

For the case where contact between tool and workpiece is restricted to the land area (i.e. the feed is less than or equal to the width of the K-land) the computer simulation of tool/workpiece contact shows that there exists a range of angle of engagement values where

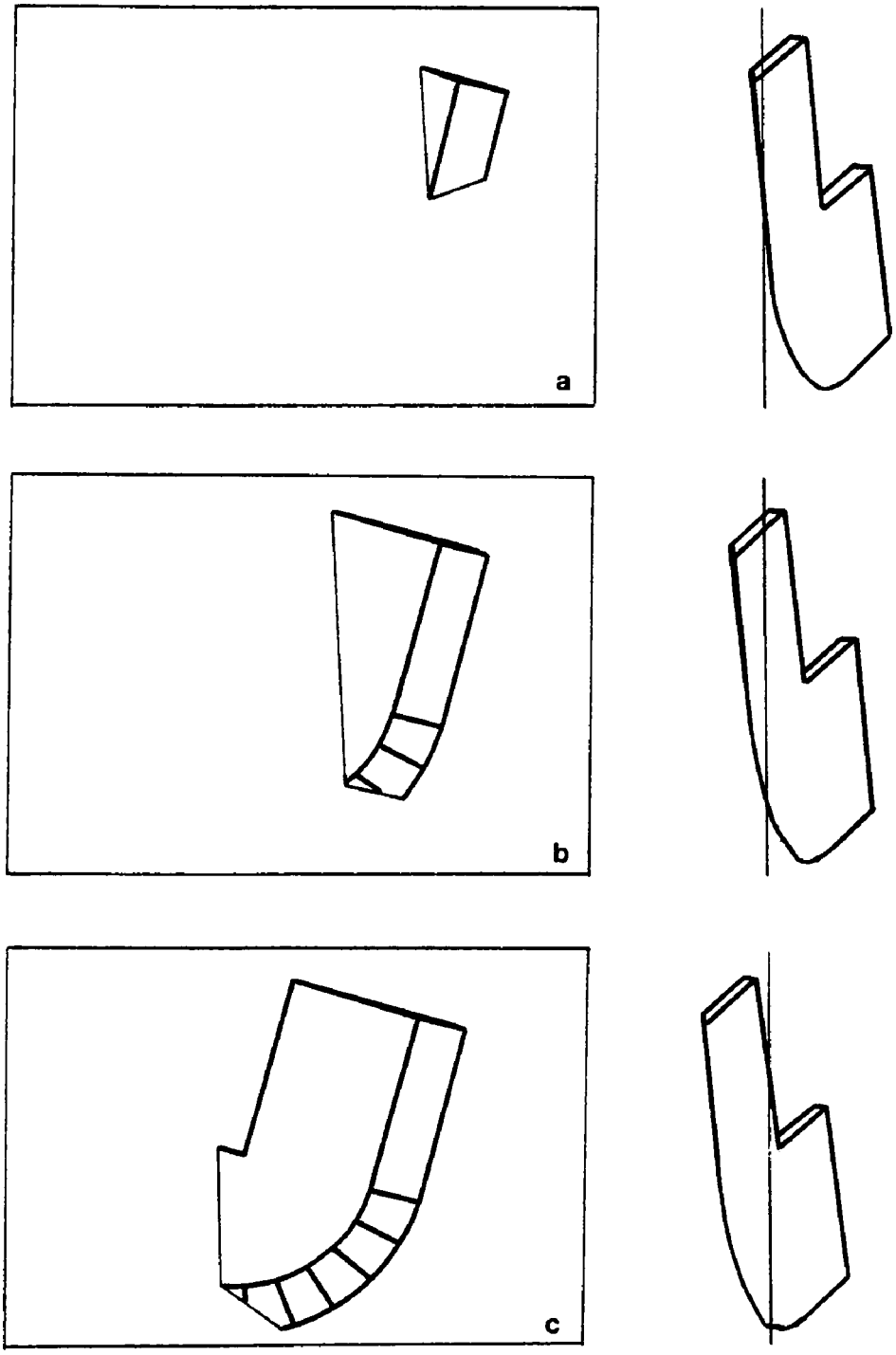

Figure 15: Simulation of the progressive tool/work engagement at ε_i=-20°.

initial contact between the tool and the workpiece occurs inside the land area, away from the major or minor cutting edges. At some of these ε_i values, ($\varepsilon_i = 0° \pm 5°$) it could be seen that a substantial part of the chip cross section was intercepted and contacted by the K-land before either major or minor cutting edges had entered the cut. The computer simulation confirmed that the tool/workpiece intersection on the region around the tool nose becomes a curve rather than a straight line, because of the surface of revolution introduced by the K-land. As the range of ε_i values was varied in both sign directions, the inclination of the intersection curve varied considerably and the initial contact point shifted to positions on the minor and major cutting edges. The variation in initial contact location and its progress is shown in Figures 16, 17 and 18 for three widely spaced values of ε_i. For each figure, the top part of the figure shows two views. These two views correspond to the front view (a) of the tool breaking through the plane of engagement (viewed in a direction perpendicular to the plane of engagement) and the side view (b) of the same system. These views were extracted from the graphic system. The bottom part of the figure shows a condensed view of initial contact and its progress. The view basically shows a tool on which the intersection curves resulting from incremental rotations of the cutter relative to the workpiece have been superimposed. These intersection curves were reproduced from hard copy prints of the simulation carried out on the graphic system. To aid

in the interpretation and the identification of initial contact point, the area of the tool that will intercept the chip cross section, given a feed/tooth less than the width of the K-land, has been superimposed on the tool with dashed lines. Also, to introduce consistency in the representation for different values of ε_i, the view is taken perpendicular to the reference plane passing through the cutter's center of rotation and the tip of the tool.

Figure 16: ε_i=-30°

This figure illustrates the type of contact condition obtained when the center line of the face mill is placed above the workpiece's plane of engagement, resulting in an angle of engagement ε_i=-30°. The side view b) of the tool's attitude relative to the workpiece shows clearly that the chip will be generated from the top down, as initial contact starts on a point located at the depth of cut line. View c) shows different stages of the intersection curve as tool/workpiece contact progresses. If it is viewed in the context of Kronenberg and Opitz's trials with carbide and HSS tools, this type of contact corresponds to a "T" type of contact. Now in the experiments reported by various researchers [25,30,35,36] and discussed in section 3.4, this type of contact does not seem to be detrimental to the tool life. It remains to be seen whether it is the case for ceramic tools.

Figure 17: ε_i=0°

This figure illustrates the type of contact obtained when the centerline of the cutter coincides with the workpiece's plane of engagement, resulting in an angle of engagement ε_i=0. Side view b) shows a tool's position relative to the workpiece where the entire cutting edge is trailing the K-land, almost parallel to the plane of engagement. It is clear that this angle of engagement will result in an initial contact point inside the K-land. View c) shows that the initial curve of contact is located entirely inside the K-land and more important, better than half of the chip cross section is intercepted by the K-land before the two extreme points on the major (depth of cut line) and minor (point tangent to the machined surface) cutting edges come into contact with the plane of engagement. Again, within the context of the experiments reported in section 3.4, this type of contact would correspond to a 'u' contact and seems to be very favorable.

Figure 18: ε_i=50°

This figure illustrates the type of contact obtained when the center line of the cutter is below the workpiece's plane of engagement, resulting in an angle of engagement ε_i=50°. Side view b) shows a tool's position relative to the workpiece where the minor cutting edge is leading the rest of the tool and will clearly be the first part of the tool to make contact with the workpiece's plane of engagement. Note from view c) that the edge of the tool (its periphery)

comes into contact with the workpiece instantly and continues to be in contact until full engagement is reached. The first contact point is located on the minor cutting edge and the last point on the tool to enter the cut is the point on the major cutting edge located at the depth of cut line. Between these two instants, the cutting edge is continuously involved in the cut. Within the context of the experiments reported in section 3.4, this type of contact would correspond to a "v" type of contact and seems to be very unfavorable. The hypothesis is that the periphery of the cutting edge, and intuitively, its most fragile part comes into contact with the workpiece instantly and bears the brunt of the impact. If this hypothesis is valid, ceramic tools should be very sensitive to this type of impact.

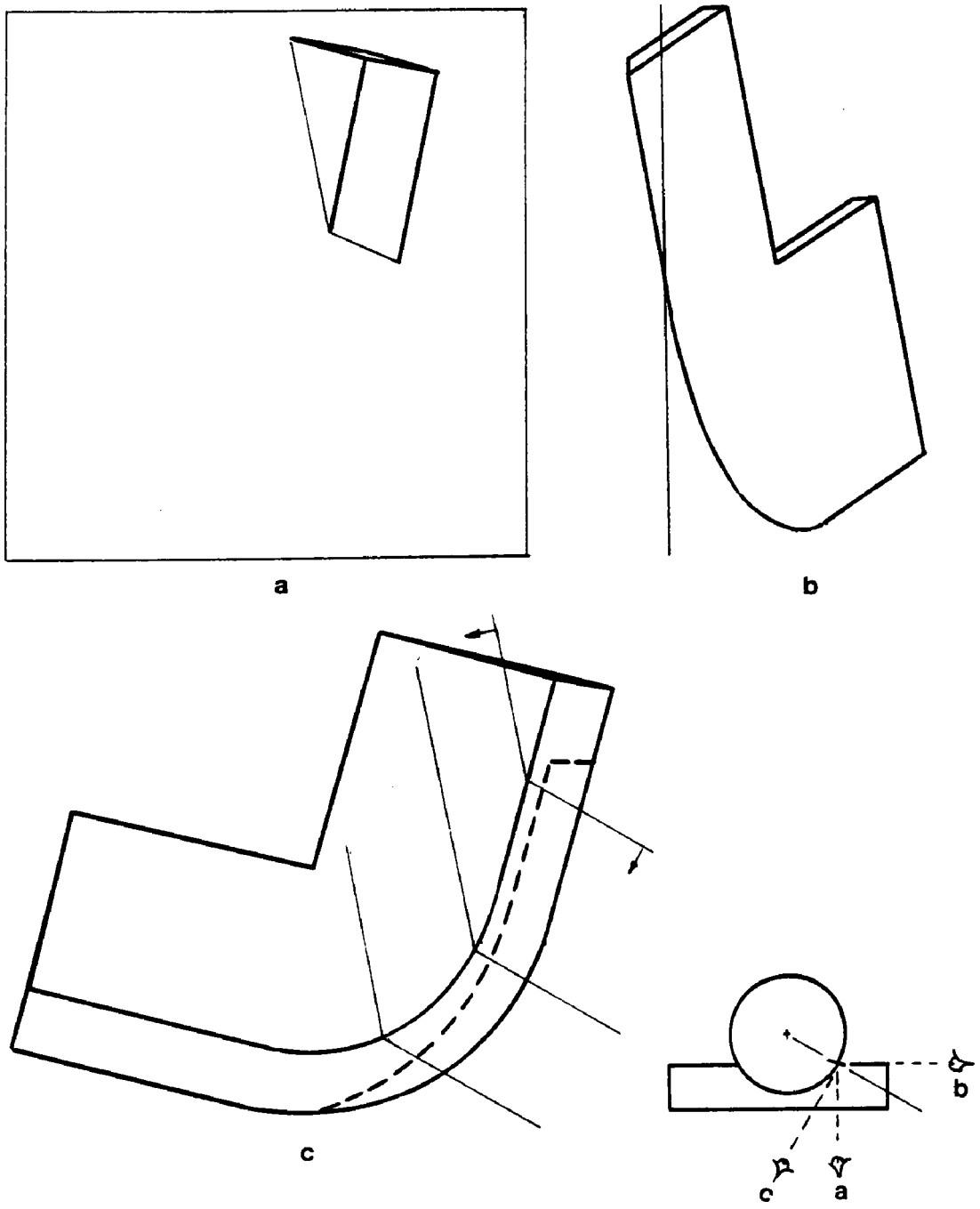

Figure 16: Tool/work intersection curves for ε_i=-30°.

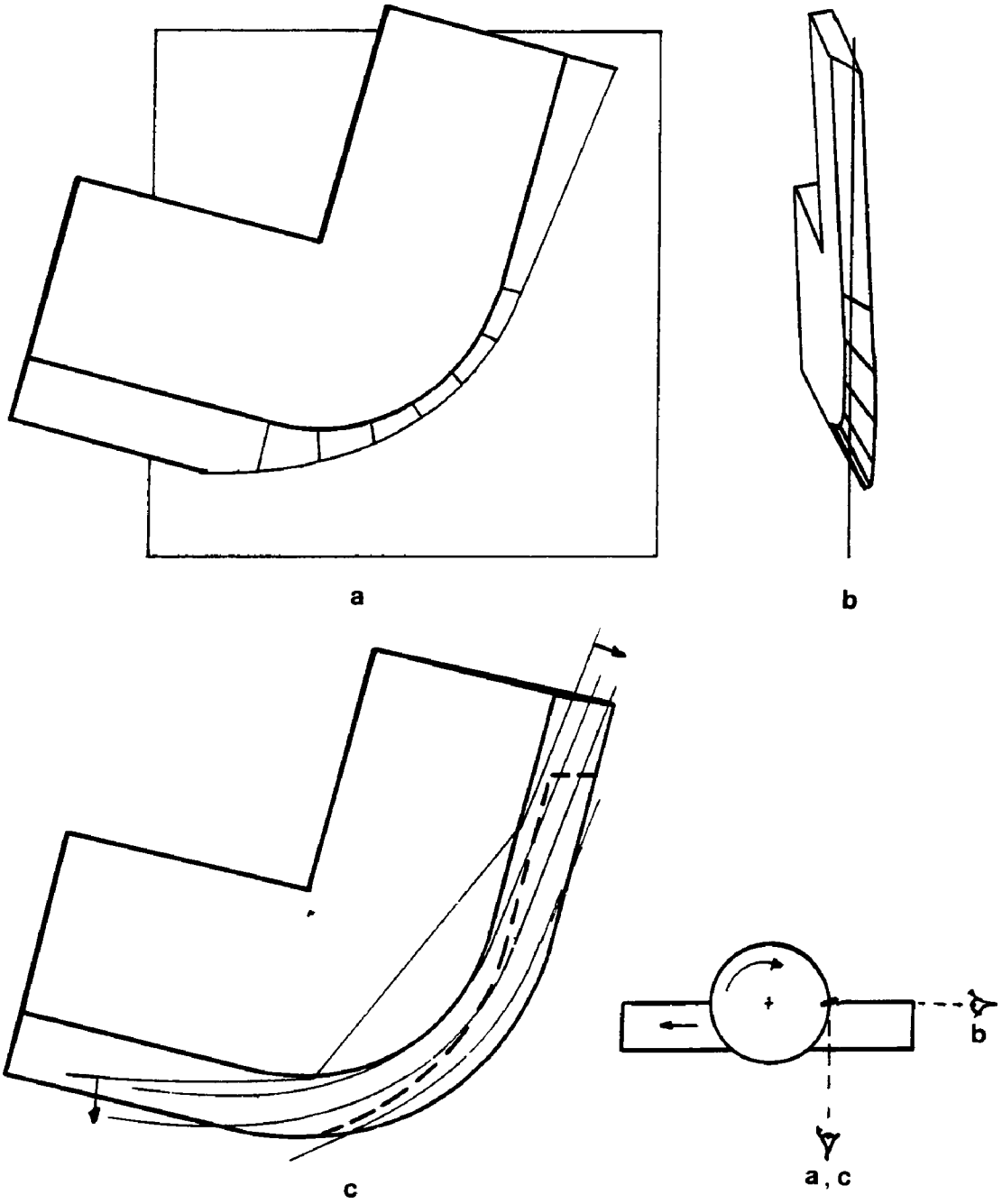

Figure 17: Tool/work intersection curves for ε_i=0°.

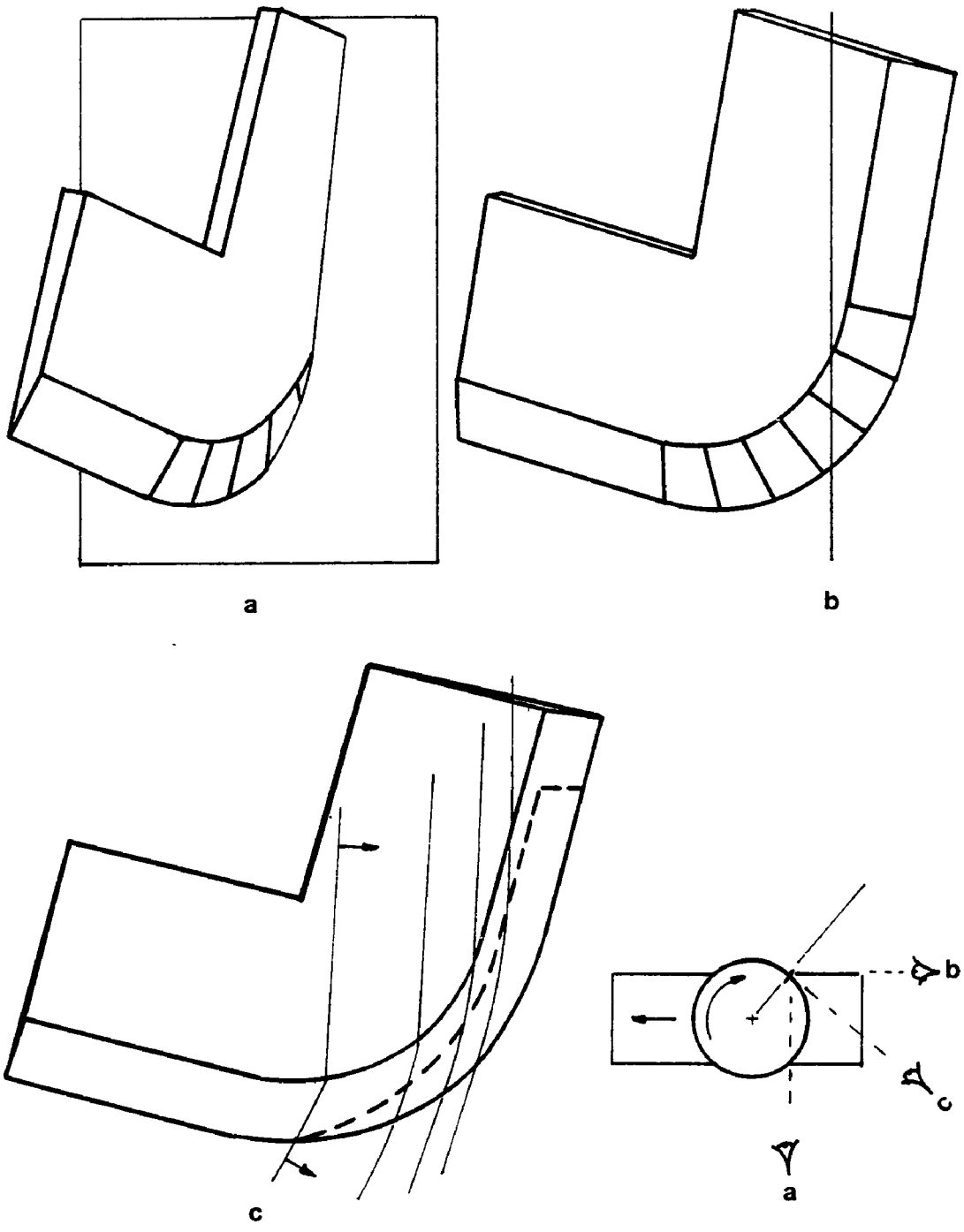

Figure 18: Tool/work intersection curves for ε_i=50°.

4.2.4 Comparison between edge preparations

In addition to SNG-433 tools having a .008x20° K land, tools in an SNG-433 configuration having a hone (.001-.002 in) rather than a K-land were also available for testing. Since the face of these tools remains planar, it is not necessary to use the graphic system in order to visualize the type of contact they make with the plane of engagement. Kronenberg's analysis for the determination of initial contact can be applied directly to these tools; and since the contact curves for the K-land tool can be obtained in a reference plane similar to that used in Kronenberg's analysis, a direct comparison is possible. The similarities and differences between the two edge preparations are summarized below.

- As ε_i varies from large negative values to large positive ones, tools with a K-land or a honed edge go essentially through the same types of contact conditions. When held in a double negative cutter, both edges are capable of initial contact at the depth of cut line (T), initial contact in the face of the tool (U) as well as initial contact on the minor cutting edge (V).

- Although these two edge preparations are capable of similar contact types when held in a common face mill, similar contact types will happen at different values of ε_i for the two tools. This is illustrated in figure 19. Figure 19 shows the cross section of the chip that will be intercepted by the tools. The intersection curves for different tools and different values of ε_i have been superposed on

the chip cross section. Note that for ε_i=-20°, the honed tool is making "T" contact (at the depth of cut line) while the K-land tool is still making contact inside the face of the tool. Therefore, by virtue of the change in axial and radial rake angles introduced by the land, a K-land tool has a theoretically wider range of "U" type of contact than a tool with just a hone.

- By virtue of the surface of revolution around its nose, a K-land tool has a curved intersection with the plane of engagement in this area. The result is that a K-land tool, compared to a tool with no edge preparation, is capable of a "U" type of contact where a much larger area of the chip cross section is intercepted inside the body of the tool, before either minor or major cutting edges come into contact with the work. This difference can also be seen in figure 19.

4.2.5 Implications for the experiments

The computer graphic simulation of the type of initial contact a K-land tool makes with the plane of engagement shows that for a given face mill diameter and rake angles, considerable variation in initial contact condition can be obtained through the variation of the angle of engagement ε_i. Furthermore, the computer simulation shows that there exists a range of ε_i values which result in an initial contact occurring inside the K-land of the tool, away from the major and minor cutting edges. Given the brittleness of ceramic

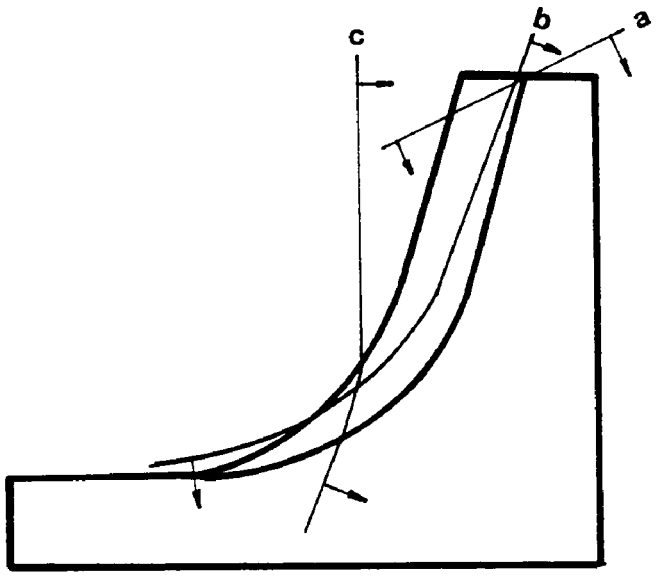

K-land tool

a. $\varepsilon_i = -20°$

b. $\varepsilon_i = 0°$

c. $\varepsilon_i = 50°$

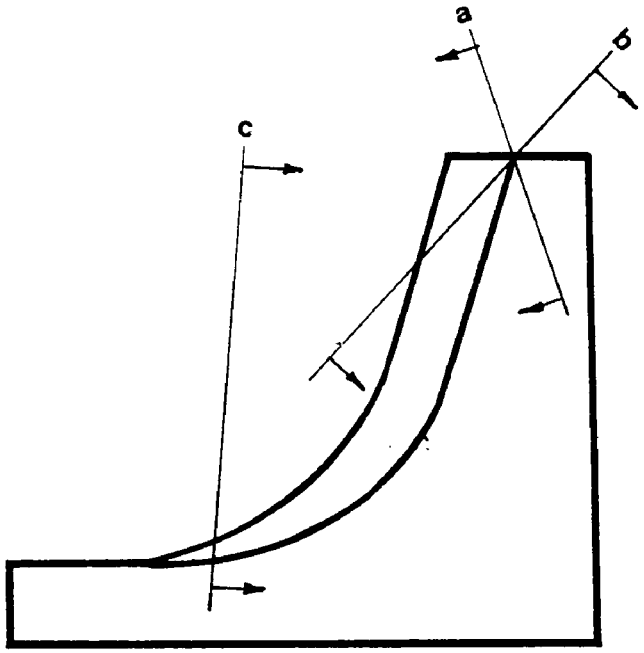

honed tool

a. $\varepsilon_i = -20°$

b. $\varepsilon_i = 0°$

c. $\varepsilon_i = 50°$

Figure 19: Tool/work intersection curves for two different edge preparations.

tools, the emphasis of the tests should be an investigation of the influence of initial contact location and progress on the performance of silicon nitride based tools. The same investigation should be extended to a tool with no K-land preparation since it was also seen, through the application of Kronenberg's analysis that there exists a narrow range of ε_i values which will cause initial contact to occur inside the face of the tool.

Keeping in mind the possible damage due to the tool's exit conditions as described by Pekelharing et al. [27,30,32,33,34], the tests should also seek to distinguish between entry and exit failure if it is possible.

5. EXPERIMENTAL EVALUATION

5.1 Previous Work

A literature search on the subject of face milling with ceramic tools revealed only scant attempts to evaluate their performance. Shortly after Kronenberg [26] published his ideas about cutter entry conditions in face milling, Krabacher and Haggerty [38] reported on some turning and milling tests with ceramic tools. The tests report on machining cast iron with some unidentified grade of ceramic. A ceramic tool with a sharp edge and one with a .08 mm x 45° K-land were used. The tests use ε_i as the independent variable and are summarized in a 32 mm x 45 mm graph. Axial and radial rakes are said to be both negative and equal to -5°. The performance of the tool with the sharp edge is shown to peak (1 data point) at $\varepsilon_i \simeq -12°$ and the authors claim that good tool life can be produced only for $-20° < \varepsilon_i < -10°$, and that this range of ε_i values results in a "u" type of contact. This interpretation does not seem to be correct since for $-20° < \varepsilon_i < -10°$, Kronenberg's analysis shows that an SNG-434 tool with $\gamma_a = \gamma_r = -5°$ will make a "T" type of contact. "U" contact is only possible for $\varepsilon_i > \gamma_r$ and in this case, $\varepsilon_i > -5°$. On either side of $\varepsilon_i \simeq -12°$, tool performance decreases sharply. Since the authors do not provide any information concerning the cutter diameter, width of the workpiece, types of tool failure and experimental procedure, it is very difficult to evaluate the performance of the sharp tool within the context of entry, exit and other potentially harmful effects. In

contrast to the sharp tool edge, the tool with the .08 mm x 45° K-land is shown to be much less sensitive to ε_i. The author's reasoning is that tool performance is better since by virtue of the 45° bevel put on the tool, the cutting edge is always trailing the face of the tool and therefore will not contact the work first. While this is true for a certain range of ε_i value, it will be seen later on that as ε_i increases beyond a certain value, this will no longer be true. Furthermore, while the initial contact point is important, the manner in which contact progresses until full engagement is reached seems to be much more important according to Opitz and Beckhauss [36]. Again, the lack of cutter diameter/workpiece width make it difficult to evaluate these tests.

Another attempt to determine the milling performance of ceramic based tools was reported byOkushima and Hoshi [39]. Their approach to the problem was based on the assumption that there existed a K-land width necessary to prevent ceramic breakage in face milling. The tests were carried out on steel workpieces and the independent variables included cutter diameter (2 levels: 94mm and 393mm), radial rake (3 levels: 15°, 5°, -5°) and width of land (3 levels: .1 mm, .2 mm, .3 mm). Axial rake was negative (-5°) and workpiece width was 90 mm. The two cutter diameters used resulted in two angles of engagement equal to 73° and 13,5° for the small and large cutter respectively. The authors conclude that for large angles of engagement, a small width of the land is preferable to a larger one, and for small angles of engagement, a strong edge (wide land and negative

axial rake) performs better than a weak one (positive radial rake and small land width). However, they also conclude at the end of the paper that for the 73° angle of engagement, good tool performance is severely limited by the amount of plastic deformation taking place. Indeed, the method used to grind the land on the tools results in a land angle at least equal to 45°. It is therefore not surprising that large land widths of this nature, used with double negative cutters result in poor tool life. In contrast, the performance of the tools in the larger diameter cutter shows some interesting features. Tools with a +5° or -5° radial rake and 45° land angle show a steady performance of 2000-3000 cutter revolutions (50-75 cm of cutter travel) until failure for the .1 mm, .2 mm and .3 mm land widths under test. The tools with a 15° radial rake show instantaneous failure for a .1 mm land width and better than 2000 cutter revolutions (50 cm of cutter travel) when the land width is .3 mm. Feed per tooth was .25 mm. This tool was modelled on the graphic system to investigate the type of contact it made with the workpiece. The authors state in their paper that the 15° radial rake is produced on the tool by grinding a groove, parallel to the cutting edge of the tool, at the desired angle. The tool geometry was reproduced on the graphic system as closely as possible, and the working portion of this tool is reproduced in figure 20(a). Figure 20(b) shows the resulting intersection curve between the .3 mm K-land and the workpiece, as the tool breaks through the plane

of engagement at ε_i = 13.5°. Note that since the feed per tooth (.25 mm) is smaller than the width of the K-land (.3 mm), contact is restricted to the K-land. Figure 20(b) clearly shows that the intersection curve is contained completely inside the K-land, and that therefore, initial contact happens inside the land of the tool. Note that as the tool continues its progressive engagement, the intersection curve will be moving parallel to itself, and the periphery of the tool will be the last part to engage the workpiece. The presence of the K-land has therefore nullified the effect of the positive 15° radial rake on contact and brought the tool's performance up to par with the stronger (-5°, +5° radial rakes) tool shapes. Finally, these tests fall short of recognizing the importance of initial contact between the tool and the workpiece. The ε_i values (13.5° and 73°) resulting from the use of two different cutter diameters are clearly not enough in order to bring out the effect of initial contact.

Extensive testing of ceramic tools on cast iron and steel was also reported by A.O. Schmidt et al. [40]. Their report presents tests carried out over a number of years. Most of the ceramic tools were specially prepared with a diamond hone to produce a .076 mm x 45° land. Within the context of ceramic tool performance under interrupted cutting and the potential influence of tool/workpiece initial contact, these tests do not offer much information. The test conditions show that a 142.8 mm cutter diameter was used on

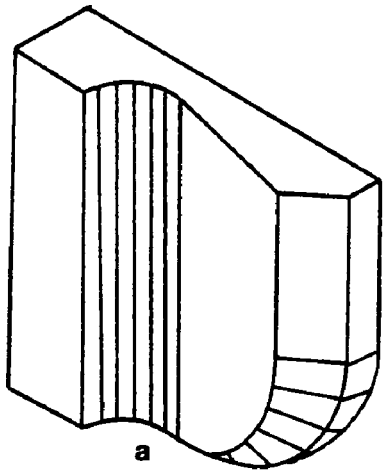

Figure 20: Modelling of tool used by Okushima and Hoshi [30]

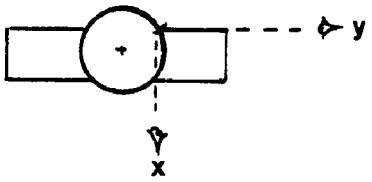

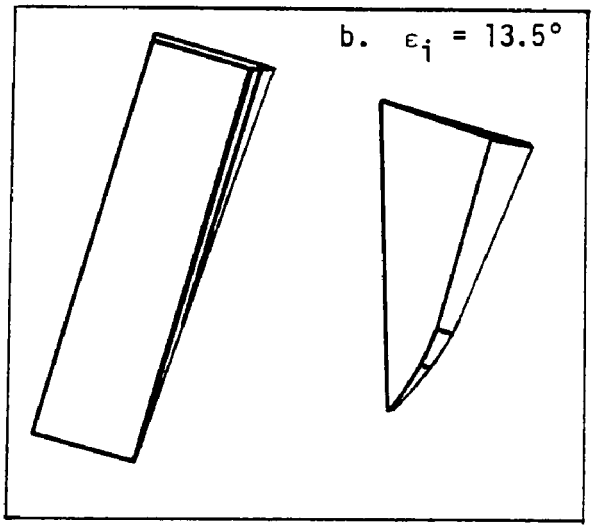

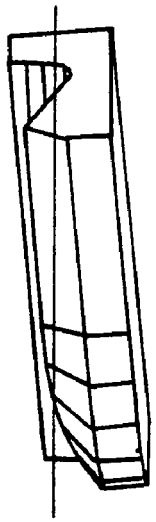

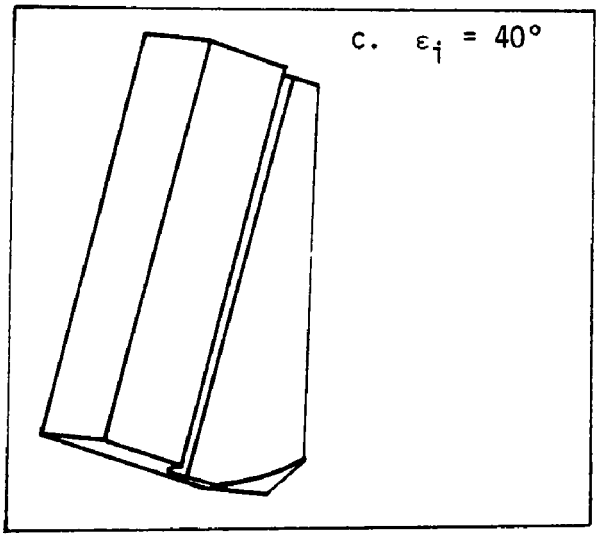

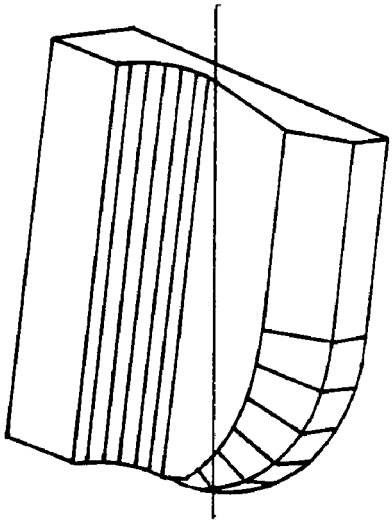

139.7 mm wide workpieces. Cutter position was central and the feed range was from .063 to .152 mm/tooth. The central position of the cutter results in an angle of engagement ε_i = 78°. Under the largest feed condition of .152 mm/tooth, it can be shown that for ε_i = 78°, the chip thickness at entry, although uncorrected for the thinning effect due to the corner angle, reduces to 20% of the nominal feed valve and is equal to .031 mm. Under these conditions, it can be seen that impact at entry is practically negligible and this test feature may very well have been intentional in order to facilitate the entry of ceramic tools into the cut. Still, the authors report that catastrophic failures were very frequent.

In the tests reviewed above, it seems therefore, that only Krabacher and Haggerty [38] attempted the use of ε_i as an independent variable. The use of a 45° land angle and the lack of test data concerning the cutter diameter and work width make their results difficult to assess.

5.2 Case #1: Tool with No Edge Preparation

The silicon nitride tool grades available for the study in an SNG 433 configuration came in two different edge preparations. One of the preparations consisted of a standard (.2 mm x 20°) K-land ground around the periphery. The other type of tool had only a lightly honed radius (.025-.05 mm) around the periphery. For this type of tool, Kronenberg's analysis is applicable and the following tests attempt to determine if premature tool failure can be avoided through careful control of entry and exit conditions.

5.2.1 Experimental approach and equipment

When a rectangular workpiece is to be face milled, the position and size of the face milling cutter relative to the work will determine the variety of entry and exit modes the cutting tool will see during one full pass over the workpiece. In figure 21(a), it can be seen that the tool will first enter and exit out of plane (a).

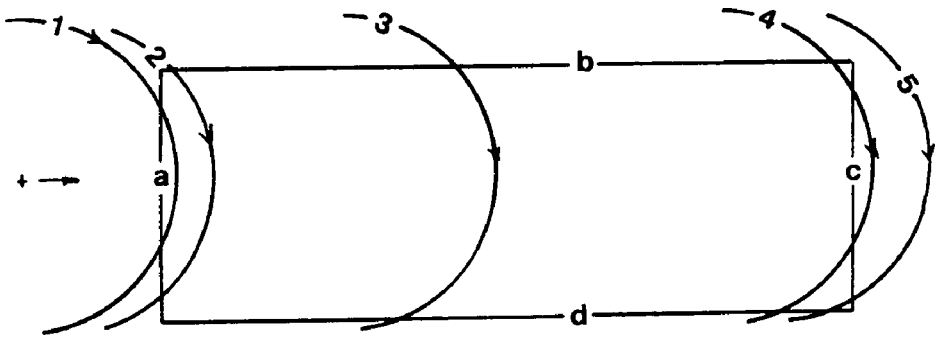

Fig. 21(a): Entry/Exit with a Rectangular Workpiece

the plane perpendicular to the feed motion. As the cutter advances to position (2), the tool is now entering the cut on plane (b) and still exiting out of plane (a). When the cutter reaches position (3), the tool enters through plane (b) and exits out of plane (d). It will continue to do so until the cutter reaches position (4) where the tool still enters through plane (b), exits out of plane (c), re-enters through plane (c) and exist again out of plane (d).

Finally, when the cutter reaches position (5), it will enter through plane (c) and exit out of (d). A change in the relative position of cutter and workpiece will result in a different sequence. It can be seen that the only part of the workpiece where entrance and exit are constant as the cutter advances is the middle part. To guard against the confounding of different entrance/exit conditions during one pass of the cutter, it was decided to confine the tests to the middle section of the workpiece where entrance and exit conditions remain constant. To achieve this, every workpiece is precut with a sharp carbide blade far enough to eliminate the possible entry or exit through plane (a). The variation at the other end of the workpiece is dealt with by disengaging the cut before the cutter reaches the point where it can enter or exit through plane (c). The resulting useful length (L) of the workpiece is shown in figure 21(b).

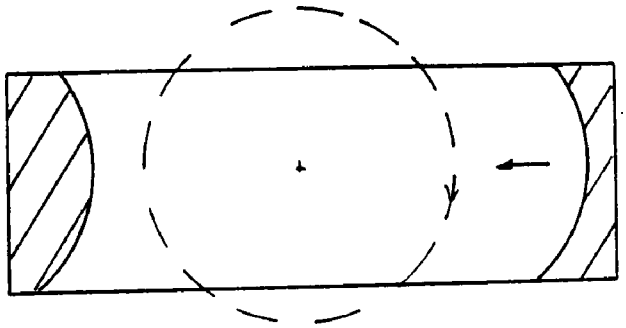

Fig. 21(b): Workpiece Preparation

The equipment used for the face milling tests contained the following elements.

Milling machine: The milling machine used is a Cincinnati vertical knee-and-column type milling machine. The machine is rated at 7.5 h.p. Spindle speed range varies from 20 to 1500 RPM in finite progressive steps. Feed range is from 12.7 to 508 mm/min also in finite progressive steps and with the capability of doubling each valve. A plain milling machine vise was secured to the table and used to clamp the work.

Face mill: Niagara double negative face mill, with 8 pockets accommodating 12.7 mm (.5 in) square negative disposable inserts. The cutter has a 101.6 mm (4 in) diameter and the cutter angles were quoted by the manufacturer to have the following values;

axial rake γ_a = -5.0°

radial rake γ_r = -5.6°

corner angle C = +15°

Toolmaker's microscope: A Fowler Instruments microscope was available for tool observation and for measurement. The instrument has x50 magnification and a table movement resolution in graduations of .001 mm. No attempts was made to calibrate the instrument for any tests carried out.

5.2.2 Initial tests

These tests sought to investigate the influence of the angle of engagement ε_i when using SNG-433 silicon nitride based tools to face mill steel workpieces. In selecting the values of the independent

variable ε_i, Kronenberg's analysis was used to ensure that different types of initial contacts were present. The target values of the independent variable were ε_i = -22°, +7.2° and 30° representing respectively a T, U and V type of contact. More values were added later as the tests progressed. The speed, feed and depth of cut were chosen following exploratory tests so that there would be an easily measurable tool life at some of the ε_i values. Workpieces 38.1 mm wide were used and the ε_i values were obtained by offsetting the cutter center by a distance d_i from the workpiece's plane of engagement such that $\varepsilon_i = \sin^{-1}(2d_i/\phi)$ where ϕ = face mill diameter.

Work material: 4340 steel, hot rolled, 28 R_C.
44.5 mm wide x 152.5 long x 127 mm deep.

Face mill: 101.6 mm diameter
axial rake γ_a = -5°
radial rake γ_r = -5.6
corner angle C = 15°

Cutting conditions: Speed: 164.5 m/min
Feed: .18 mm/tooth
Depth: 1.52 mm

Independent variables:

angle of engagement ε_i = -22°, 7.2°, 14.5°, 18.2°, 22°, 30°,48.5°

Tool material: - SNT Grade
- AY6 Grade

both tool grades came in an SNG-433 configuration with a .025-.05 mm hone on the edge.

Dependent variable: Tool life.

Tool life was measured as the total distance travelled by the cutter to tool failure. Tool failure was reached when the cutter ceased to cut. With ceramic tools, this invariably meant the point at which the edge was completely chipped out or at which catastrophic failure occurred.

note: For ε_i = -22°, a workpiece 25.4 mm was used so that successive passes would not cause the tool to rub against a workpiece wall.

Because of the preparatory operation needed to start the cut, as well as the set up operation needed to fix an ε_i value, the tests were not completely randomized. Instead, an ε_i value was picked, workpiece(s) prepared and all data points at that ε_i value were taken with the tool grades and replicates randomly allocated. The procedure was followed until all ε_i values were run.

Table 1 gives the distances travelled until tool failure and the averages at each ε_i level are plotted in figure 22.

Observations:

Although all tools ultimately failed through edge fracture, there were some distinct differences in the type of fractures that occurred.

TABLE 1: DISTANCE TRAVELLED (CM) UNTIL FAILURE. VARIABLE EXIT ε_o.

$\varepsilon_i \rightarrow$		-22.0°	+7.2	+14.5	+18.2	+22.0	+30.0	+48.5
SNT-H		89.0	207.0	111.1	2.5	1.9	3.8	1.5
		48.2	233.7	134.6	3.2	2.0	1.3	1.0
		68.6	198.1	96.5	3.8	1.5	2.5	1.5
						1.9	2.0	2.0
	$\bar{x}$	68.6	213.0	114.0	3.2	1.8	2.4	1.5
AY6-H		30.5	47.0	62.2	10.8	2.5	2.5	1.0
		43.2	53.3	48.3	6.1	1.9	8.9	2.0
		38.1	61.0	57.2	14.0	1.9	1.3	1.5
						2.5	2.5	2.0
	$\bar{x}$	37.3	53.8	55.9	10.3	2.2	3.8	1.6

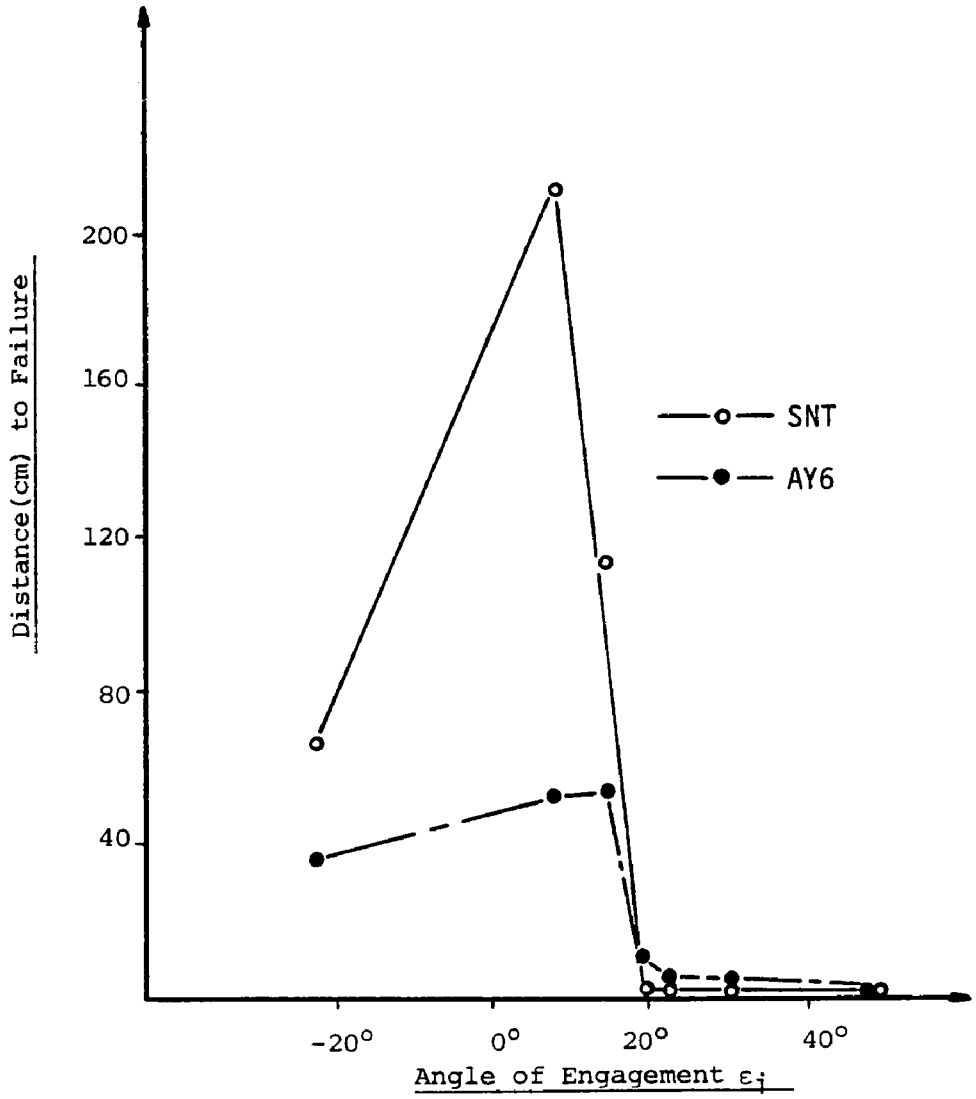

Figure 22: Tool performance vs. angle of engagement.
Initial tests with honed tools on 4340 steel.

SNT grade: At ε_i = -22°, the tools developed a crack which seemed to start at the depth of cut line and extended to the face of the tool. Fracture usually followed and involved the whole cutting edge. Crater wear had started developing.

At ε_i = 7.2°, the tools exhibited a smooth type of flank wear, and continued to cut even though a large crater developed. Failure resulted when the crater reached the edge of the tool.

At ε_i = 14.5°, the tool exhibited the same behavior as for ε_i = 7.2° but then failed suddenly through a fracture of the cutting edge before the crater reached the edge.

For $\varepsilon_i \geq$ 18.2, the tools invariably fractured in an area below the depth of cut line but above the nose radius. The fracture occurred very quickly and always at the same spot. No evidence of crater or cracks was visible on the unfractured area of the tool.

AY6 Grade: For $\varepsilon_i \leq$ 14.5°, the AY6 developed a large crater and fracture involving the whole length of the cutting edge followed. Sometimes, a crack running parallel to the cutting edge, in the center of the crater can be seen prior to fracture.

For $\varepsilon_i \geq$18.2, the AY6 tools failed in a manner identical to the SNT grade tools. Fracture was in the same area and of the same type.

Discussion:

On the basis of this experiment, the following conclusions seem appropriate:

- When failure was not premature, the AY6 grade seemed to crater and wear much more rapidly than the SNT grade. For $\varepsilon_i \leq 14.5°$, crater for this grade seems to be responsible for tool life termination.

- The SNT grade showed its best performance at $\varepsilon_i = 7.2°$. Note that this angle of engagement results in initial contact in the face of the tool (U type of contact) and tool life termination seems to have been invaraibly caused by the crater reaching the edge of the tool. In contrast, an angle of engagement of $\varepsilon_i = -22°$ which results in initial contact at the depth of cut line (type T contact) seems to be responsible for the crack development at the depth of the cut line and subsequent failure.

- The negligible tool life, irrespective of tool grade, which characterized the tool performance for $\varepsilon_i \geq 18.2°$ cannot be explained in terms of the independent variable ε_i. Indeed, keeping in mind the potentially harmful effect of the exit angle ε_o exposed by Pekelharing and others [27,30,33,34], it seems that the criticism applied to the experiments of Lucht and Kronenberg in sections 3-4-1 and 2 also applies to this experiment. By keeping the width of the workpiece constant and offsetting the cutter center with respect to the plane of engagement in order to set higher ε_i values, the exit angle ε_o is also systematically varied. The values of ε_i and corresponding ε_o at the test points are listed below.

ε_i	-22.0°	7.2°	14.5°	18.2°	22.0°	30.0°	48.5°
ε_o	61.0°	48.5°	38.7°	34.2°	30.0°	22.0°	7.2°

Note that as ε_i increases, ε_o decreases and certainly ε_o = 7.2° is well inside the range of harmful exit angles observed by Pekelharing in the face milling of steel with carbide tools. While a direct comparison is not possible, the possibility remains that as ε_i increases, the potential effects of entry andexit become confounded. The need, therefore, exists for an experiment that will ensure that these effects are separated. Only then can a statement be made on the potential effect of a V type of contact on tool performance.

- Even though the failure mechanism operating for $\varepsilon_i \geq$ 18.2° is not clear at this point, the plot shows clearly that indiscriminate testing of different tool grades in this range of ε_i values will mask the potential differences between the grades.

5.2.3 Revised tests

The tests described in section 5.2.2 resulted in a possible confounding of the effects of ε_i and ε_o over the range of ε_i values greater or equal to 18.2°. An easy way to dissociate these effects is to manipulate the widths of the workpieces at each data point in order to control the value of ε_o. In the previous tests, the SNT grade performed best at ε_i=7.2°. Associated with this data point was an ε_o=48.5°. There was no chipping or premature failure

of the tool under these conditions and tool life was terminated strictly by the crater wear. So the value of ε_o = 48.5° seems to have no adverse effect and it was selected as the minimum value for the new tests. Indeed, when viewed in the light of Pekelharing's tests [34], this type of exit seems to be located well beyond the dangerous exit zone.

Since the first tests showed that the AY6 grade was very prone to cratering when machining steel, this grade was dropped from consideration since it was felt that no additional information could be gained by running it again.

The test points selected are listed below with the associated ε_o and workpiece width (w) values.

ε_i	-22.0°	7.2°	14.5°	22°	30°	38.7°	48.5°
w(mm)	25.4	44.5	50.8	63.5	63.5	76.2	76.2
ε_o	61°	48.5°	48.5°	61°	48.5°	61°	48.5°

Note that this scheme results in different values of the arc of contact between the tool and the workpiece but there is no evidence to suggest that this has any influence on premature tool failure. Different lengths of the arc of cut will probably result in different heating/cooling cycles of the tool. These heating/cooling cycles can have an influence on the type of thermal cracking in ceramic tools, but thermal cracking is not known to cause premature tool failure through catastrophic breakage.

Except for the width of cut modifications introduced at the present test points, all other test conditions and procedures prevailing in section 5.1.2 were used in the revised test. For comparative purposes, an SNT grade tool with a K-land was also run at some selected data points but will not be considered in this discussion.

Table 2 shows the distance travelled until tool failure for the SNT-grade (honed tools) and figure 23 shows a plot of the average values for this test and the earlier test.

Discussion:

The plots in figure 23 show that as the exit angle ε_o was increased to a value $\geq$ 48.5°, a substantial increase in tool life resulted at ε_i = 14.5°, 22° and 30°. The sudden and quick failures below the depth of cut line characteristic of $\varepsilon_i \geq 18.2$ in the previous test were not encountered. The initial tests with ε_o variable can then be interpreted as follows:

- For $\varepsilon_i \leq 7.2°$, the data points show the influence of the angle of engagement ε_i.
- For $\varepsilon_i > 7.2°$, it seems clear that the effect of ε_i and that of ε_o are confounded, and very likely that ε_o is the dominant cause of failure.

On the assumption that the different widths of the arc of cut, resulting from the variation in workpiece widths introduced in the revised tests, have no effect on tool breakage, the revised tests can be

TABLE 2: DISTANCE TRAVELLED (CM) UNTIL FAILURE.
CONSTANT EXIT CONDITIONS ε_o=48.5°.

	$\varepsilon_i \rightarrow$	-22.0	+7.2	+14.5	+22.0	+30.0	+38.7	+48.5
SNT-H		76.2	160.0	219.7	68.6	63.5	15.2	1.3
		88.9	198.1	193.4	139.7	71.1	7.6	5.1
		57.2	209.6	102.9	86.4	88.9	20.3	3.8
		71.2	193.0	165.1	101.6	76.2	12.7	5.1
	$\bar{x}$	73.4	190.2	170.3	99.1	74.9	14.0	3.8
SNT-K		284.5	381.0			139.7		2.0
		406.5	329.0			97.8		3.8
		393.7	343.0			158.8		1.3
	$\bar{x}$	360.7	350.5			132.0		2.3

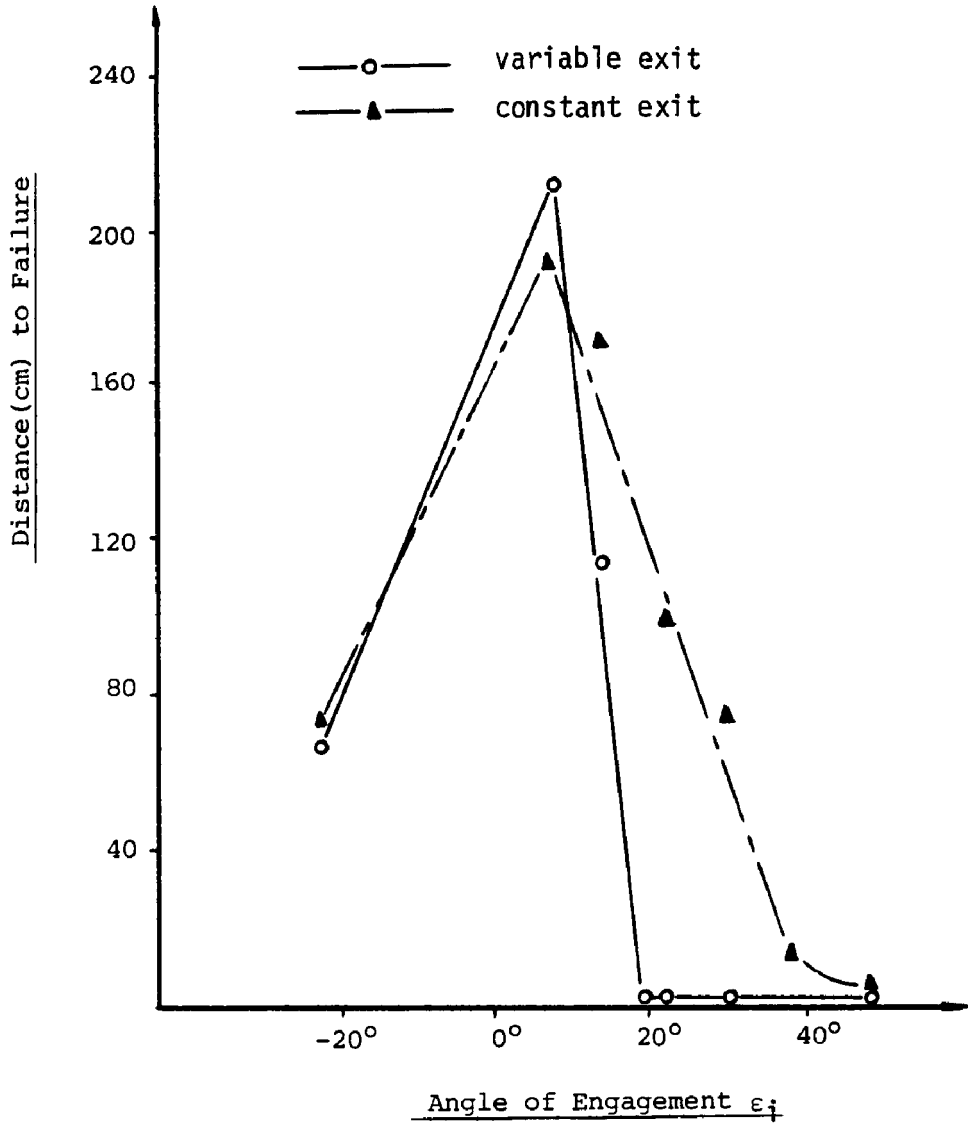

Figure 23: Tool performance vs. angle of engagement.
Revised tests with honed tools on 4340 steel.

considered to show the influence of the angle of engagement ε_i on tool performance. The following conclusions can then be drawn:

- At ε_i=-22°, initial contact on the major cutting edge at the depth of cut line results in premature tool failure. In both tests, this data point was characterized by the development of a visible crack at the depth of cut line and subsequent catastrophic failure of the whole cutting edge.
- At ε_i=7.2 and ε_i=14.5, initial contact correspond to a U and V type of contact respectively. Tool performance at these two data points is best, with no chipping or breakage. Except for one tool fracture (at ε_i=14.5°) after 102.9 cm of travel, all data points taken at these two ε_i values exhibited a tool life terminated strictly by the crater reaching the edge of the tool.
- As ε_i increased above 14.5°, tool life decreased drastically to become negligible at ε_i=48.5°. Tool failure shifted from a failure dominated by the cratering rate to one where small chipping appeared in the region where the tool nose meets the major cutting edge. This chipping progressed rapidly to include the whole cutting edge and frequently led to a total edge fracture. This progression could easily be followed at ε_i=22° and 30° but failure was rather quick at the last two ε_i values. It does seem therefore that as V contact becomes more pronounced, making the inclination of the tool/workpiece

intersection line more vertical and thus bringing the periphery of the cutting edge into immediate contact with the work at entry, the tool life deteriorates quickly and the ceramic edge is not able to withstand interrupted cutting for long.

5.2.4 Exit breakage boundary

The immediate breakage caused under certain ε_0 angles at the cutting conditions used in the initial tests was investigated further by recalling that Loladze [20] theorized that there must be a so-called "breaking feed" that creates stresses which the tool cannot withstand. Loladze's photoelastic studies also showed that the stresses on the tool are intensified at the exit phase. Pekelharing [27] blamed the so-called "negative shear" formation for the exit failure of carbide tools. In the experiments reported by Pekelharing et al. [33,34], it is not clear whether feed adjustments were made so that the chip thickness at exit was constant for different values of the exit angle ε_0. It seemed interesting therefore to investigate the influence of the chip thickness on the exit breakage and to see whether there was a value of the chip thickness that would not cause failure irrespective of the angle of exit ε_0. In other words, a breakage boundary was sought in function of three independent variables: feed, speed and exit angle. To construct such a test, the influence of the angle of engagement ε_i has to be

controlled. Since the experiments in sections 5.2.2 and 5.2.3 showed that tool life at ε_i=7.2° was invariably controlled by the evolution of the crater on the rake face, it is safe to conclude that at this ε_i value, entrance conditions are favorable to the tool and do not damage it. This ε_i value was therefore selected to be kept constant for the test. Next, the angle of exit ε_o had to be varied. This was achieved by preparing workpieces of different widths. For each workpiece width, representative of an exit angle ε_o, a search could then be initiated to find the feed value at which it would be safe to operate without incurring breakage. This search was done for two speed values. The test conditions are listed below:

- Work material, face mill, tool geometry and depth of cut of 1.52 mm were retained from experiments of sections 5.2.2 and 5.2.3.
- Angle of engagement ε_i = 7.2° = constant.
- Angle of exit ε_o and associated workpiece widths:

ε_o	0	7.2	14.5	22.0	30.0	38.7°
w(mm)	6.35	12.7°	19.1°	25.4	31.8	38.1

- Tools: SNT Grade in SNG-433 with a light hone (.025-.05 mm)
- Feed selection available on the machine (mm/tooth)

  at 165 m/min: .0635; .089; .10; .127; .178; .229; .28

  at 249 m/min: .051; .0635; .089; .114; .140; .178; .229; .292
- Speeds: 165 m/min and 249 m/min.
- Test criterion: After considering the previous tests, carrying out some exploratory trials and assessing the tools and work material available, the following rule was adopted: At a given ε_o value,

the breakage boundary is set at the maximum feed at which two consecutive starts, using two new edges, can be made up to a travelled distance of 50.8 cm at 165 m/min and 38.1 cm at 249 m/min.

Table 3 shows the results of the search. The cross hatched boxes indicate those feeds at which no breakage was observed for two consecutive starts. At some values of ε_o, the longest distance travelled at the feed adjacent to the maximum safe feed is recorded. When no value is recorded, failure happened in the first 10 cm of travel. Irrespective of feed, speed or ε_o value, failures were remarkably similar to those described in section 5.1.2 for $\varepsilon_i \geq 18.2°$. The breakage was invariably located in an area below the depth of cut line and on or just above the junction between the tool nose and the major cutting edge.

Figure 24 shows a plot of the breakage boundary.

The plot clearly shows that for small ε_o angles (<20°) the feed that can be tolerated without breakage is minimal. As ε_o increases, the permissible feed increases. At ε_o=38.7°, the permissible feed, for a speed of 165 m/min, is double that of ε_o=30°. No satisfactory explanation could be found for this behavior. Speed did not seem to make a difference, as the boundary for 249 m/min seems to be very close to that of 165 m/min. Ideally, a wider range of speeds should have been investigated but the extremely rapid cratering of SNT grade tools at higher speed made this consideration difficult to implement.

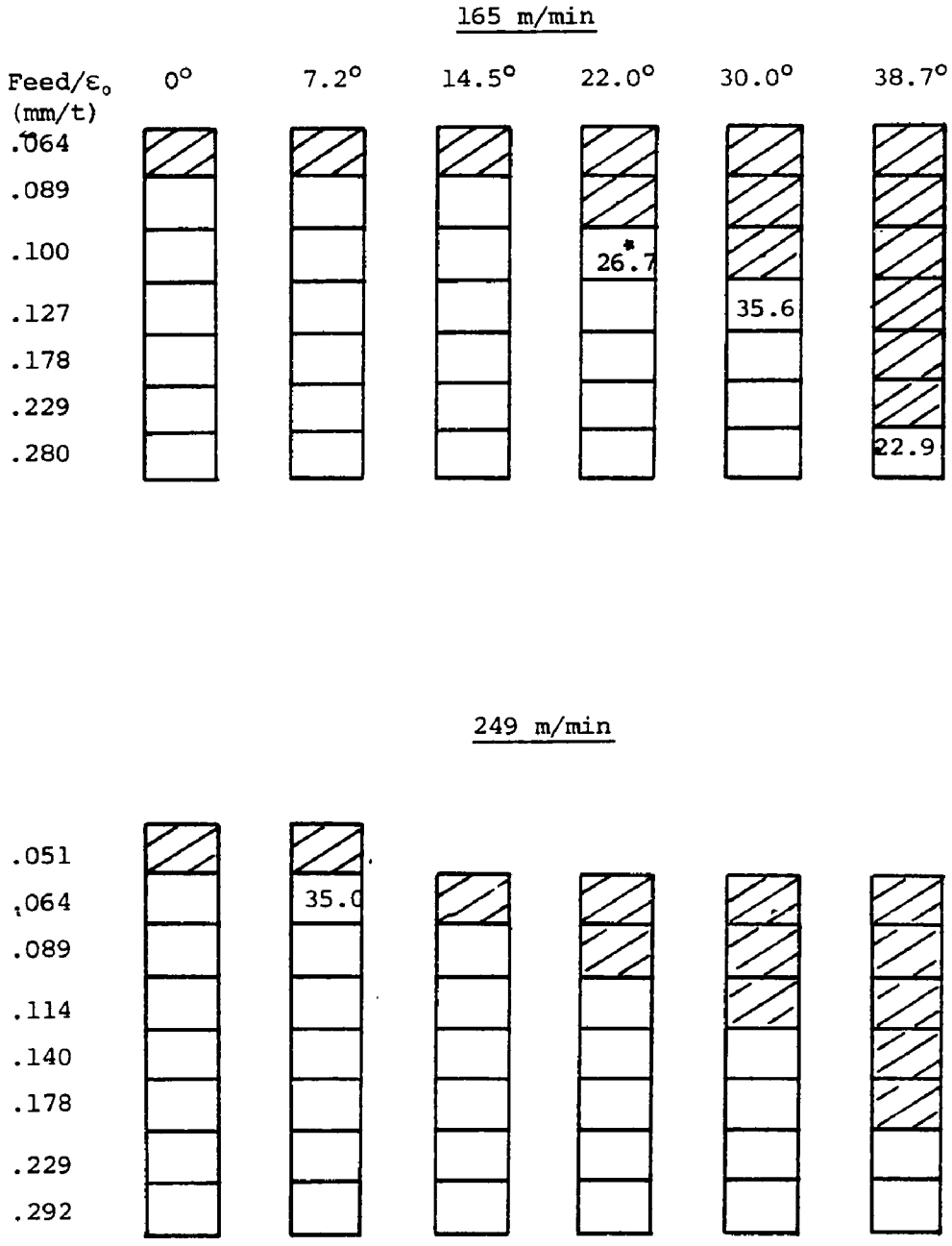

* Distances in cm

Table 3: Exit breakage boundary conditions

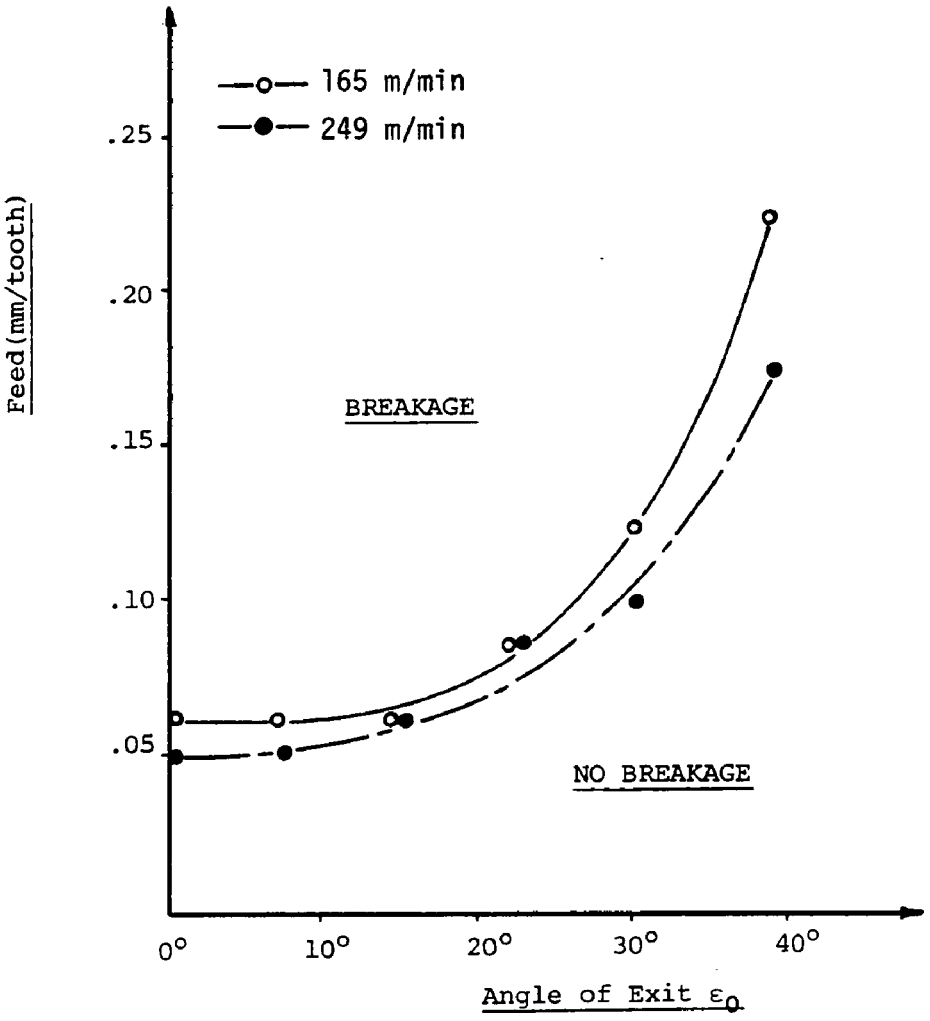

Figure 24: Exit breakage boundary in function of feed/tooth and angle of exit.

5.3 Case #2: Tool with a K-land Preparation

5.3.1 Experimental approach

The previous tests have clearly shown that the angles ε_i and ε_o have an influence on the tool performance when face milling with an SNT tool having no K-land. It was also shown that initial contact in the face of the tool (U type) seemed to prevent chipping or breakage. The computer graphic model used to visualize initial location and progress of contact between a K-land tool and the workpiece showed that depending on the value of ε_i, this tool was capable of a type of contact such that a large portion of the chip cross section is intercepted inside the K-land, before the major or minor cutting edges contact the work. Intuitively, this type of contact would seem beneficial. The computer simulation also showed that as ε_i increased, the intersection curve shifted to a vertical direction, such that the minor cutting edge of the tool was the initial area of contact and that the periphery of the tool followed into the cut throughout the engagement phase. This type of contact is similar to that which seemed very unfavorable in the experiments using tools with no K-land. The purpose of this test is to check the sensitivity of a K-land tool to the type of contact it sees at entry, and verify the notion that the indiscriminate use of a K-land tool, should it result in an unfavorable entry condition, may very well negate the potential benefit of the K-land. The procedure used in the initial tests of section 5.2.1 regarding workpiece

preparation was followed for these tests. Workpiece material was different since not enough of the original 4340 stock remained. Some 4340 plate steel was ordered and arrived with a hardness ≈ 24 Rc. This steel was sent to an outside contractor for heat treating, quenching and tempering. Final hardness averaged 35 Rc and showed very little variation across the 5 cm sections.

As the purpose of the experiment was to investigate the influence of the entrance contact condition as expressed by the angle of engagement ε_i, potential problems associated with the exit condition were eliminated through the use of workpieces of various widths, such that the angle of exit was constant and equal to 48.5°.

For comparative purposes, it was also decided to run a control tool. A coated steel cutting grade tungsten carbide tool was chosen to be run at a selected number of ε_i values. More specifically, three ε_i values resulting in T, u and v contact were chosen for the control tool. The complete test conditions are given below.

5.3.2 Test conditions and results

- Work material: 4340 steel plate; heat treated, quenched and tempered to 35 Rc. Scale removed.
- Face Mill: 106 mm diameter
  axial rake $\gamma_a = -5°$
  radial rake $\gamma_r = -5.6°$
  corner angle c = 15°

- Cutting conditions: speed: 202 m/min

feed: .15 mm/tooth

depth: 1.52 mm

- Tools: SNG 433: silicon nitride SNT grade ,2mm x 20°land

Tungsten carbide CC-6 (TiC coating)

Carboloy 514

- Work dimensions: 203 mm long, depth and width variable.

Independent variable ε_i: ε_i, ε_o and associated work width w were:

ε_i	-22.0°	-7.2°	+7.2°	14.5°	22.0°	30.0°	38.7°
w(mm)	19.0	31.8	44.5	50.8	57.2	63.5	69.9
ε_o	48.5	48.5	48.5	48.5	48.5	48.5	48.5

note: The tungsten carbide control tool was run at ε_i=-22°, 7.2°, and 38.7°.

Dependent variable: Tool life.

As with the tests of sections 5.2.1 and 5.2.2, tool life was measured by the total distance (cm) travelled until total tool failure. With ceramics, this invariably meant tool fracture. With tungsten carbide, this meant tool fracture or .76 mm flank wear in the absence of fracture.

A procedure identical to that used in section 5.1.1 was adopted for the order in which the data points were taken. The results appear in table 4 and are plotted in figures 25 and 26. Figure 25 shows a plot of the distances travelled to tool failure. Figure 26 takes the width of cut into account and shows a plot of volume removed (cm^3) until tool failure.

TABLE 4: DISTANCE TRAVELLED UNTIL FAILURE (CM)

	ε_i	-22.0	-7.2	+7.2	+14.5	+22.0	+30.0	+38.7
SNT-K		293.4	231.1	268.0	190.5	163.8	35.6	2.54
		317.5	203.2	249.0	78.7	106.7	22.9	5.1
		261.6	266.7	99.0	182.8	124.5	17.8	3.8
				283.2	140.0		30.5	2.5
							17.8	
	$\bar{x}$	290.8	233.7	224.8	148	131.7	24.9	3.5
CC-6		330.2		213.4				68.6
		294.6		175.0				81.3
		275.6		195.6				94.0
								61.0
	$\bar{x}$	300.1		194.7				76.2

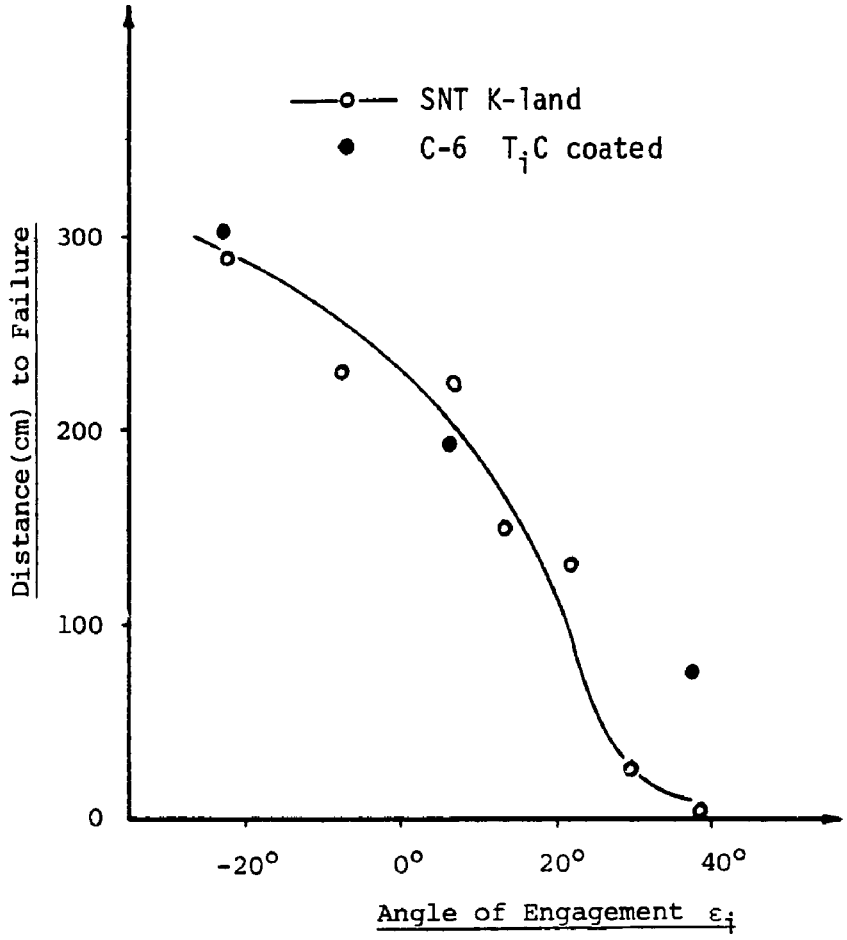

Figure 25: Tool performance vs. angle of engagement. SNT grade K-land tool on 4340 steel.

From figure 25, it can be seen that the tool performance, expressed in terms of the distance machined until tool failure, is very sensitive to the value of the angle of engagement ε_i. The performance of the silicon nitride based tool (SNT-grade) having a K-land preparation can be characterized by the following observations.

- As ε_i increased from the negative range to the positive range, two distinct modes of tool failure became apparent. For $\varepsilon_i \leq 7.2°$, the tool edge developed no chipping or fracture and the mode of failure was directly related to the tool's crater wear. Except for one premature tool failure by chipping (99.0 cm at $\varepsilon_i = 7.2°$), tool life for $\varepsilon_i \leq 7.2°$ was terminated when the crater reached the edge of the tool.

For $\varepsilon_i > 7.2°$, chipping and fracture gradually became the dominant mechanism of tool failure. Tool performance at $\varepsilon_i = 14.5°$ was characterized by small chipping along the whole cutting edge which eventually resulted in a complete destruction of the edge. Small chipping was gradually replaced by larger chips developing on the cutting edge in the area of the junction between the nose radius and the major cutting edge. Catastrophic failure was predominant when ε_i reached a value $\geq 30.0°$. Photographic records of the tool edges typical of the performance at $\varepsilon_i = 7.2°$ and $\varepsilon_i = 30°$ can be seen in the appendix.

- Since ε_o was constant and large enough for its effect to be considered negligible in these tests, the tool performance can be related to the entrance conditions resulting from the value of ε_i.

The computer graphic model shows that for the k-land tool under consideration, $\varepsilon_i \leq 7.2°$ results strictly in an initial contact point inside the tool face, on the K-land, and away from the major or minor cutting edges. Furthermore, the model also shows that for $-7.2 \leq \varepsilon_i \leq 7.2$, a considerable portion of the chip cross section area is intercepted by the K-land before the major cutting edge comes into contact with the work. The results returned by this experiment therefore lend credibility to the notion that ceramic tool brittle failure can be avoided by insuring that initial contact between the tool and the workpiece is located away from the sensitive cutting edge. In contrast, the graphic model also shows that as ε_i increases in the positive direction, the intersection curve shifts to a vertical position, moving the initial contact to the minor cutting edge. More important, the sensitive periphery of the cutting edge comes into contact instantaneously with the work. The experimental results show that this type of contact is characterized by chipping and brittle failure as ε_i increases. So it can be concluded that in this range of ε_i values resulting in poor initial contact, the presence of the K-land does not, in any way strengthen the edge of the ceramic tool. It's potential benefit is clearly not realized under these conditions.

The control tool, which consisted of a C-6 tungsten carbide grade coated with TiC was also very sensitive to ε_i. This tool was run at 3 chosen values of ε_i.

- At ε_i=7.2°, initial contact is deep in the face of the tool with the intersection line making an angle of 21° with the vertical. The experiments showed that the periphery of the tool edge did not show any chipping. The tool performed until a large crater developed and tool life was terminated when the crater reached the edge. During machining, cracks appeared on the rake face of the tool and had the characteristic pattern of the so-called "comb cracks" described in section 2.4.2. At this ε_i value, the cracks were evenly spaced and appeared to be perpendicular to the tool edge. A photographic record of this pattern can be seen in the appendix.

- At ε_i=38.7°, initial contact is on the minor cutting edge of the tool with the intersection line making an angle of 5.5° with the vertical. Termination of tool life at this data point was invariably due to gross chipping or fracture usually located in the upper portion of the tool nose. A photographic record of this type of failure can be seen in the appendix.

- At ε_i=-22.0°, initial contact is at the depth of cut line on the tool edge with the intersection line making an angle of -16.0° with the vertical line (the intersection line is moving from the tool edge to the inside face of the tool in this case). Although the tool continued to perform for a long distance, tool life at this data point was characterized by small chipping along the tool edge and from the rake face. The "comb cracks" which developed appeared to be inclined to the cutting edge and invariably branched in the vicinity of the cutting edge. Tool life was terminated invariably when the face of the tool was chipped out. A photographic record of this type of tool edge can be found in the appendix.

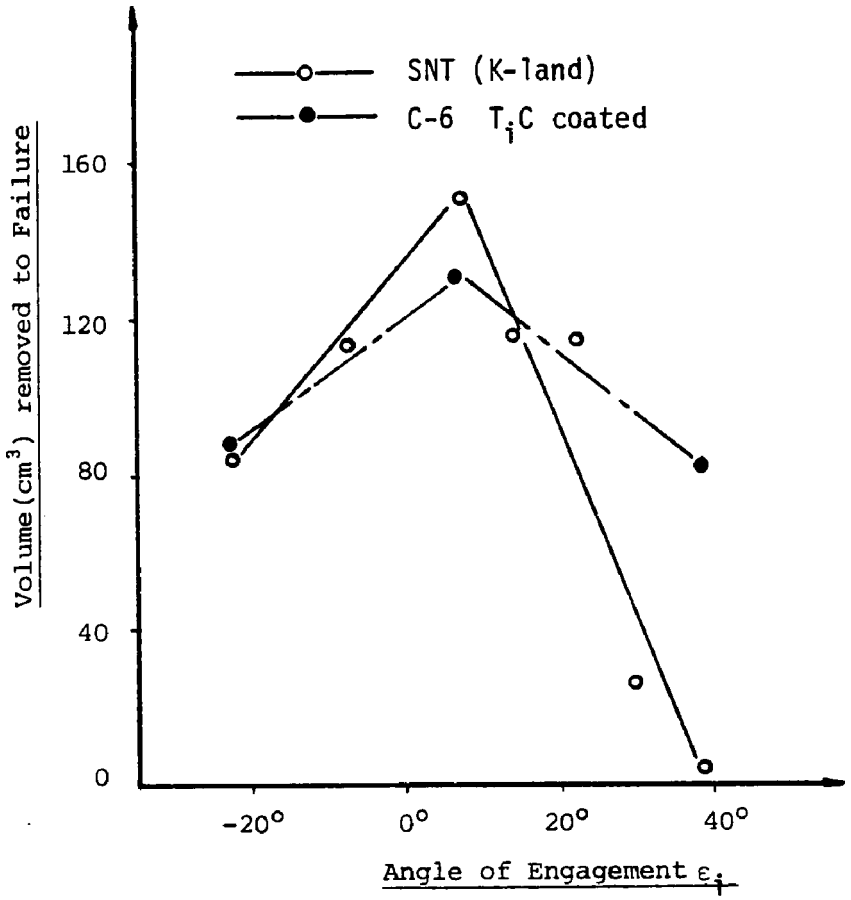

Figure 26: Volume of metal removed vs. angle of engagement. SNT grade K-land tool on 4340 steel.

Figure 26 shows a plot of the data transformed in terms of the volume of material removed per tooth until failure. This plot rectifies the distortion in performance introduced by the variable width of cut in the experiment. It can be seen that tool life, expressed in terms of volume of metal removed can be maximized in a definite range of ε_i values. This range of ε_i values corresponds to an initial tool workpiece contact inside the face of the tool, and away from the cutting edge.

5.3.3 Exit conditions

An attempt to investigate the behavior of SNT-grade tools with a K-land preparation under different exit conditions was undertaken. The approach taken was similar to that used for the evaluation of the honed SNT-grade tools in section 5.2.4. All test conditions including work material were similar to those of section 5.2.4. The breakage characteristic of the exit failure with the honed SNT-grade tools was not observed with the K-land tools. These tools behaved adequately over the whole range of test conditions. The attempt was not pursued any further. While it certainly appears that a K-land tool is able to withstand exit far better than a tool with no edge preparation, the test conditions used here may not have been severe enough to challenge the K-land tool. This area should certainly be investigated further in the future.

5.4 Comparative Tests

In addition to investigating the effects of ε_i and ε_o on the performance of silicon nitride based tools, tests were also run in an attempt to differentiate between tool material compositions as well as tool edge preparations. The results of these comparative tests are given below.

5.4.1 Comparison between tool grades

The tests described in section 5.2.2 indicated that the AY6 grade had an inferior performance compared to the SNT grade when both grades were run in an SNG 433 configuration with a honed edge. During the discussion of these tests, it was noted that AY6 performance for $\varepsilon_i \leq 14.5°$ seemed to be limited by a fast cratering rate. It was thus clear that the SNT grade had a better crater resistance and that the tests of section 5.2.2 were simply highlighting this difference. The tests therefore were not indicative of the relative toughness of the two grades. So, in order to distinguish between the toughness of the two grades, a material more challenging than 4340 steel had to be found. Some exploratory tests on leftover pieces of a manganese steel alloy known to be very difficult to machine showed that this material could discriminate between the tools. The exact composition of this manganese steel is not known. The workpiece blocks could not be cut on a band saw and had to be sized on a milling machine at speeds no higher than 21 m/min (~ 70 SFPM). Its importance

in this test is strictly limited to its potential ability to highlight differences between tool grades and the expense needed to obtain a chemical analysis of the material did not seem justified at this point. The test conditions were as follows:

Work Material: Manganese steel

50.8 mm wide; 304.8 mm long; 152.4 mm deep

Face mill: 101.6 mm double negative

axial rake $\gamma_a = -5°$

radial rake $\gamma_r = -5.6°$

corner angle C = 15°

Cutting conditions: speed: 85 m/min

feed/tooth: .127 mm/tooth

depth of cut: 1.27 mm

Independent Variables:

$\varepsilon_i/\varepsilon_o$: Due to the restricted shape of the available workpieces, variation in ε_i was obtained by offsetting the cutter centerline with respect to the plane of engagement without keeping ε_o constant by varying the width of the workpiece. As ε_i increases, the effects of ε_i and ε_o may very well become confounded.

Tool grades: SNT grade, AY6 grade.

Tool geometry: SNG 433 tools a) with a .2 mm x 20° K land

b) .025-.050 hone and no land

Dependent variable: Tool life as expressed by the distance (cm) travelled by the cutter until tool failure. Tool failure invariably meant total breakage of the cutting edge.

The procedures regarding workpiece preparation and data point allocation described in the experiments of section 5.2.2 were also applied here.

The test results are shown in Table 5 and figure 27 shows a plot of the averages at each data point. The following observations can be made:

- Performance of the SNT grade, irrespective of tool edge preparation was negligible. Tool failure invariably took the form of total edge breakage after a few revolutions of the cutter. Angles of engagement ε_i which result in a favorable entry condition did not make any difference as the tools failed at each data point.

- In contrast to the SNT grade, the AY6 tools, under favorable entry conditions were able to cut this material without immediate failure. The performance of the two different edge preparations under test seemed to peak around ε_i=7.2°. Note that this ε_i valve was shown previously to result in favorable entry conditions. Tests interrupted before tool failure showed that the AY6 tools were developing a large crater on the rake face with no apparent chipping of the cutting edge. Failure by breakage in this range seemed to

TABLE 5: DISTANCE TRAVELLED (CM) TO FAILURE

	ε_i	0°	7.2°	14.5°	22.0°	30.0°	38.7
AY6-K		29.2	31.8	21.6	11.4	5.4	4.5
		25.4	30.5	22.9	16.5	14.0	1.9
		27.3	22.9	21.0	15.2	8.9	1.3
		24.8	25.4	21.6	12.7	9.5	1.3
AY6-H		6.4	9.2	9.5	6.4	5.1	4.5
		11.4	13.3	10.5	11.4	8.9	5.1
		12.7	10.2	12.1	8.9	7.6	1.9
		12.1	8.9	10.8	6.4	5.1	7.6
SNT-K		1.3	5.1	1.3	.3	.3	.3
		.3	15.2	1.3	.3	.3	.3
		1.0	2.5	.3	.3	.3	.3
		.3	1.9	.3	.3	.3	.3
SNT-H		.3	1.3	.3	.3	.3	.3
		.3	.3	.3	.3	.3	.3
		.3	.3	.3	.3	.3	.3
		.3	.3	.3	.3	.3	.3

Note: a value of .3 was assigned when breakage was immediate.

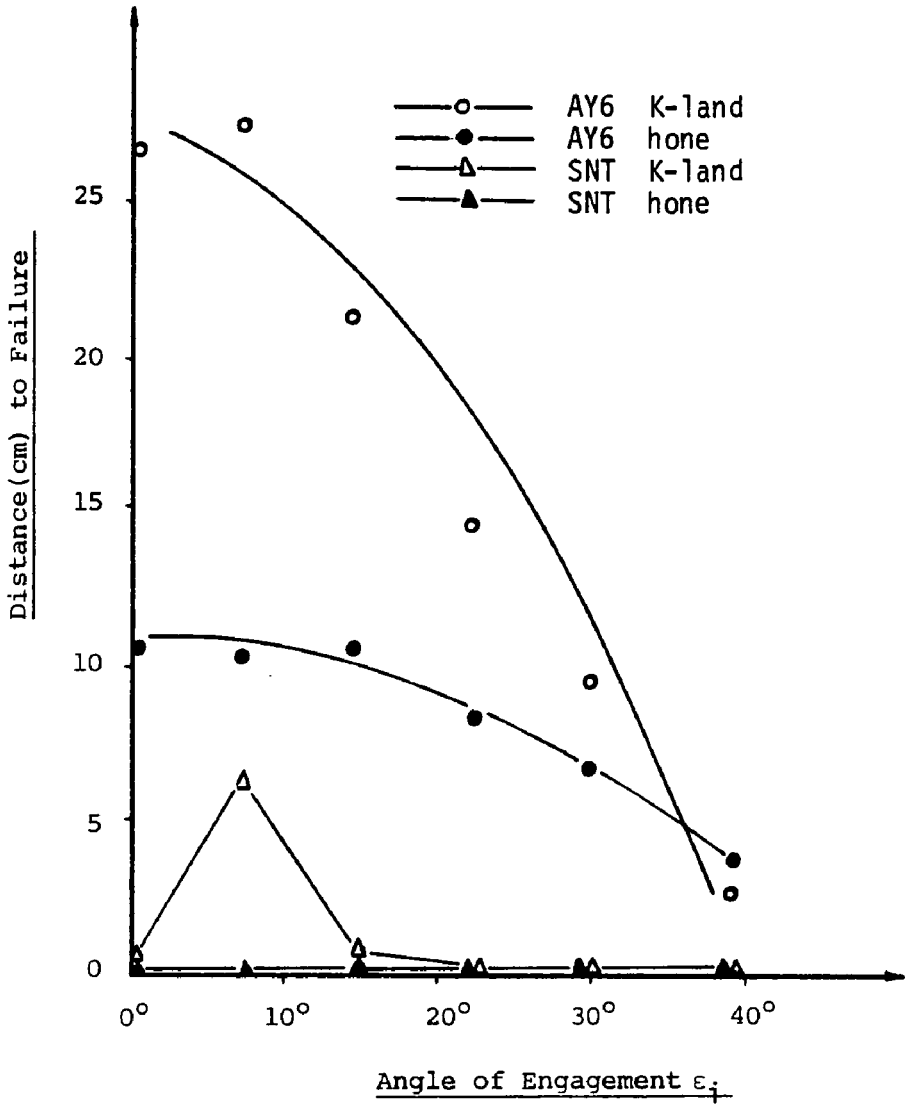

Figure 27: Comparative tests of silicon nitride grades and preparations on Manganese steel.

happen invariably when the crater reached the cutting edge. As ε_i increased, tool life decreased but interpretation in this range is difficult. As noted before, the variable ε_o values resulting from the fixed workpiece width do not allow the separation between the potential ε_i and ε_o effects.

- In conclusion, the tests clearly show the superior impact resistance and strength of the AY6 grade compared to the SNT grade. It should also be noted that if testing had been run indiscriminately at a high ε_i value (ε_i=38.7°), differences between tool grades as well as differences between tool preparations would have been masked. The interpretation of the apparent difference between tool edge preparations will be discussed in the next section.

5.4.2 Comparison between edge preparations

The test described in section 5.2.3 can best illustrate the comparative performance of tools with a honed edge and tools with a k-land preparation. The test conditions can be found in section 5.2.3 and the test results are shown in table 2 in that section. Figure 28 shows a plot of tool performance in function of ε_i.

- The comparison regarding contact conditions of different edge preparations discussed in section 4.2.4 showed that a K-land tool was capable of a wider range of contact inside the face of the tool ('u' type of contact). As an example, for ε_i=-22°, it could be seen that a k-land tool was making a 'u' type of contact while the tool with a honed edge was making a "T" type of contact at the depth of cut line. Figure 28 shows that at ε_i=-22°, the honed tool failed

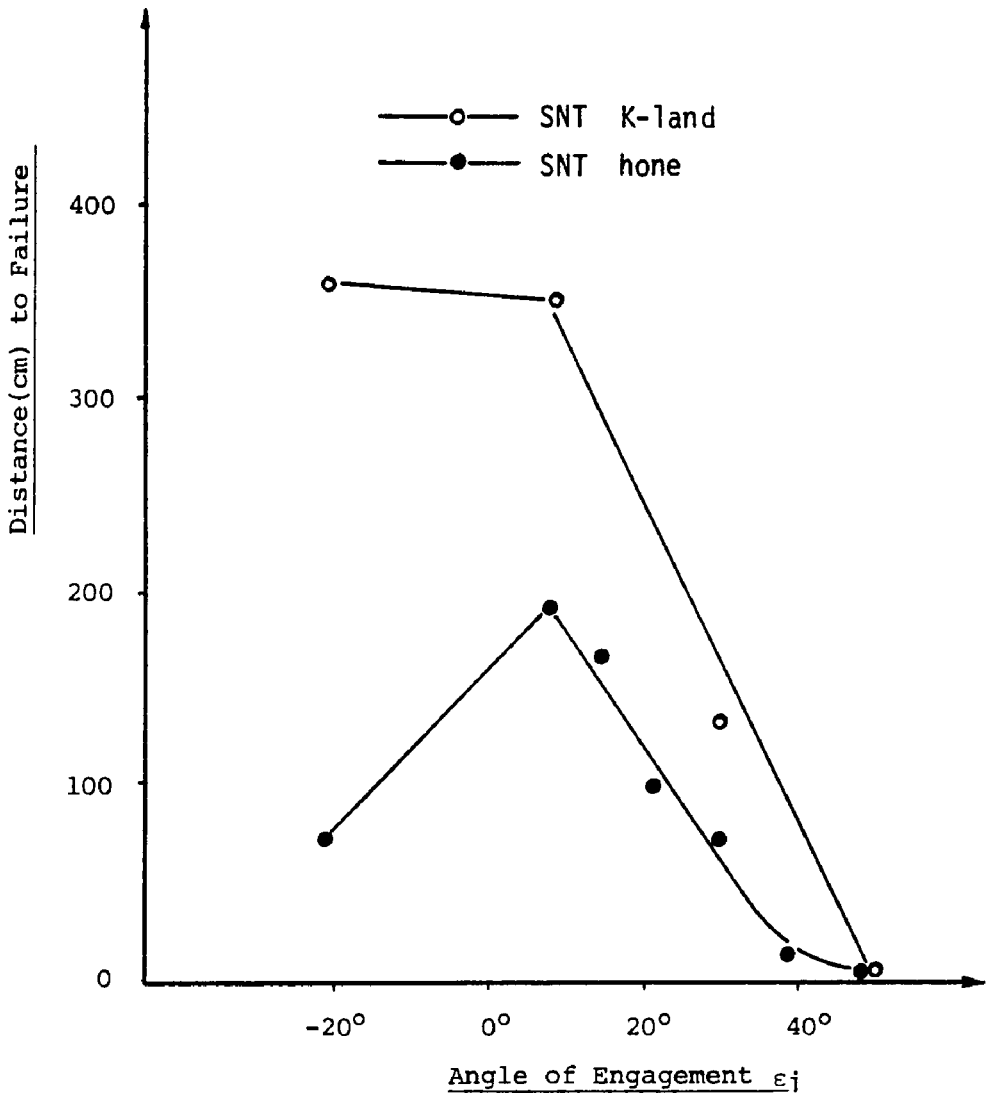

Figure 28: Comparative tests with different edge preparations on 4340 steel.

prematurely by fracture while the K-land tool continued to perform free of premature failure. The performance difference at ε_i=-22° clearly shows the influence of the presence of the K-land.

- When ε_i increases to large values ($\varepsilon_i \geq 30°$), the graphic model of section 4.2.3 showed that the tool/workpiece intersection curve at entry assumed a more vertical position, shifting initial contact location at entry to the minor cutting edge of the tool and causing the cutting edge of the tool to contact the work early. Kronenberg's analysis showed that a similar contact resulted at this ε_i values for the honed tool. Figure 28 shows that tool performance deteriorates for both edge preparations in this ε_i range and tool life was invariably terminated by premature chipping and fracture of the cutting edge. So under what appears to be unfavorable contact conditions, the K-land tool and the honed tool fail prematurely through chipping and fracture. Under these conditions, the presence of a K-land on the tool appears to be redundant.

- At ε_i=7.2°, both edge preparations seem to be performing at their best and tool life was terminated when the crater reached the edge. The test points were free of premature chipping or fracture. Note that initial contact is deep in the face of the tool for both edge preparations. However, since the mode of tool failure was largely due to the crater weakening or reaching the edge, a direct comparison of the strength of these two edge preparations is not

possible. Indeed, by virtue of its bevel, and for the crater to reach the edge, more tool material has to be removed from the K-land tool than from the honed tool. Assuming that cratering takes place at the same rate, a K-land tool will outperform a honed tool when cratering is the dominant mode of tool failure. Ideally, such a comparison should be carried out under a tool material/work system where cratering is not the dominant mode of wear. Under such conditions, the strength of the two shapes, rather than the material's resistance to cratering would be the independent variable.

5.4.3 Coated tools

Since under favorable entry conditions, chipping or brittle failure of the cutting edge were eliminated, cratering and the subsequent weakening of the cutting edge became the leading failure mechanism. The thought was therefore given to the possible application of a wear resistant coating on both silicon nitride grades. Tool samples in both grades and edge preparations were coated by GTE-Valeron with a film of aluminum oxide. Although aluminum oxide is not immune to cratering in contact with steel, it has been shown [7] to be one of the least reactive materials when put into contact with different metals. The method used to coat these tools is not known. In general, the aluminum oxide coating showed a very poor adherence to the AY6 grade and the coating could easily be scraped off with a sharp object. This was a disappointing result since

wear and crater resistance provided by a coating, combined with the toughness exhibited by this grade seemed to point toward a very promising grade. The SNT grade, however, showed a somewhat better coating adherence and testing was undertaken to evaluate its performance. The test conditions are given below.

Work material: 4340 steel, hot rolled, 28 Rc.
50.8 mm wide, 152.4 mm long rectangular pieces.

Face mill: 101.6 mm diameter
axial rake $\gamma_a = -5°$
radial rake $\gamma_r = -5.6°$
corner angle C = 15°

Cutting conditions: speed: variable
feed: ~.14 to .18 mm/tooth
depth: 1.52 mm
$\varepsilon_i = 7.2°$
$\varepsilon_o = 61°$

Tools: SNG 433, .025-.05 mm hone on the edge
Grade: SNT and SNT+AL_2O_3 coating.

Test criterion: Distance (cm) travelled until tool failure.
Tool failure invariably meant fracture of the cutting edge.

Workpiece preparation and test procedures used in the tests of section 5.2.2 were followed in these tests. The results are shown in table 6 and test point averages are plotted in figure 29 using a logarithmic scale.

Figure 29 shows that the coated tool did not perform as well as the uncoated tools. The uncoated tools behaved as expected and failed invariably when the crater on the rake face reached the edge. As the crater grew larger, a crack could be seen running parallel to the cutting edge and in the middle of the crater. The coated tools in contrast appeared to be very brittle. The coating had a tendency to come off in plaques, very early. Edge chipping, particularly in the lower speed range seemed to be the dominant mode of failure. Another manifestation of the embrittlement of these coated tools was very clear during the insertion and removal of these tools from the face mill pockets. It seems that the clamping force was enough to cause breakage along all edges contacted by the pocket.

The coating of these tools was not pursued any further at this stage.

TABLE 6: DISTANCE (CM) TRAVELLED TO FAILURE

Speed (m/min)		164	203	249	310
SNT-H		135.9	67.3	45.7	26.7
		198.1	76.2	38.1	27.9
		179.0	73.7	53.3	33.0
	$\bar{x}$	171.0	72.4	45.7	29.2
SNT-H + AL_2O_3 coating		68.6	58.4	45.7	20.3
		44.5	61.0	43.2	30.5
		55.9	49.5	61.0	34.3
	$\bar{x}$	56.3	56.3	50.0	28.4

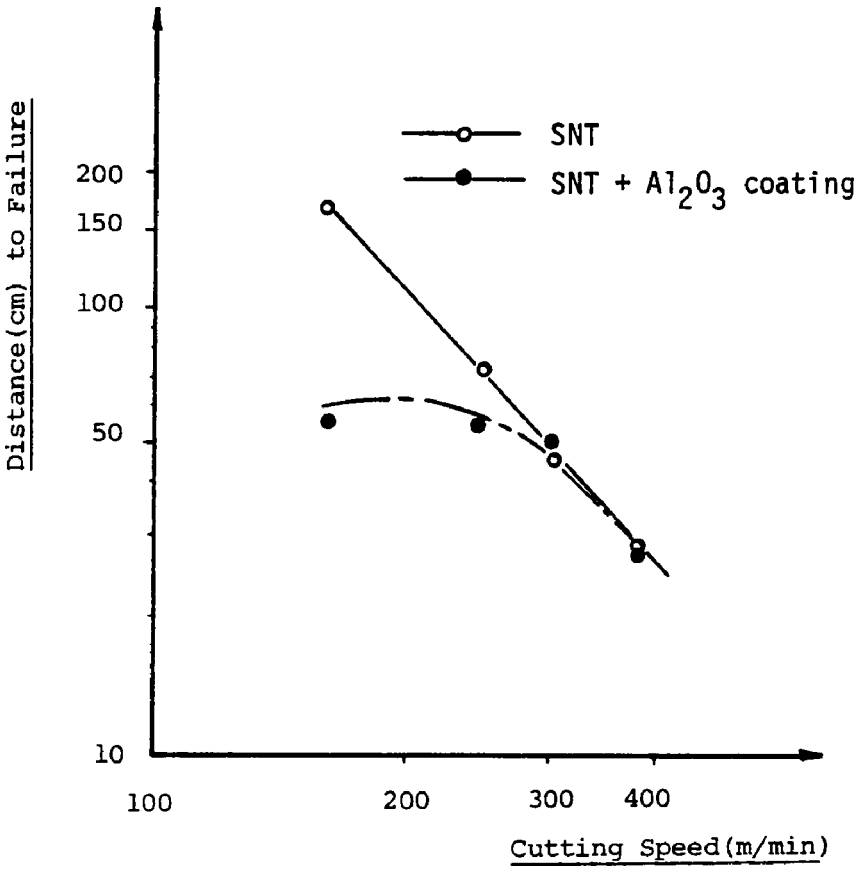

Figure 29: Comparative tests with coated and uncoated SNT grade honed tools on 4340 steel.

5.5 Tests on Titanium and Waspalloy Alloys

One of the aims of this study was to investigate the feasibility of machining some of the more difficult to machine materials at higher speeds than those typical of tungsten carbide or high speed steel tools. T_i6AL4V alloy as well as Waspalloy are typical of difficult to machine materials. The attempts made to address these materials in face milling using silicon nitride based tools were not successful. Irrespective of tool composition, geometry, angle of engagement ε_i, angle of disengagement ε_o, feed, speed or depth of cut, failure by total disintegration of the cutting edge was immediate. Another commercially available silicon nitride based material (Kyon 2000) that was claimed able to address Waspalloy at very high speed was tried but fared no better. The testing on these alloys was not pursued any further.

5.6 Tests on a Silicon Aluminum Alloy

5.6.1 The material

Among the properties of aluminum which chiefly affect its use as a metallurgical material are its low relative density, high thermal conductivity and ease of casting. If an alloy can then be formulated such that it possesses a low coefficient of thermal expansion and good wear characteristics, it will have all the required properties to qualify as a potential replacement for cast iron in automobile engines as well as a host of other wear parts. A hypereutectic aluminum-silicon system, AL 390 seems to fulfill these requirements and has emerged as the prime candidate for future engine blocks. It is also appearing in a variety of other automotive and mechanical wear parts. However, the presence of a large amount of silicon was bound to create difficulties in machining. Of the cutting tool systems available today, successful machining was reported [43,43,44,45] using a grade of tungsten carbide at moderate speeds, or polycrystalline diamond at much higher speeds. While the difference in cutting speed range for these two cutting tool materials is substantial, the ratio of the price per edge is also as high as 40:1. This alloy was therefore retained for the evaluation of the silicon nitride based tool materials.

The material for the tests was contributed by a major aluminum producer in the form of cast slabs 61 cm long x 20 cm wide x 7.6 cm thick. Although no chemical analysis was supplied with the material,

the pieces supplied were said to be representative of AL 390 compositions used in industry. A sample cut from one of the slabs was analysed by the G.T.E. Laboratory in Towanda and the results showed a major difference in the silicon content when compared to the nominal AL 390 composition. The chemical composition returned by the G.T.E. Laboratory is given below.

Chemical analyses:

Ag	0.5-5 ppm	Mo	1-10 ppm
Al	80%	Ni	1-10 ppm
Ca	1-10 ppm	Pb	10-100 ppm
Cr	10-100 ppm	Si	13%
Cu	4.9%	Sn	1-10 ppm
Fe	0.29%	Ti	10-100 ppm
Mg	0.65%	V	1-10 ppm
Mn	10-100 ppm	Zn	0.068%

Density: 2.74 g/cc Hardness: $\bar{x}$ = 43.6 R_B σ = 3.4

The chemical analyses, tabulated above were reported to have been obtained by atomic absorption for Si, Mg, Cu, Fe, Zn and Al. Qualitative emission spectrography was used for all other metallic elements. The major elements of the alloy are compared below to the nominal Al 390 composition reported in the literature [41].

	Nominal %	Analysed %
Al	Balance	80
Si	16-18	13
Cu	4.0-5.0	4.9
Fe	0.6-1.1	0.29
Mg	0.45-0.65	0.65

The possibility remains that the sample analysed may have come from a part of the casting which had a silicon depleted region. This phenomenon has been known to occur [41]. However, since the purposes of the tests were to evaluate the performance of some silicon nitride based tools against a tungsten carbide control tool, the alloy available proved as difficult to machine as the 390 alloys described in the literature.

5.6.2 Tests with negative geometry inserts

The first tools available were all square negative inserts (SNG 433) having a .025-.050 mm hone on the edge. These tools were available in the SNT and AY6 compositions. C-2 tungsten carbide tools in an SNG-433 configuration were obtained for the comparative test since this grade of carbide seems to be the standard grade used for the machining of silicon aluminum alloys. Since the new aluminum alloy parts seem to be mostly die cast "near net shape" parts, the face milling tests were confined to be representative of finishing operations. The test conditions are given below.

Workpiece: Silicon aluminum alloy. 7.6 cm wide x 20 cm long

Face mill: 101.6 mm diameter

$\gamma_a = -5°$; $\gamma_r = -5.6°$; $c = 15°$

Depth: .5 mm (.020 in)

Speeds and Feeds:

speed: m/min:	249	310	383
feed: mm/tooth:	.137	.122	.122
speed; sfpm:	816	1016	1257
feed: in/tooth:	.0054	.0048	.0048

Tools: SNG 433 in three compositions

- SNT grade (.025-.050 mm hone)
- AY6 grade (.025-.050 mm hone)
- C-2 (walmet W-A2)

Length of Test: 10 passes for a total distance travelled of 203.2 cm (80 in)

Dependent variable: Nose wear. The average value of the nose wear land was measured using the toolmaker's microscope described in section 5.2.1.

The results of the tests are shown in table 7. Initially, two data points were taken at each test condition. The order of the experiment was random and data collection was performed over two days.

TABLE 7: Nose wear ($x10^{-3}$ in) for C-2, SNT and AY6 grades on silicon aluminum alloy.negative tools.

SPEED (SFPM)	816	1016	1257
(m/min)	249	310	383
C-2	15.8	28.4	43.3
	14.6	31.0	39.4
SNT	11.8	17.7	24.0
	9.8	16.5	21.3
AY6	7.1	9.1	12.6
	7.1	8.7	12.6

(a)

SNT	10.8	17.1	23.8
	9.8	15.6	26.0
AY6	6.7	9.6	13.0
	7.1	9.3	12.8

(b)

NOTE: nose wear measurements should be read in 10^{-3} inches or $25.4x10^{-3}$ mm

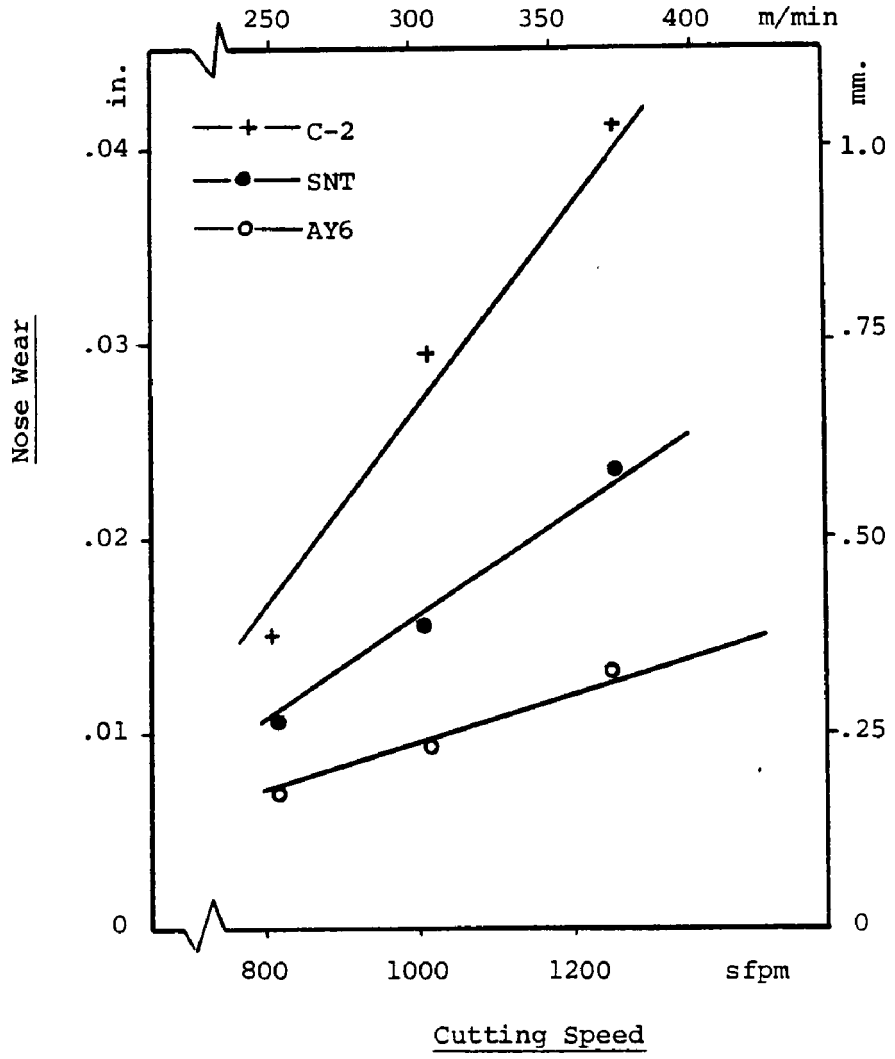

Figure 30 : Comparative tests on silicon aluminum with negative geometry tools.

In table 7.a, it can be seen that the difference between the first and second measurement is positive in 8 out of 9 cells. This raised some questions and the SNT and AY6 grades were run again as shown in table 7.b. Inspection did not reveal anything questionable and the two tables were pooled for analysis.

Measurement of the width of the wear land on the nose of the tool turned out to be difficult. Invariably, all 3 grades tended to have a layer of aluminum over the wear land. All 3 grades also had a built up edge of varying height on the rake face of the tool. Before the wear land could be measured, the built up edge as well as the aluminum covering the underside of the nose had to be removed. This was done by using a fine grade of sand paper to remove the aluminum layer. Still, the location of the boundary between worn and unworn parts of the tool was not easily seen under the microscope. Also, the honed edge of the silicon nitride grades made it difficult to focus the microscope on the tool's edge. Fortunately, table 7 shows that differences between grades are substantial and therefore, the difficulties encountered in measuring the nose wear do not diminish the information sought from these tests.

The average value at each data point is plotted in figure 30 for each tool. A nonlinear least square package available in the Bethlehem Steel library of statistical packages was used to fit a model to the data. The general model was:

$$y = y_o + (b_1 + b_2MS + b_3MC)(V-S_o) \qquad \text{where}$$

y = tool's nose wear x 10^{-3} inches

V = cutting speed SFPM

MS = MC = 0 for the AY6 grade

MS = 1; MC = 0 for the SNT grade

MS = 0; MC = 1 for the C-2 grade

The resulting models for the three different tool grades were as follows:

AY6 grade: $y = 4.66 + .0125\ (V-633.16)$

SNT grade: $y = 4.66 + .0309\ (V-633.16)$

C-2 grade: $y = 4.66 + .0603\ (V-633.16)$

The complete computer print out showing the number of iterations taken to reach a minimum residual sum of squares, the ANOVA representation, the parameter estimates and their 95% confidence interval can be found in appendix B.

The models show substantial differences in the wear characteristics of the three tool grades, with the AY6 composition giving the best wear performance. Some qualitative observations were also made during the tests:

- all tools showed evidence of a built-up-edge. This built-up-edge was very severe at the slow speeds. Although its height diminished considerably at the higher speeds, it was still present on all 3 grades.

- The SNT grade developed a crater that could easily be seen upon removal of the built-up-edge. This crater was filled with aluminum and often caused the breakage of the tool nose. Cratering and subsequent breakage of the tool nose did not happen with the AY6 grade.
- Although the SNT grade is known to be harder than the AY6 grade, the latter showed better wear performance, less built up edge and less aluminum adherence. It is strongly suspected that chemical interaction was present between the SNT grade and the work material.
- The C-2 tungsten carbide grade showed the worst performance. At the higher speeds, the tool tended to pick up large amounts of aluminum under the tool nose. This material accumulation seems to fit the so-called "deceptive chip formation" described by W. Konig [42].

Finally, although aluminum machining practice and characteristics dictate the use of high positive rake angles, the tests run with negative inserts showed clear differences between tool grades and a possible incompatibility between the SNT grade and the work material.

5.6.3 Tests with positive geometry inserts

Upon reception of silicon nitride based inserts in an SPG 433 configuration, comparative wear tests similar to those described in 5.6.2 were conducted. Except for the positive face mill size and the resulting speeds and feeds obtained on the machine, all other

test conditions were identical to those of section 5.6.2. They are listed below.

Workpiece: Silicon aluminum alloy. 7.6 cm wide x 20 cm long

Face mill: Sandvik modulmill, 203.2 mm (8 in) diameter.

$\gamma_a = +7°$; $\gamma_r = 0°$; $C = 15°$

Depth of cut: .5 mm (.020 in)

Speeds and Feeds:

speed: m/min:	.212	264	328	405	498
feed: mm/tooth:	.132	.129	.134	.145	.140
speed: sfpm:	697	867	1078	1330	1634
feed: in/tooth:	.0052	.0051	.0053	.0057	.0055

Tools: SPG 433 in three compositions

- SNT grade (.025-.050 mm hone)
- AY6 grade (.025-.050 mm hone)
- C-2 (walmet WA2)

Length of Tests: 10 passes for a total distance travelled of 203.2 cm (80 in)

Dependent variable: Nose wear. The average value of the nose wear land was measured using the toolmaker's microscope described in section 5.2.1.

The tests were randomized and the measurement difficulties encountered in the tests of section 5.6.2 were also encountered in these tests. The results are shown in table 8.

The least square method was used to fit linear models to the data. The models are described by:

AY6 grade: $y = 5.16 \exp\{.770(V-600)10^{-3}\}$

SNT grade: $y = 8.02 \exp\{1.07(V-600)10^{-3}\}$

C-2 grade: $y = 5.48+.032\ (V-600)$

where y = nose wear in 10^{-3} inches

V = cutting speed in sfpm

The computations and analysis of variance representations for these least square models can be found in appendix B.

The average value of each data cell and the least square model for each tool grade are plotted in figure 31.

note: In table 8, it can be seen that the C-2 grade is not run at the highest speed of 498 m/min (1634 sfpm). Wear and excessive accumulation of aluminum material under the tool nose under these conditions made it impossible to complete 10 passes. 635 m/min (1330 sfpm) was the highest speed at which the C-2 could be run and an additional speed of 212 m/min (697 sfpm) was introduced for this grade as a fourth data point.

TABLE 8: Nose wear ($x10^{-3}$ in) for AY6, SNT and C-2 grades on silicon aluminum alloy. Positive tools.

SPEED (SFPM)	697	867	1078	1330	1634
(m/min)	212	264	328	405	498
AY6	-	6.7	7.0	9.3	11.4
	-	6.3	7.5	8.7	11.8
SNT	-	11.0	13.4	17.0	24.8
	-	10.6	12.6	18.9	23.4
C-2	8.7	13.4	20.1	29.9	-
	8.0	14.7	22.5	27.0	-

NOTE: Nose wear measurements should be read in 10^{-3} inches or $25.4x10^{-3}$ mm.

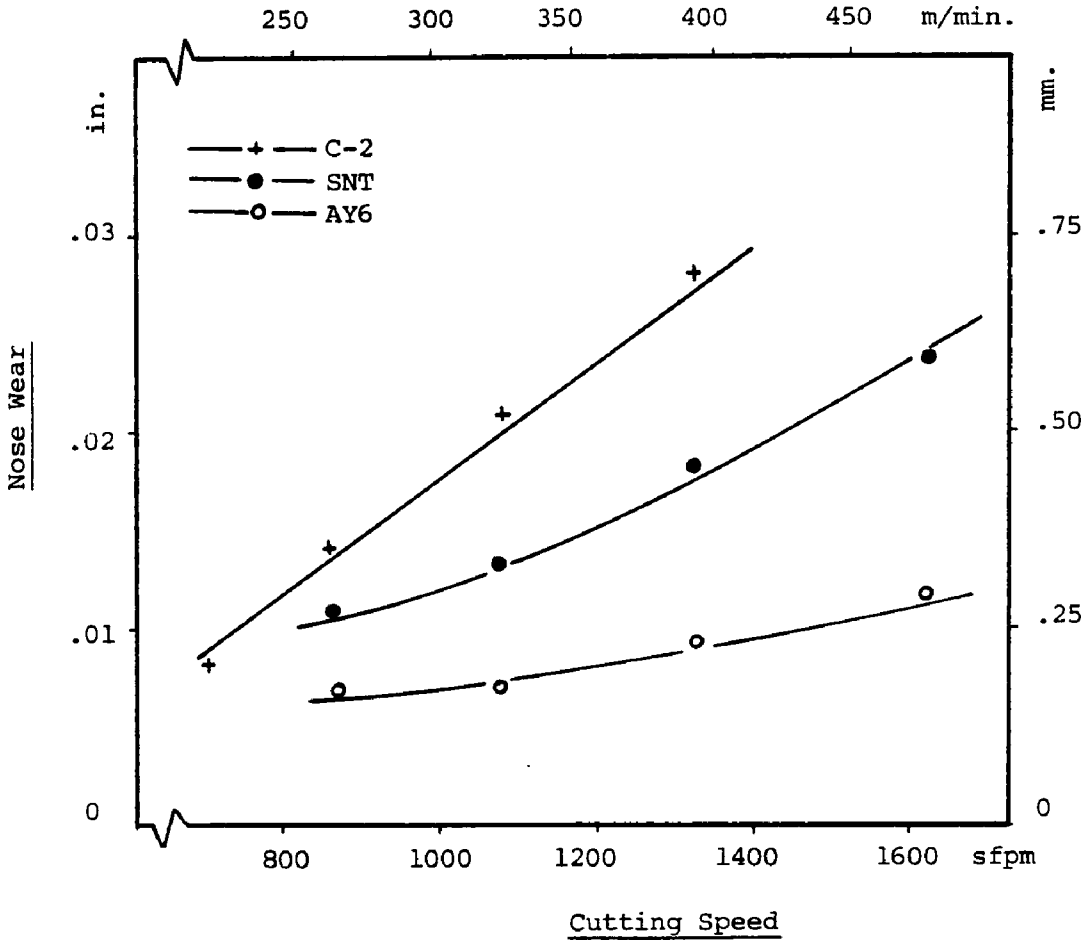

Figure 31 : Comparative tests on silicon aluminum with positive geometry tools .

The comparative performance of the positive inserts can be characterized by the following conditions:

- Again, the AY6 grade showed the best performance in terms of wear resistance. Second best performance was that of the SNT grade and the least wear resistant grade was the C-2 tungsten carbide.

- Positive geometry did not eliminate the built up edge. This was applicable to all grades although the built up edge for the AY6 grade was minimal in the high speed range.

- Positive geometry did not eliminate the cratering and subsequent breakage of the tool nose observed on the SNT grade in section 5.6.2. This observation reinforces the idea that the SNT composition is interacting with the work material.

- Attempts to increase the speed while using the AY6 grade resulted in excessive accumulation of workpiece material under the tool nose. This pick up of material seems to fit the description of the so-called "deceptive chip formulation" discussed by W. Konig [43]. Konig identifies tool wear and the subsequent blunting of the cutting edge as the main factor in the formation of deceptive chips. This phenomenon is said to be independent of tool material.

- The positive geometry tools, as expected, appear to perform substantially better than their negative counterparts. However, a direct quantitative comparison on the basis of these tests is not possible given that the 2 cutters having different diameters result in a substantially different arc of cut. Over 10 passes, the smaller, negative cutter causes the SNG tools to be in contact with the work over a substantially longer linear distance. Since abrasive wear seems to be the dominant mode of tool wear, direct comparison between SNG and SPG tools in these tests should acknowledge the 'disadvantage' incurred by the smaller cutter.

5.6.4 Comparison with polycrystalline diamond

Polycrystalline diamond tips, in solid inserts or brazed to a tungsten carbide substrate have been shown by many studies [42, 43, 44,45] to be the ideal tool material for the machining of the high silicon aluminum alloys and particularly the hypereutectic AL 390 alloy. The only question which seems to arise concerning their use is their economic justification for a given production case. Some polycrystalline (PCD) tools were obtained in order to situate the AY6 performance with respect to both the C-2 and PCD tools.

Figure 32 shows the progression of nose wear with time for the three grades. The AY6 and C-2 grades are shown at a speed of 264 m/min (867 sfpm) while the PCD tool is shown at speeds of 960 m/min (3150 sfpm) and 767 m/min (2520 sfpm). Other test conditions were

identical to the tests of section 5.6.3. These conditions are listed below.

Workpiece: silicon aluminum alloy 7.6 cm wide x 20 cm long

Face mill: Sandvik modullmill, 203.2 mm (8 in) diameter.

$\gamma_a = +7°$; $\gamma_r = 0°$; $C = 15°$

Depth of cut: .5 mm (.020 in)

Feed/tooth: ~.132 mm (.005 in)

Tools: C-2 SPG 433

AY6 SPG 433 with .025-.050 mm hone

PCD SPG 433

The tests were interrupted periodically to measure the width of the wear land under the tool nose. The tests were terminated when the C-2 and AY6 grades reached a wear land of .38 mm (.015 in). The plot of figure 32 shows the average value of two measurements for the AY6 and C-2 grades. The plots for the PCD show one measurement resulting from one trial at each speed.

Figure 32 clearly shows that if the AY6 grade is superior to the C-2 grade, it is clearly not in the same class as the PCD tools. As these PCD tools were consuming a large amount of work material and showing very little wear, the comparison was not pursued any further. The PCD tools did not show any built up edge or aluminum accumulation on the wear land.

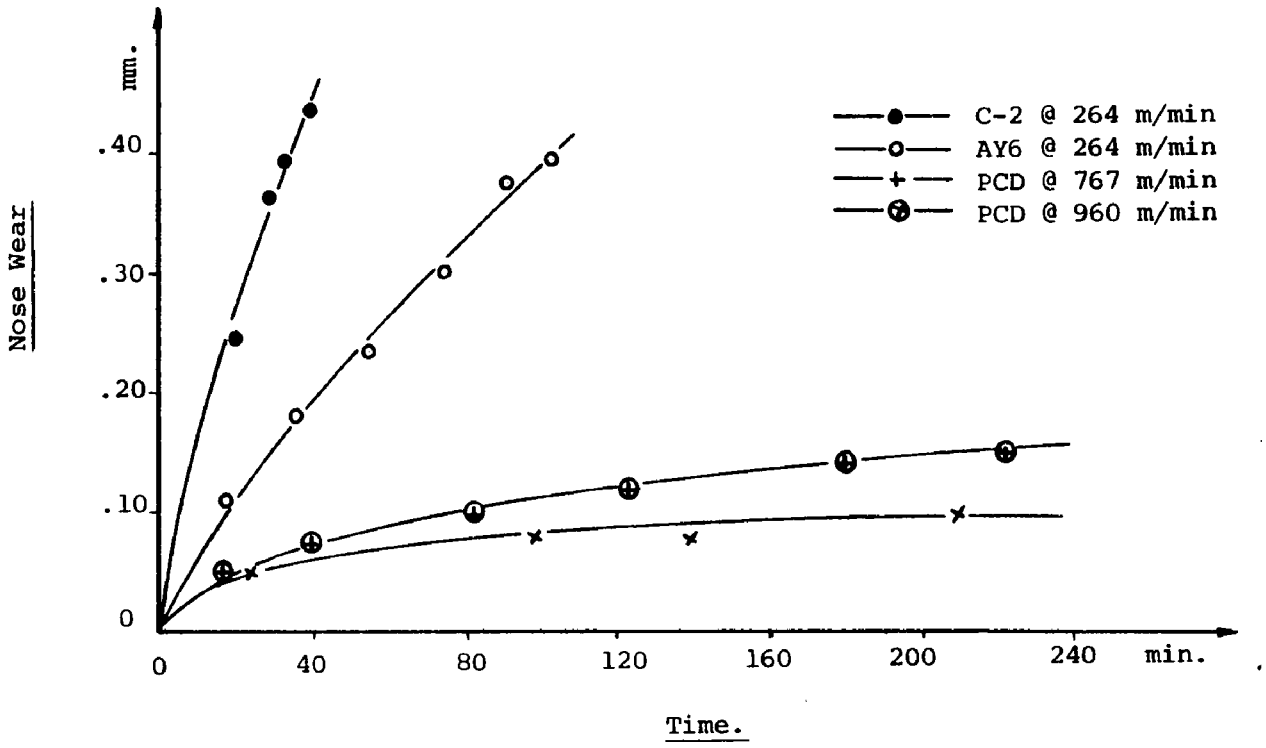

Figure 32 : Comparative tool wear tests . C-2 , AY6 and P.C.D. tools on silicon aluminum.

The comparative performance of the AY6 and C-2 grades was extended to cover a wider range of speeds. Other test conditions and procedures were identical to those previously described for figure 32. Table 9 gives the time taken to develop a .38 mm (.015 in) wear land under the nose. Figure 33 shows a plot of the data in a log-log scale. The least square lines for this data can be found in appendix b. It is clear that the AY6 grade is substantially more wear resistant than the C-2 grade.

TABLE 9: Time (min) to .38 mm (.015 in) nose wear.

SPEED	sfpm	867	1078	1330	1634	2030
	m/min	264	328	405	498	619
AY6		103.0	43.0	22.0	20.7	10.2
		100.0	47.6	24.3	18.8	8.7
C-2		37.2	14.0	6.0	5.7	1.5
		33.4	12.8	6.6	4.0	2.0

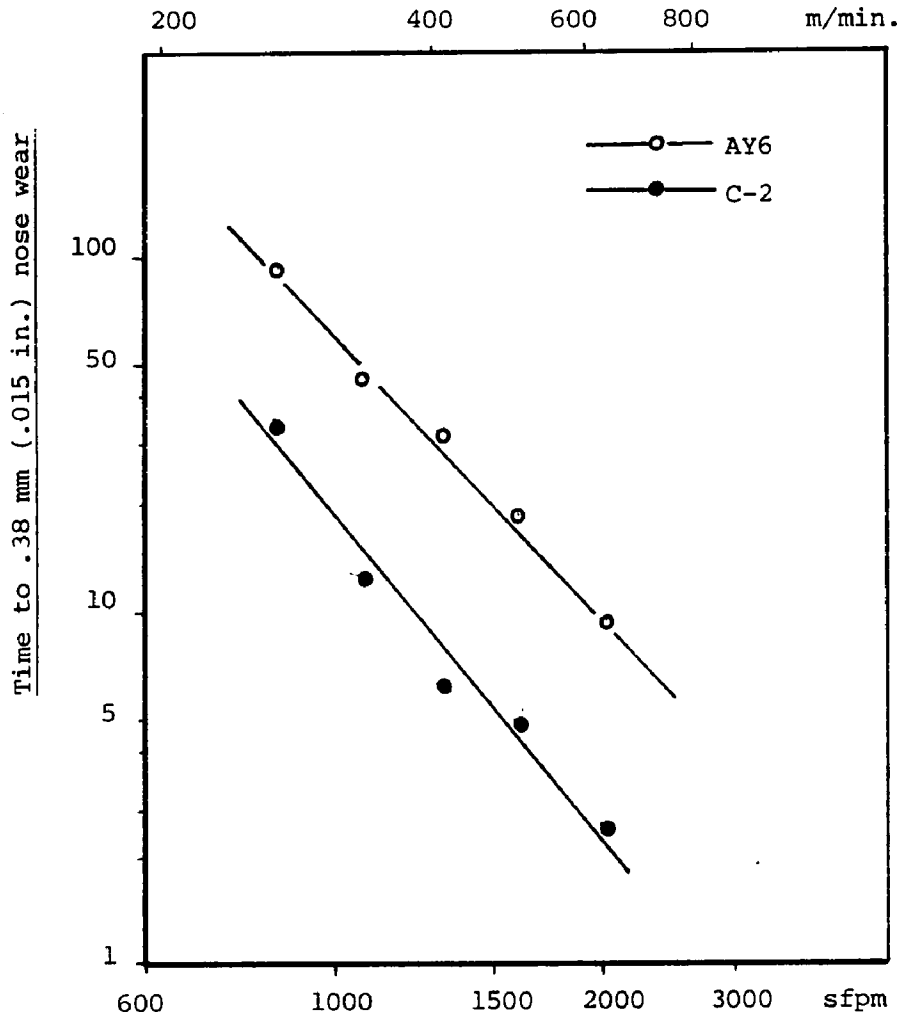

Figure 33 : Comparative performance of AY6 and C-2 grades on silicon aluminum .

6. Conclusions

The results of this study can be separated into two general parts. The first one includes observations, conclusions and problems associated with face milling when using a brittle ceramic type material. The second part pertains to those conclusions and observations specific to the performance of the different silicon nitride based compositions used in the tests. These conclusions are summarized below.

6.1 Face Milling with Ceramic Materials

6.1.1 Influence of the entry condition

The tests carried out in sections 5.2 and 5.3 clearly show that the entry condition, as expressed by the value of ε_i and the tool geometry is critical when milling with ceramic tools. For the SNG 433 tools having a honed edge, it was demonstrated that initial impact in the face of the tool, away from the fragile cutting edge could eliminate premature tool failure due to fracture or chipping. In contrast, initial contact at the depth of cut line resulted in premature failure through gross fracture, often preceded by the appearance of a crack at the depth of cut line. Also resulting in premature tool failure were geometric conditions which placed the initial tool/workpiece contact on the minor cutting edge, causing the periphery of the cutting edge to lead during entry. Note that these conditions in general, include symmetric and up milling.

6.1.2 Influence of the exit condition

The tests also showed that the SNG 433 having a honed edge were also susceptible to severe breakage at unfavorable exit conditions. Angles of disengagement ε_0 of up to 30° were found to cause severe fracture at relatively small feeds. A feed dependent breakage boundary was found but no explanation can be offered for this relationship. For $0 \leq \varepsilon_0 \leq 25$, the maximum allowable chip thickness at exit appears fairly constant. As ε_0 increase above 30°, the maximum allowable chip thickness increases substantially. This relationship needs further investigation.

6.1.3 The role of the K-land

Bearing in mind the potentially harmful effects of unfavorable entry and/or exit conditions on the performance of ceramic tools in face milling, this study has shown that the K-land should not be treated as an undefined strengthening preparation. Through the use of the graphic system, it was shown that the K-land should be treated as a geometric feature that can be exploited to protect the periphery of the cutting edge against unfavorable entry conditions. The graphic simulation of tool/workpiece initial contact location and progress showed that there exists a range of ε_i values for which initial contact is located on the K-land. Within this range, a substantial portion of the chip cross-section is intercepted by the K-land before the fragile periphery of the cutting edge enters the cut.

Experimental tests showed that ceramic type tools were free of chipping or breakage under these conditions. As ε_i increased towards values typical of upmilling situations, it was shown that the inclination of the tool/workpiece intersection curve shifted to a more vertical position, causing initial contact to occur on the minor cutting edge. It was noted that this type of contact was similar to the unfavorable "V" contact observed by Kronenberg and others. The tests showed that under these conditions, a K-land tool failed prematurely by chipping or fracture of the cutting edge. A K-land tool cannot therefore be used indiscriminately since for high ε_i values, initial contact and progress are such that the presence of a K-land offers no protection to the periphery of the cutting edge. Indeed, for extreme positive values of ε_i, it was shown that the performance of tools with or without a K-land was comparable, and invariably characterized by premature failure due to gross fracture of the cutting edge.

In contrast, when ε_i had large negative values, a substantial difference could be seen between the two tool geometries. The tools having a honed edge made initial contact at the depth of cut line and failed through gross fracture of the cutting edge. Under identical ε_i conditions, the geometric modification introduced by the K-land caused initial contact to remain on the K-land, away from the cutting edge, and tool performance was free of fracture.

Under favorable entry conditions, both the honed and K-land tools were free of chipping or fracture. Although the K-land tool fared better than the honed tool, this could not be interpreted as a manifestation of the higher strength of the K-land edge. Indeed, in both cases, cratering was the dominant mode of failure and by virtue of the bevel present on a k-land tool, more material has to be removed from the face of this tool than from that of the honed tool before the crater reaches the edge. Had the tests been carried out on a work material which did not promote cratering, and had flank wear been the tool life criterion, it does not seem evident that the K-land tool performance would have been superior to that of the honed tool. It would seem worthwhile to repeat this comparison on a work material where cratering is not the dominant wear mechanism.

An attempt was made to investigate the influence of exit conditions in a manner similar to that used for the SNG 433 tools with a honed edge. The K-land tool showed no sensitivity to exit conditions and no chipping or breakage was observed in the ε_0 range tested. As noted in the discussion of these tests, the conditions may not have been severe enough for the k-land tool. In addition, the negative range of ε_0 remains to be explored. This area therefore deserves more investigations.

6.1.4 The approach to ceramic cutting tool geometry

The results discussed above lead to the conclusion that ceramic tool geometry for potential face milling applications can be approached in a rational way. The tests using an SNG 433 tool with no edge preparation showed that unfavorable entry and/or exit conditions could cause premature tool failure, and a method was shown whereby these effects can be separated. The tools with a K-land preparation showed that under similar conditions, they could exit from the cut with no fracture. In addition, the computer simulation of initial tool/work contact location showed that this type of tool section could be exploited to ease entry through the selection of suitable geometric parameters.

While it was clear that a ceramic tool with no edge preparation offered a rather weak tool edge, it was not at all evident whether the standard K-land tool represented an optimum tool shape. It is believed that the realization that both entry and exit conditions can be harmful to the tool, augmented by the ability to identify favorable entry conditions for different tool edge preparation by 3-D graphic simulation, will enable the design of experiments permitting movement towards an optimum or near optimum ceramic tool shape for milling.

6.2 Performance of the Silicon Nitride Grades

With regard to the two silicon nitride based compositions available for the study, the tests conducted lead to the following conclusions:

- Based on the 4340 steel tests, it was obvious that the SNT grade had a better crater resistance than the AY6 grade. However, it appears that, because of severe cratering, neither grade is suitable for machining this type of steel.

- Based on the manganese steel tests, the AY6 grade was clearly the tougher grade. Whereas the SNT grade could not cut this material and fractured almost immediately, the AY6 grade, under favorable entry conditions showed no chipping or fracture. Failure under these conditions was strictly controlled by the cratering rate.

- Since severe cratering was the dominant tool failure mechanism under favorable milling conditions, the coating of these tools with a less steel reactive material was considered. Both compositions were sent out to be coated with Al_2O_3. The coating showed no adherence to the AY6 tool. The SNT grade showed relatively better adhesion but comparative tests showed that uncoated tools outperformed the coated ones. Poor coating adhesion and possible embrittlement of the substrate as a result of the coating process are likely causes.

- Neither grade was able to machine the Titanium or Waspalloy alloys. Failure through a total disintegration of the cutting edge was immediate. This was true for all conditions of geometry, speed, feed, depth of cut or contact condition tried.

- The tests on the silicon aluminum alloy showed that the AY6 grade was clearly superior to the SNT and C-2 grades in terms of wear resistance. The SNT grade, although known to be harder than the AY6 grade, performed poorly. The rapid cratering observed on the rake face of the SNT grade as well as the strong adherence of work material to the tool suggest that this composition does not seem to be chemically compatible with the work material. AY6 performance was best under positive geometry and for silicon aluminum alloy applications considering machining with a C-2 grade of tungsten carbide, the AY6 grade is clearly an alternative. Additional tests should be carried out using sharper tools (without the .025-.05 mm hone) and a polished rake face to reduce built up edge and aluminum adherence.

A brief comparative test using a commercial grade of polycrystalline diamond showed that this tool material could operate very successfully in a speed range prohibited to either silicon nitride or tungsten carbide based grades of tool material. Unless the number of parts in a silicon aluminum machining application is too small to justify the initial purchase of PCD tools, this tool material seems ideal for the highly abrasive silicon aluminum alloys.

7. Recommendations for Further Study

7.1 Optimization of the K-land parameters

K-land angle and width can be used as the independent variables. The graphic system can be used to determine an "equivalent" initial contact condition for each K-land under study and comparative tests can then be run under identical $\varepsilon_i, \varepsilon_o$ conditions.

7.2 The Effect of K-land Parameters on the Exit Failure

It was found that a tool with no edge preparation had a clearly defined feed dependent exit breakage boundary while under the same conditions, a K-land tool (20°x.20mm) was insensitive to the same types of exits. The variation in this exit breakage boundary can be studied as a function of the K-land angle. Also, the relationship between the maximum tolerated chip thickness at exit and the exit angle ε_o needs a fundamental investigation.

7.3 Simulation and Testing of Curved Edge Preparations

The chamfered K-land edge is only one possible edge preparation. Other shapes can be designed for the purpose of protecting the cutting edge at entry and exit. These shapes can readily be designed and simulated on the graphic system. Promising designs could eventually be produced and tested on the machine.

7.4 Beginning and Ending the Cut in Face Milling

In this study, ε_i and/or ε_o were maintained constant throughout the length of cut by precutting the workpiece at entry and disengaging the tool at the end before it started entering or exiting out of the plane perpendicular to the feed motion. It can easily be checked that ceramic tools will fail prematurely under any conditions if these steps are not taken. The study of ways to begin and end the cut during the milling of rectangular workpieces should be undertaken. One possible approach would be the use of numerically controlled tool path so that favorable ε_i and ε_o angles are maintained during the beginning and at the end of the cut.

7.5 Interactive Tool/Work Contact Simulation Package

The procedure to visualize tool/workpiece initial contact and progress under different angles of engagement can be formulated and implemented into an interactive simulation package. Ideally, the user would define and construct the tool under study then call upon the system to display the tool/work intersection by simply specifying the parameters γa, γr, c, ϕ and ε_i.

8. Bibliography

[1] King, A.G., and Wheildon, W.M. Ceramics in machining processes. New York: Academic Press Inc., 1966.

[2] Rea, R.F. "Background and properties of oxide cutting tools" A.S.T.E. collected papers, paper #17 (1957).

[3] Cook, N.H. "A review of published Russian work" A.S.T.E. collected papers, paper #18 (1957).

[4] Kennedy, W.B. "Experimental machining with ceramics" A.S.T.E. collected papers, paper #25 (1957).

[5] Tabuchi, N., et al. "Performance of Sumiboron" The Carbide and Tool Journal, May-June (1980).

[6] King, A.G. "Ceramic tool wear" A.S.M.E. paper 63-Prod-11 (1963).

[7] Whitney, E.D. "Ceramics and ceramic tool technology" The Carbide and Tool Journal, May-June (1980).

[8] Moore, H.D., and Kibbey, D.R. "Ceramic tool geometry and preparation" A.S.T.E. collected papers, paper #19 (1957).

[9] Pekelharing, A.J. "A story about the cracking of ceramic tools when cutting steel" C.I.R.P. Annals, XI (1961).

[10] Whitney, E.D., et al. Final report on development of improved cutting tool materials. Technical report AFML-TR-65-306, Ohio: U.S. Air Force Materials Laboratory, October 1965.

[11] Kalish, H.S. "New developments in cutting tools" The Carbide and Tool Journal, May (1981), pp. 163-176.

[12] Jack, K.H. "Review of Sialons and related nitrogen ceramics" Journal of Material Science, 11 (1976), pp. 1135-1158.

[13] Gazza, G.E., Journal of the American Ceramic Society, 56 (1973), p. 662. Cited from [12].

[14] Vasilos, T. Development of oxynitride materials for ceramic tool bits. Contract #DAAG46-77-C-0005, Army Materials and Mechanics Research Center, 1977.

[15] Gnesin, G.G., et al. "Optimization of the properties of a tool material based on silicon nitride" Soviet Powder Metall. Met. Ceram. (English Translation), 17[2] (1978), pp. 124-127.

[16] Wyman, V. "Cutting a dash with Sialons" Engineer, September 24 (1981), p. 29.

[17] Trent, E.M. Metal Cutting, 2nd ed. Butterworths, 1984.

[18] Baker, R.D. "Kyon 2000: a new world of high speeds and performances" The machinability of engineering materials, American Society for Metals, Proceedings of an International Conference, Rosemont, Illinois (1982), p. 292.

[19] Martellotti, M.E. "An analysis of the milling process" Trans. A.S.M.E., vol. 63, Nov. (1941), pp. 677-700.

[20] Loladze, T.N. "Nature of brittle failure of cutting tools" Annals of the C.I.R.P., Vol. 24/1/1975.

[21] Zorev, N.N. "Machining steel with a carbide tipped tool in intermittent heavy cutting condition" Russ. Engg. Jl., Vol. 43, #2 (1963), p. 43.

[22] Panday, P.C., Bhatia, S.M., and Shan, M.S. "Thermo-Mechanical failure of cemented carbide tools in intermittent cutting", Annals of the C.I.R.P., Vol. 28/1/1979.

[23] Schmidt, A.O., and Armitage, J.B. "An investigation of radial rake angles in face milling" Trans. A.S.M.E., Nov. (1944), pp. 633-643.

[24] Boston, O.W., and Gilbert, W.W. "Influence on tool life and power of nose radius, chamfer and peripheral cutting edge angle when face milling a 40,000 psi cast iron" Trans. A.S.M.E., Feb. (1947), pp. 117-124.

[25] Lucht, F. "Some effects of work positioning when face milling steel", Trans. A.S.M.E. Feb. (1946), pp. 151-160.

[26] Kronenberg, M. "Analysis of initial contact of milling cutter and work in relation to tool life" Trans. A.S.M.E. April (1946), pp. 217-228.

[27] Pekelharing, A.J. "The exit failure in interrupted cutting" Annals of the C.I.R.P., vol. 27/1/1978.

[28] Zorev, N.N. "Uber das wesen der niedrigen Zerspanbarkeit austenitischer chrom-Nikel-Stahle" Annals of the C.I.R.P., vol. 12 (1964), pp. 159-165. Cited from [36].

[29] Lehwald, W. Prufung von Hartmetallen im hinblick auf die Schneidenbeanspruchung beim unterbrochenen Schnitt. Dr. Thesis, TH Aachen (1962). Cited from [27].

[30] Hoshi, T., and Okushima, K. "Optimum diameter and positions of a fly cutter for milling steel at light cuts" Trans. A.S.M.E., Journal of Engineering for Ind., Nov. (1965), pp. 442-446.

[31] Beckhaus, H. Einfluss der Kontaktbedingungen auf das steinduerhalten von fraswerkzeugen beim strirnfrasen. Dr. Thesis, TH Aachen (1969). Cited from [27].

[32] Shaw, M.C., Sampath, W.S. and Lee, Y.M. "Tool fracture probability of cutting tools under different exiting conditions" Trans. A.S.M.E., Journal of Engineering for Ind., vol. 106, May (1984).

[33] Pekelharing, A.J. "The exit failure of cemented carbide face milling cutters Part I - Fundamentals and Phenomenae" Annals of the C.I.R.P., vol. 33/1/1984, pp. 47-50.

[34] Van Luttervelt, C.A., and Willemse, H.R. "The exit failure of cemented carbide face milling cutters Part II - Testing of commercial cutters" Annals of the C.I.R.P., vol. 33/1/1984, pp. 51-54.

[35] Kronenberg, M. Grundzuge der Zerspanungslehre. Bd. II Springer Verlag (1963).

[36] Opitz, H., and Beckhaus, H. "Influence of initial contact on tool life when face milling high strength materials" Annals of the C.I.R.P., Vol. XVIII (1971), pp. 257-264.

[37] Kane, G.E., et al. Mechanism of Wear and Performance of Multicomponent Ceramic Oxide Cutting Tool Materials. Fourth Annual Progress Report, N.S.F., May 1 (1975).

[38] Krabacher, E.J. and Haggerty, W.A. "Performance characteristics of ceramic tools in turning and milling" A.S.T.E. semi-annual meeting Los Angeles (1958), paper #145.

[39] Okushima, K., and Hoshi, T. "Utilizing TiC Cermet in Face-Milling" Bulletin J.S.M.E., vol. 6, No. 24 (1963).

[40] Schmidt, A.O., Roubik, J.R., Lanergan, J.J., and Hug, G. "Comparative carbide and ceramic millint tests" I.J.M.T.D.R., vol. 3, no. 1, Jan.-March (1963).

[41] Reynolds Metal Company. 390 Alloy Technology. Foundry Characteristics. Report, June (1975).

[42] Konig, W., and Erinsky, D. "Machining and machinability of aluminum cast alloys" Annals of the C.I.R.P., vol. 32/2/1983.

[43] Devor, R.E., and Miller, J.C. "Machinability of high silicon cast aluminum alloy with carbide and diamond cutting tools" 9th NAMRC, May (1981), pp. 296-304.

[44] Stashko, D. "Aluminum machining - a practical approach" S.A.E. Technical Paper Series 800490.

[45] Miller, J.C. "Machining high silicon aluminum" Society of Die Casting Engineers, paper no. G-T81-035 (1981).

APPENDIX A.

Typical edge conditions when machining 4340 steel R_c 35

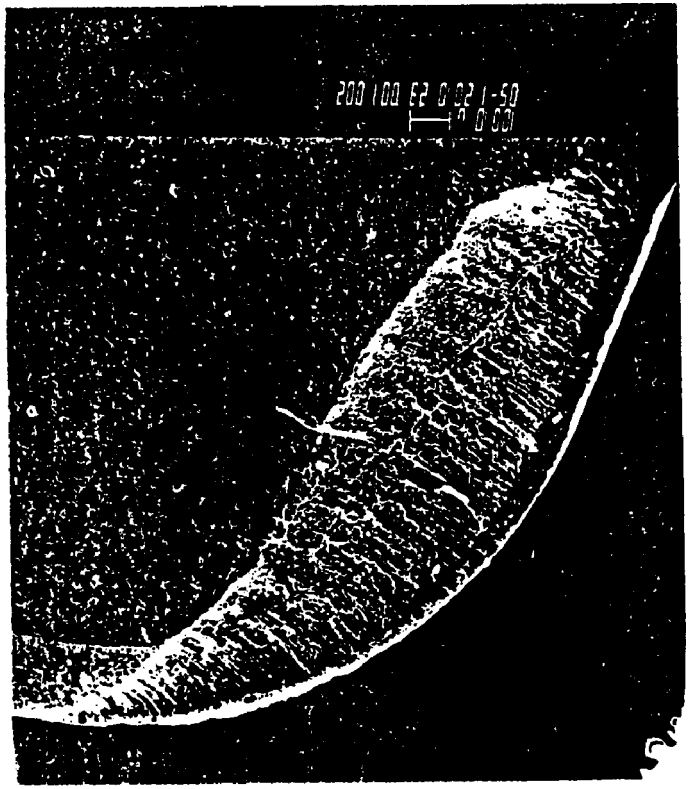

a. SNT K-Land at $\varepsilon_i = 7.2^\circ$

b. SNT K-Land at $\varepsilon_i = 30.0^\circ$

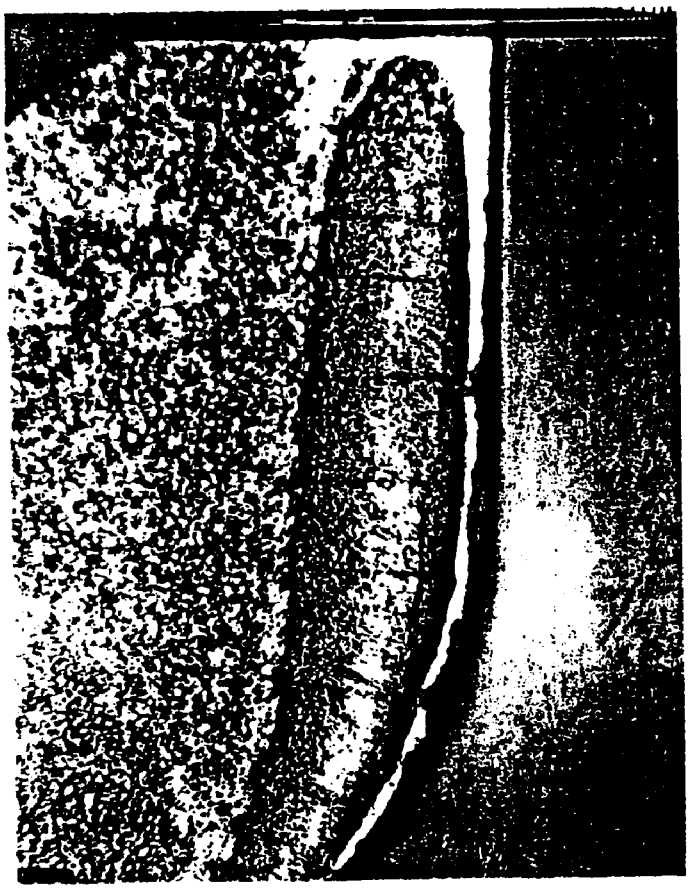

c. Coated C-6 carbide at $\varepsilon_i = 7.2^{\circ}$

d. Coated C-6 carbide at $\varepsilon_i = 38.7^{\circ}$

APPENDIX B.

1. MODEL FOR SNG TOOLS

$y = y_o + (b_1 + b_2.MS + b_3.MC)(V - S_o)$ where

y = tool's nose wear $x10^{-3}$ in.

V = cutting speed SFPM

OBS	SPEED	WEAR	MS	MC	PWEAR	RESID
1	816	7.1	0	0	6.9426	0.1574
2	816	7.1	0	0	6.9426	0.1574
3	816	6.7	0	0	6.9426	-0.2426
4	816	7.1	0	0	6.9426	0.1574
5	1016	9.1	0	0	9.4402	-0.3402
6	1016	8.7	0	0	9.4402	-0.7402
7	1016	9.6	0	0	9.4402	0.1598
8	1016	9.3	0	0	9.4402	-0.1402
9	1257	12.6	0	0	12.4499	0.1501
10	1257	12.6	0	0	12.4499	0.1501
11	1257	13.0	0	0	12.4499	0.5501
12	1257	12.8	0	0	12.4499	0.3501
13	816	11.8	1	0	10.3056	1.4944
14	816	9.8	1	0	10.3056	-0.5056
15	816	10.8	1	0	10.3056	0.4944
16	816	9.8	1	0	10.3056	-0.5056
17	1016	17.7	1	0	16.4820	1.2180
18	1016	16.5	1	0	16.4820	0.0180
19	1016	17.1	1	0	16.4820	0.6180
20	1016	15.6	1	0	16.4820	-0.8820
21	1257	24.0	1	0	23.9246	0.0754
22	1257	21.3	1	0	23.9246	-2.6246
23	1257	23.8	1	0	23.9246	-0.1246
24	1257	26.0	1	0	23.9246	2.0754
25	816	15.8	0	1	15.6756	0.1244
26	816	14.6	0	1	15.6756	-1.0756
27	1016	28.4	0	1	27.7260	0.6740
28	1016	31.0	0	1	27.7260	3.2740
29	1257	43.3	0	1	42.2468	1.0532
30	1257	39.4	0	1	42.2468	-2.8468

NON-LINEAR LEAST SQUARES SUMMARY STATISTICS DEPENDENT VARIABLE WEAR

SOURCE	DF	WEIGHTED SS	WEIGHTED MS
REGRESSION	5	6654.49066821	1330.89813364
RESIDUAL	25	20.48263189	0.81930528
UNCORRECTED TOTAL	30	6674.97330011	
(CORRECTED TOTAL)	29	1152.97741084	

PARAMETER	ESTIMATE	ASYMPTOTIC STD. ERROR	ASYMPTOTIC 95 % CONFIDENCE INTERVAL LOWER	UPPER
Y0	4.65922518	0.52182584	3.58451336	5.73393701
B1	0.01248326	0.00092825	0.01057650	0.01440003
B2	0.01839375	0.00138471	0.01554192	0.02124558
B3	0.04776384	0.00355754	0.04043700	0.05509069
S0	633.16194580	21.85822528	588.14444845	678.17944315

ASYMPTOTIC CORRELATION MATRIX OF THE PARAMETERS

	Y0	B1	B2	B3	S0
Y0	1.000000	-0.788918	0.624696	0.696565	0.845265
B1	-0.788918	1.000000	-0.465713	-0.417237	-0.455598
B2	0.624696	-0.465713	1.000000	0.687330	0.765229
B3	0.696565	-0.417237	0.687330	1.000000	0.845691
S0	0.845265	-0.455598	0.765229	0.845691	1.000000

NOTE: ALL ASYMPTOTIC STATISTICS ARE APPROXIMATE. REFERENCE: FALSTON AND JENNRICH, TECHNOMETRICS, FEBRUARY 1978, P 7-14.

2. MODELS FOR SPG TOOLS

AY6, SNT and C-2 Grades

y = nose wear data in 10^{-3} in. or 25.4×10^{-3} mm

V = cutting speed in SFPM

			697	867	1078	1330	1634
y	AY6		-	6.7	7.0	9.3	11.4
			-	6.3	7.5	8.7	11.8
	SNT		-	11.0	13.4	17.0	24.8
			-	10.6	12.6	18.9	23.4
	C-2		8.7	13.4	20.1	29.9	-
			8.0	14.7	22.5	27.0	-
ln(y)		AY6		1.902	1.946	2.230	2.433
				1.840	2.015	2.163	2.468
		SNT		2.397	2.595	2.833	3.211
				2.361	2.534	2.939	3.153

a. AY6 Least Square Model: $\ln y = \ln a + b\,x$ where $x = v-600$

Fitted Model: $\ln y = 1.641 + .770 \cdot 10^{-3}\, x$

ANOVA REPRESENTATION

SOURCE	SS	DF	MS	F
REGRESSION	.38966	1		
ERROR	.01042	6		
LACK OF FIT	.00309	2	.00309/2	<1
PURE	.00733	4	.00733/4	

$$S_{xx} = \sum_{i}^{4} \sum_{j}^{2} (x_{ij} - \bar{x}..) = 656117{\cdot}50$$

$$S_{yy} = \sum_{i}^{4} \sum_{j}^{2} (y_{ij} - \bar{y}..) = .400$$

$$S_{xy} = \sum_{i}^{4} \sum_{j}^{2} (x_{ij} - \bar{x}..)(y_{ij} - \bar{y}..) = 505{\cdot}628$$

$$b = S_{xy}/S_{xx} = .770.10^{-3}$$

$$\ln(a) = \bar{y} - b\bar{x} = 1.641$$

95% C.I $\quad b \pm .126 \times 10^{-3}$

$\quad \ln a \pm .087$

b. SNT Least Square Model

Fitted Model: $\ln y = 2.082 + 1.07 \cdot 10^{-3} x$ where x = V-600

ANOVA REPRESENTATION:

SOURCE	SS	DF	MS	F
REGRESSION	.75121	1		
ERROR	.01287	6		
LACK OF FIT	.00306	2	.00306/2	<1
PURE ERROR	.00981	4	.00981/4	

$$S_{xx} = \sum_{i}^{4} \sum_{j}^{2} (x_{ij} - \bar{x}..) = 656117 \cdot 50$$

$$S_{yy} = \sum_{i}^{4} \sum_{j}^{2} (y_{ij} - \bar{y}..) = .7641$$

$$S_{xy} = \sum_{i}^{4} \sum_{j}^{2} (x_{ij} - \bar{x}..)(y_{ij} - \bar{y}..) = 702.06$$

$b = S_{xy}/S_{xx} = 1.07 \times 10^{-3}$

$\ln(a) = \bar{y} - b.\bar{x} = 2.082$

95% C.I. $b \pm .14 \times 10^{-3}$

$\ln(a) \pm .133$

c. C-2 Least Square Model

Fitted Model: $y = 5.48 + .032.x$ where x = V-600

ANOVA REPRESENTATION

SOURCE	SS	DF	MS	F
REGRESSION	457.422	1		
ERROR	9.125	6		
LACK OF FIT	.977	2		<1
PURE	8.148	4		

$$S_{xx} = \sum_{i}^{4} \sum_{j}^{2} (x_{ij} - \bar{x}..) = 448572.0$$

$$S_{yy} = \sum_{i}^{4} \sum_{j}^{2} (y_{ij} - \bar{y}..) = 466.547$$

$$S_{xy} = \sum_{i}^{4} \sum_{j}^{2} (x_{ij} - \bar{x}..)(y_{ij} - \bar{y}..) = 14324.34$$

$b = S_{xy}/S_{xx} = .0319$

$a = \bar{y} - b\bar{x} = 5.483$

95% C.I. $b \pm .0045$

$a \pm 2.06$

VITA

The author was born on July 25, 1953, in El-Khroub, Algeria, the son of Mohamed and Djamila Lehtihet. He graduated from the Lycee du Mansourah (Constantine, Algeria). In 1977 he obtained a Bachelor of Science Degree (Honors) in Mechanical Engineering from Portsmouth Polytechnic (England) and in 1980 a Master of Science Degree in Industrial Engineering from Lehigh University. He will be joining the Industrial Engineering and Management systems faculty at the Pennsylvania State University.